

AD-A083 725

ARMY MILITARY PERSONNEL CENTER ALEXANDRIA VA
INITIAL ANALYSIS OF THE SULFUR-EXTENDED TEST TRACK CONSTRUCTED --ETC(U)
MAR 80 R L GARMAN

F/G 11/4
--ETC(U)

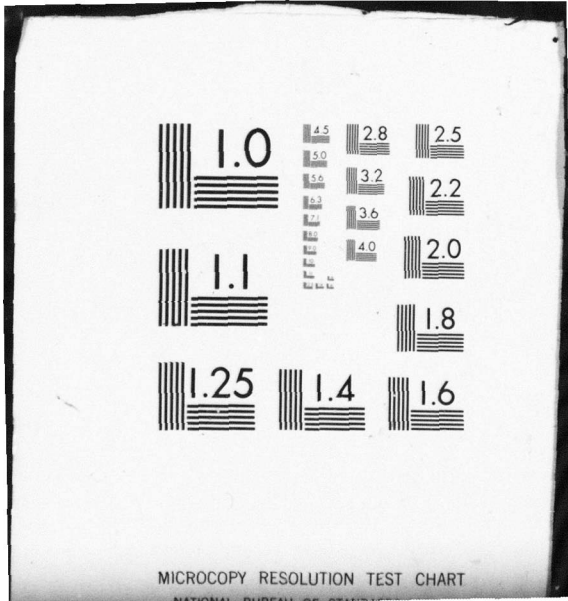
UNCLASSIFIED

NL

1 of 3

AD
A083 725





MICROCOPY RESOLUTION TEST CHART
NATIONAL BUREAU OF STANDARDS

LEVEL

② SC

INITIAL ANALYSIS OF THE SULFUR-EXTENDED TEST TRACK CONSTRUCTED AT WASHINGTON STATE UNIVERSITY

ADA 083725

CAPTAIN ROBERT L. GARMAN
HQDA, MILPERCEN (DAPC-OPP-E)
200 Stovall Street
Alexandria, VA 22332

DTIC
ELECTED
APR 25 1980
C

Final Report 18 March 1980

Approved for public release; distribution unlimited.

A thesis submitted to The University of Washington at Seattle, Washington in partial fulfillment of the requirements for the degree of Master of Science in Civil Engineering.

80 3 28 037

COPY

6 Initial Analysis of the Sulfur-Extended Test Track
Constructed at Washington State University

by

10 Robert Lawrence/Garman

11 4 Mar 80

12 209

A thesis submitted in partial fulfillment
of the requirements for the degree of

9 Final rept.,

Master of Science in Civil Engineering

University of Washington
1980

Approved by Ronald L. Jeml
(Chairperson of Supervisory Committee)

Program Authorized
to Offer Degree Civil Engineering

Date March 4, 1980

391191

mt

In presenting this thesis in partial fulfillment of the requirements for a Master's degree at the University of Washington, I agree that the Library shall make its copies freely available for inspection. I further agree that extensive copying of this thesis is allowable only for scholarly purposes. It is understood, however, that any copying or publication of this thesis for commercial purposes, or financial gain, shall not be allowed without my written permission.

Signature _____

Date _____

Accession For	
NTIS GRA&I	<input checked="" type="checkbox"/>
DDC TAB	<input type="checkbox"/>
Unannounced	<input type="checkbox"/>
Justification	
By _____	
Distribution/	
Availability Codes	
Dist	Avail and/or special
A	

TABLE OF CONTENTS

	Page
List of Figures	iv
List of Tables	viii
Acknowledgments	x
Chapter I: Introduction	1
Background	1
Sulfur-Asphalt Technologies	4
Processes	4
Shell Canada Limited	4
Gulf Oil Canada	10
Societe National Elf-Aquitaine	22
Pronk	23
U.S. Bureau of Mines	26
Chapter II: Current U.S. Field Tests	36
Introduction	36
Lufkin Field Trial	36
Boulder City Field Test	50
Chapter III: Mix Design and Resilient Modulus Evaluation of Sulfur-Extended Asphalt Pavements	66
Background	66
Materials Characteristics	68
Sample Preparation	69
Sample Testing	73
Results of Marshall Mix Design	76
Results of Hveem Mix Design	86
Resilient Modulus	98
Pavement Thickness	99
Chapter IV: Construction and Instrumentation of Test Track	113
WSU Test Track Equipment	113
Preparation of Track Prior to Placement of Test Sections	118

	Page
Test Track Instrumentation	124
Test Sections, Background	129
Test Track Thicknesses	130
Test Track Placement Temperatures	130
Test Track Densities	133
Quality Control	137
Chapter V: Fatigue Characteristics and Comparison of Measured to Theoretical Pavement Responses	140
Fatigue	143
Comparison of Bison Indicated Initial Strains and Deflections to BISAR Predicted Initial Strains and Deflections	151
Chapter VI: Conclusions and Recommendations	162
Conclusions	162
Recommendations	163
Bibliography	165
Appendix A: WSU Summary of Daily Track Operators Journal . .	170
Appendix B: Calibration of Bison Strain Gauges	179

LIST OF FIGURES

	Page
1.1 Effect of Mixing Sequence on Marshall Stability	8
1.2 Batch Mixing Plant Asphalt and Liquid Sulfur System . . .	11
1.3 Relationships between Tensile Strength and Sulfur Content	14
1.4 Relationships between Tensile Strength and Temperature .	16
1.5 Relationship Between Tensile Strength and Binder Content for Sulfur-Asphalt Mixtures with 40/50 Pen Asphalt	17
1.6 Relationships Between Resilient Modulus and Sulfur Content	19
1.7 Relationships Between Resilient Modulus of Elasticity and Temperature for Sulfur-Asphalt Mixtures	20
1.8 Relationships Between Resilient Modulus of Elasticity and Binder Content for Sulfur-Asphalt Mixtures	21
1.9 Size Gradation for Aggregate Materials	29
1.10 Viscosity of Sulfur-Asphalt Binder vs Temperature	32
1.11 Stress Fatigue Curve, Limestone Aggregate	33
1.12 Stress Fatigue Curve, Volcanic Aggregate	34
2.1 Layout of SNPA Sulfur Bitumen Binder Pavement Test-- U.S. Highway 69, Lufkin, Texas	40
2.2 Aggregate Gradations for Lufkin Field Trials	41
2.3 Colloid Mill Furnished by SNPA for Preparation of Sulfur-Asphalt Emulsion	42
2.4 Schematic Drawing of Sulfur-Asphalt Mixing Station . . .	43
2.5 Hveem Stability vs Pavement Age for HMAC Mixtures, U.S. 69	46
2.6 Marshall Stability vs Pavement Age for HMAC Mixtures, U.S. 69	48

	Page
2.7 Resilient Modulus at 68°F (20°C) vs Pavement Age for HMAC Mixtures, U.S. 69	51
2.8 Profile of Sulfur-Asphalt (SA) Concrete and Asphalt Concrete (AC) Test Sections and Specimen Specifications	53
2.9 SEA Experimental Project Schematic of Test Items	54
2.10 Aggregate Gradation Chart Showing the Grading Limits and Composition of Blend	55
2.11 Schematic of S/A System	57
2.12 Peak Deflection Profile Due to Dynaflect Loading for the Various Test Sections of U.S. 93-95, Boulder City, Nevada (Slow Lane O-W-P)	59
2.13 Deflection Basins from the Average Observations for the Various Test Items of U.S. 93-95, Boulder City, Nevada (Slow Lane O-W-P)	61
2.14 Relationship Between the Average Resilient Modulus and Temperature for Each Section of U.S. 93-95, Boulder City, Nevada	64
3.1 Plan and Cross-Sectional View of SR 220	67
3.2 Aggregate Gradation, WSDOT Class B	72
3.3 Hveem and Marshall Sample Preparation	74
3.4 Marshall Sample Testing Sequence	75
3.5 Hveem Sample Testing Sequence	75
3.6 Marshall Mix Design Data Curves 100/0 Asphalt/Sulfur Ratio	81
3.7 Marshall Mix Design Data Curves 70/30 Asphalt/Sulfur Ratio	82
3.8 Marshall Mix Design Data Curves 50/50 Asphalt/Sulfur Ratio	83
3.9 Hveem Stabilometer	87
3.10 Hveem Mix Design Data Curves 100/0 Asphalt/Sulfur Ratio .	92
3.11 Hveem Mix Design Data Curves 70/30 Asphalt/Sulfur Ratio .	93
3.12 Hveem Mix Design Data Curves 50/50 Asphalt/Sulfur Ratio .	94

	Page
3.13 Comparison of Marshall Stabilities of Various Asphalt/Sulfur Ratio Samples	96
3.14 Comparison of Hveem Stabilities of Various Asphalt/Sulfur Ratio Samples	97
3.15 M_R vs Binder Content and Days of Cure, Marshall Samples, Varying Asphalt/Sulfur Ratios	100
3.16 M_R vs Binder Content and Days of Cure, Hveem Samples, Varying Asphalt/Sulfur Ratios	102
3.17 Cross-Section of M_R Values of Hveem Samples at 5.5% Binder Content	104
3.18 5.5% Binder Content, M_R vs Temperature: Marshall Samples	105
3.19 5.5% Binder Content, M_R vs Temperature: Hveem Samples	106
3.20 BISAR Predicted Maximum Initial Horizontal Strain vs Various Base Course Thicknesses	108
3.21 BISAR Predicted Maximum Initial Vertical Strain vs Various Base Course Thicknesses	109
3.22 Predicted Load Repetitions to Failures vs Thickness of Base Course	111
4.1 Test Track -- Washington State University	114
4.2 Wheel and Tire Arrangement	115
4.3 Schematic of Dual Size and Spacing	116
4.4 Load Distribution in Wheel Path	117
4.5 Schematic Profile of Test Track	121
4.6 Plan View of Test Track	122
4.7 Moisture Content (%) of the Subgrade as Placed and Average Moisture Content per Section	123
4.8 Vertical Soil Extensometer	125

	Page
4.9 Partial Cross-Section of Two WSU Test Track Sections Illustrating Position of Strain Gauges	127
4.10 Partial Plan View of Two WSU Test Track Sections Illustrating Position of Strain Gauges	127
4.11 Bison Strain Gauge Layout	128
4.12 Schematic Profile of Test Track as Planned Compared to as Built	131
4.13 Actual Pavement Thicknesses Achieved at Test Track . .	132
4.14 Temperature-Viscosity Curve for Liquid Sulfur	134
4.15 Density vs Number of Passes with a 10-Ton Smooth Steel Wheel Gallion Roller	136
4.16 Sulfur-Asphalt Binder Composition vs Specific Gravity .	138
5.1 Bison Strain Gauge Layout	142
5.2 Fatigue Criteria for Horizontal Tensile Strain at the Bottom of the Test Track Pavement	146
5.3 Initial Horizontal Tensile Strain vs the Number of Load Repetitions to Failure for the 0/100 S/A Sections (BISAR and Bison)	148
5.4 Initial Horizontal Tensile Strain vs the Number of Load Repetitions to Failure for the 30/70 S/A Sections (BISAR and Bison)	149
5.5 Surface Deflections as Computed by Bison, BISAR and Bison/BISAR Hybrid	161

LIST OF TABLES

	Page
1.1 Summary of Available Sulfur-Asphalt Technologies	5
1.2 Stiffness and Fatigue Life of Regular and Simultaneous Mixes	9
1.3 Physical Properties of S/A Binders	13
1.4 Specific Gravity of Sulfur Asphalt	25
1.5 Emulsion Stability	25
1.6 Typical Air Emission Data for Pronk Sulfur Asphalt Trial.	27
1.7 Marshall Design Data Comparison	31
2.1 Survey of Sulfur-Asphalt Field Trials	37
2.2 Toxicity of Hydrogen Sulfide Gas	58
2.3 Variations in Marshall Stabilities, Test Results at 60°C Within Each Layer for Various Test Items of U.S. 93-95, Boulder City, Nevada, Sections A, B, C & D .	63
3.1 Relative Density of Various S/A Binders	70
3.2 Equivalent Binder Content for 30/70 and 50/50 S/A Binders Compared to Conventional 0/100	70
3.3 Aggregate Gradation WSDOT Class B	71
3.4 Marshall Design Criteria	77
3.5 Marshall Mix Design Data, 100/0 Asphalt/Sulfur Ratio . .	78
3.6 Marshall Mix Design Data, 70/30 Asphalt/Sulfur Ratio . .	79
3.7 Marshall Mix Design Data, 50/50 Asphalt/Sulfur Ratio . .	80
3.8 Hveem Mix Design Data, 100/0 Asphalt/Sulfur Ratio . . .	89
3.9 Hveem Mix Design Data, 70/30 Asphalt/Sulfur Ratio . . .	90
3.10 Hveem Mix Design Data, 50/50 Asphalt/Sulfur Ratio . . .	91

	Page
4.1 Test Track Subgrade Densities	120
4.2 Location of Thermocouples at WSU Test Track	129
4.3 Placement Temperatures of S/A Mixes at WSU Test Track .	135
5.1 Initial Strains Manually Computed and Coil Spacing . .	141
5.2 Coil Distance from Innermost Edge of Wheel Path to Coils and Angular Location of Each Coil Set	143
5.3 Location of Duals in Relation to Bison Coils for Initial Strain Readings	144
5.4 BISAR Predicted Compared to Bison Indicated Surface Deflections for S/A 30/70 and S/A 0/100 Sections	152
5.5 BISAR Predicted Compared to Bison Indicated Longitudinal Horizontal Strains for S/A 30/70 and S/A 0/100 Sections	153
5.6 BISAR Predicted Compared to Bison Indicated Transverse Horizontal Strains for S/A 30/70 and S/A 0/100 Sections	154
5.7 BISAR Predicted Compared to Bison Indicated Vertical Strains for S/A 30/70 and S/A 0/100 Sections .	155
5.8 BISAR Predicted Compared to Bison Indicated Deflection at top of Extensometer for S/A 30/70 and S/A 0/100 Sections	156
5.9 Calculated Surface Deflection	160

ACKNOWLEDGMENTS

A project of this magnitude could not have been completed without the encouragement and assistance of many individuals. I wish to express my sincere gratitude to my Committee Chairman, Dr. Ronald L. Terrel and to my Committee Members Professors Albert L. Hoag and Joe P. Mahoney for their constant guidance and support. My deepest appreciation goes to Dr. Mahoney, who served as my chief mentor throughout.

The financial assistance provided by the Federal Highway Administration, Sulfur Development Institute of Canada, Washington Asphalt Pavers Association and the Washington State Department of Transportation is appreciated.

I am truly grateful to Captain Paul D. Sharkey, U.S. Army, for assistance and friendship during the initial phases of this project. The technical assistance of Derald Christensen is appreciated. My deepest thanks go to Barbara Blackman for her typing of this thesis.

Above all, my deep-felt appreciation to my wife, Lin, and my children, Bobby and Ronni, for their support, faith and love during this study.

CHAPTER I

INTRODUCTION

BACKGROUND

Asphalt is an extremely important construction material, especially with respect to flexible pavement for roads and airfields. In the United States about 32 million tons of asphalt are used annually for the construction and resurfacing of roadways [1].

Asphalt is a very versatile material because it is a strong cement with excellent waterproofing and durability characteristics. Asphalt is a viscoelastic material which imparts controllable flexibility to a paving material when combined with mineral aggregates [3].

Asphalt has been utilized by man for more than 5000 years. Archeologists discovered that it had been utilized as a waterproofing material for temple paths and water tanks in ancient India during the period 3200 to 540 B.C. It was also used by the ancient Egyptians in their mummification process [1, 3].


The first modern application of asphalt as a paving material was in France in 1802, where it was utilized for the surfacing of floors, bridges and sidewalks. The first asphalt pavement was laid in the United States during the 1870's by Professor E. J. De Smedt in Newark, New Jersey [1]. The first street asphalt pavement was laid in Washington, D.C. with imported lake asphalt

in 1876. In 1902 approximately 20,000 tons of asphalt were refined from petroleum products in the United States. The use of petroleum derived asphalt has increased steadily from approximately 3 million tons in 1926 to more than 8 million tons in 1946; 24 million tons in 1974 to more than 32 million tons in 1977 [1].

Although asphalt is found in natural deposits known as rock asphalt, the vast majority of construction asphalt is a product of crude petroleum. The crude petroleum is refined and separated into various fractions such as gasoline, kerosene, diesel and lubricating oils. The residuals of this process are further processed into various grades of asphalts.

Unfortunately, due to rapidly increasing petroleum prices, it has become more profitable for oil companies to use the asphaltic residue in blending of heavy fuel oils rather than market the asphalt per se. This has caused a reduction in asphalt production over the last few years. Consequently, with the asphalt shortages and constant or even increasing demand, the price for asphalt has been escalating rapidly [12].

→ Due to the aforementioned shortages and price increases of asphalt, researchers, oil companies and governmental agencies are exploring the possible utilization of substitute binders and asphalt extenders for pavement construction. These explorations have produced new emerging technologies such as the recycling of asphalt, asphalt rejuvenation, and asphalt extension through the



use of wood lignins or sulfur [3]. This report will evaluate the sulfur-extended asphalt, and is based upon recently acquired data from the Washington State University (WSU) test track.

As will be discussed, many laboratory studies have been conducted by various research organizations to investigate the effects of combining sulfur, asphalt and various aggregates. Additionally, several full-scale highway projects have been built. The laboratory analytical results have been promising and have shown sulfur-extended asphalt (SEA) binders to be possibly superior to conventional pavements. The results of the full-scale highway projects are at this time incomplete and still somewhat inconclusive [23].

In an attempt to fill this gap between laboratory data and the full-scale highway projects, full-depth pavement structures for repetitive wheel load testing were constructed at the WSU test track. Further details on the construction of the test track will be given in Chapter IV.

A brief description of the state-of-the-art of the extension of asphalt with sulfur is presented in the remainder of Chapter I. A brief description of the Lufkin, Texas and the Boulder City, Nevada field trials will be presented in Chapter II to give the reader a better understanding of current field trials.

SULFUR-ASPHALT TECHNOLOGIES

Sulfur-asphalt binder is generally incorporated into paving mixtures by two methods. The first method is a sulfur-asphalt emulsion which is a dispersion of liquid sulfur into molten asphalt cement. The sulfur-asphalt emulsion is then added to preheated aggregates using one wet-mix cycle to produce the hot mix used in construction of the pavement. The second method is a two-step process utilizing two wet-mix cycles. In the first cycle, molten asphalt is mixed with preheated aggregates, then liquid sulfur is introduced to the hot mix and the second wet-mix completes the process.

Table 1.1 shows the various sulfur-asphalt technologies that have been developed to date. It should be noted that with the exception of the U.S. Bureau of Mines process, all processes are patented.

Processes

Shell Canada Limited (Sand-Asphalt-Sulfur)

Shell Canada Limited has conducted a study for using elemental sulfur in asphaltic hot mixes which permits greater flexibility in mix design and the possible utilization of poorly graded aggregates and even uniformly graded sands [4,3]. It has been shown that the

Table 1.1. SUMMARY OF AVAILABLE SULFUR-ASPHALT TECHNOLOGIES

Process	Patent	Year of Development	Mix Type	Optimum S/A Ratio by Weight	Additive	Aggregate Quality
Shell Canada Limited	Yes	1964	S-A-S	70:30	No	Poor
Gulf Oil Canada Limited	Yes	1973	S/A Emulsion Concrete	30:70	NO	Good
S.N.E.A.	Yes	1973	S/A Emulsion Concrete	30:70	No	Good
Pronk	Yes	1973	S/A Emulsion Concrete	40:60	Yes	Good
U.S. Bureau of Mines	No	1976	S/A Concrete	35:65	No	Good

S-A-S: Sand - Asphalt - Sulphur

S/A: Sulphur Asphalt

S.N.E.A.: The Societe Nationale Elfa-Aquitaine of France [3]

mixes made with these materials are equal or superior to conventional asphaltic mixes made with normally accepted aggregate gradation.

Shell Canada has developed three different mixing sequences of sand-asphalt- sulfur (SAS):

1. REGULAR PROCESS - Sand is premixed with asphalt, followed by the addition of sulfur in a second wet-mixing cycle.
2. REVERSE PROCESS - Sand is premixed with sulfur, followed by the addition of asphalt and then mixing of the three components in a second wet-mixing cycle.
3. SIMULTANEOUS PROCESS - As the name implies, all three components are mixed together simultaneously in a single wet-mixing cycle.

All three mixing sequences were used in the preparation of mixes to study the effects of the different sequences on the mix properties. Standard Ottawa sand was used because of its translucence. The mixes were made using 4 and 6 per cent 150/200 penetration grade asphalt combined with 14 per cent sulfur, by weight.

All three components were brought to 300°F prior to combination. Each wet-mixing time was 30 seconds for the Regular and Reverse sequences, but 60 seconds for the single cycle of the Simultaneous sequence. Microscopic examination of thin sections of the samples indicated no major differences between the dispersion achieved in the three different cycles.

Further laboratory testing by Shell Canada with one sized medium coarse (50 per cent between No. 8 and No. 100 sieves) sand,

150/200 penetration grade asphalt and varying amounts of sulfur was conducted. High and low workability mixes cast in Marshall molds were subjected to various one face compactive efforts. It was discovered that the amount of compactive effort had little impact on the densities of the highly workable mixes, but the stiffer sand-asphalt mixes benefited from compaction [4].

The mixing sequence (Regular, Reverse or Simultaneous) did not greatly impact upon bulk density, Marshall stability and flow of medium-coarse sand mixes.

Figure 1.1 shows the results of the Marshall stability tests. The Regular process sequence consistently yielded higher Marshall stability than the Simultaneous or Reverse processes. Additionally, the Regular process yielded the highest tensile strength, bulk density, and flexural strength. Table 1.2 shows the differences in stiffness and fatigue life of the Regular and Simultaneous processes. The Reverse process showed consistently lower Marshall stability and tensile flexural strength properties than the other two processes.

The general conclusions of this study follow:

1. Medium and coarse sands are the best aggregates to be used with SAS.
2. The mixes can be placed without rolling and compactive effort.
3. The mixes were shown to have construction properties comparable to or superior to conventional mixes.

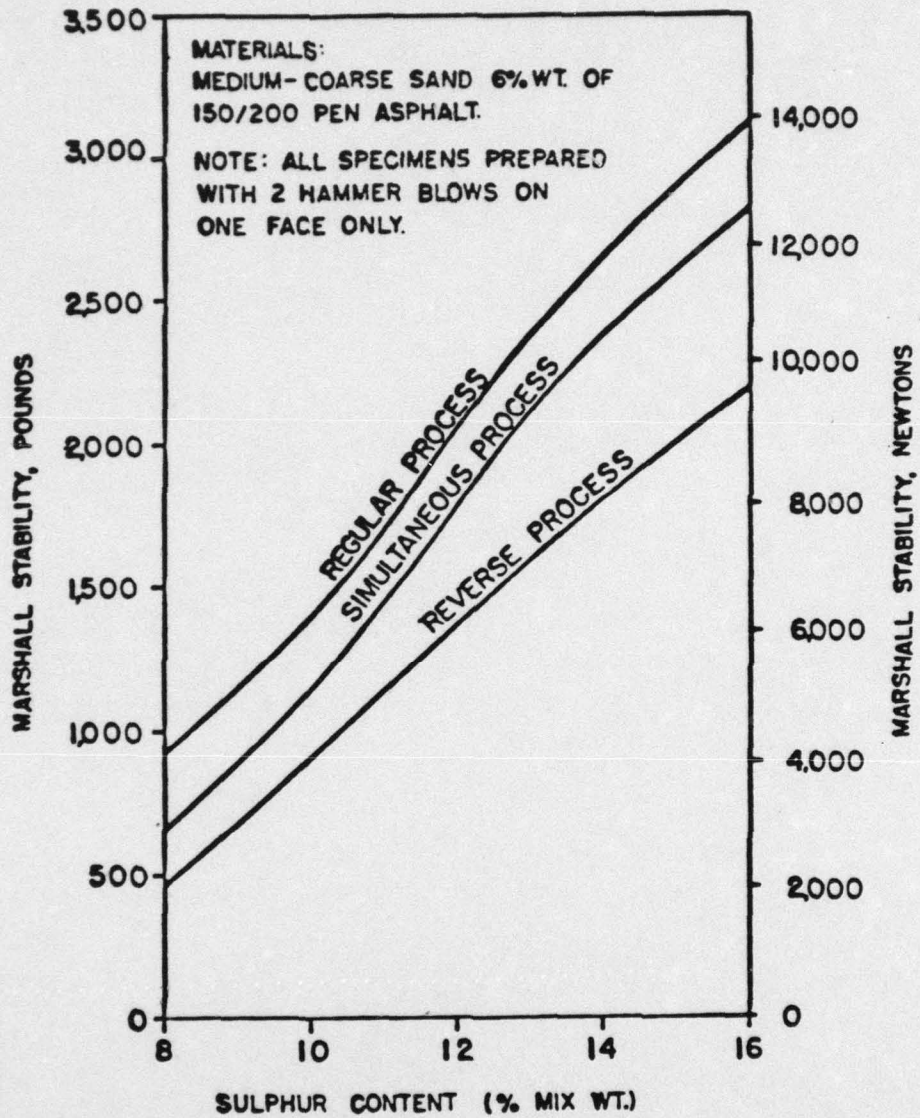


Figure 1.1 EFFECT OF MIXING SEQUENCE ON MARSHALL STABILITY
[3,5]

Table 1.2
STIFFNESS AND FATIGUE LIFE
OF REGULAR AND SIMULTANEOUS MIXES
[3,5]

	Regular Mix	Simultaneous Mix
Bulk Density, g/cc	1.971	1.961
Stiffness Modulus, N/m ²	5.7×10^9	4.8×10^9
Fatigue Life, cycles	7.23×10^5	6.05×10^5

Mix composition: 82% medium-coarse sand
6% asphalt (150/200 pen)
12% sulfur

Test Conditions: Temperature at 10°C
Frequency 60 Hz
Unit Strain 1.5×10^{-4}

4. The Regular mixing process yielded the best results when compared to the Reverse and the Simultaneous processes.
5. The use of sulfur in asphalt mixes could permit design for a predetermined stability level by variance of the per cent of sulfur added.
6. Sand-asphalt-sulfur (SAS) mixes can be produced using conventional hot mix plants equipped with liquid sulfur storage tanks fitted with a recirculating system. Such a system is illustrated in Figure 1.2.
7. SAS mixes are promising for areas with hot climates because it is less susceptible to softening at higher temperatures than conventional mixes.

Limitations of this study were that it was mainly laboratory oriented (though later field trials were conducted), weather and environmental considerations were not taken into account, and no attempt was made at predicting the optimum sulfur contents or ratios.

The Gulf Oil Canada Limited Sulfur - Asphalt System

Gulf Oil Canada has developed and field-tested a procedure for the introduction of sulfur into conventional asphaltic mixes. In this system the total amount of binder is approximately the same as it would be in a conventional mix. The advantage, however, is that the sulfur acts as a partial replacement agent for asphalt.

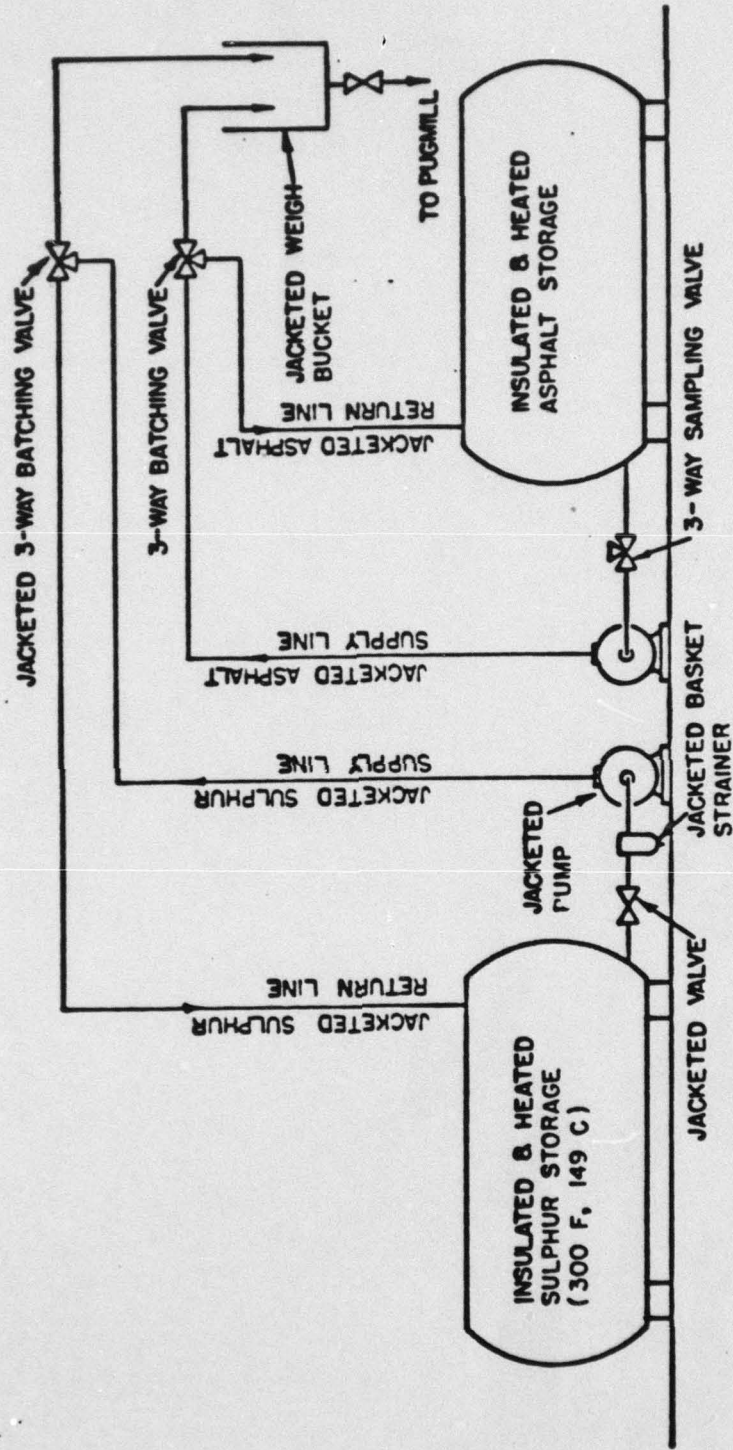


Figure 1.2. BATCH MIXING PLANT ASPHALT & LIQUID SULFUR SYSTEM [5]

Liquid sulfur is dispersed into liquid asphalt to produce a sulfur-asphalt binder. This process has the advantage that the mixes can be handled with conventional mixing and paving equipment while eliminating the hazards of dangerous buildup of high concentrations of hydrogen sulfide in storage and transfer tanks. Up to 50 per cent replacement (by weight) of asphalt by liquid sulfur was dispersed in the sulfur-asphalt (S/A) binder.

Preliminary laboratory tests indicated the coagulation and settlement of sulfur particles after approximately three hours, though some plasticizers have improved the stability of the S/A binder [6]. The physical properties of several different S/A binders is shown in Table 1.3. The viscosity characteristics of 85/100 grade asphalt is compared with the viscosity of a 50 per cent by weight S/A binder in Figure 1.3. A viscosity range of 200-600 cs was found to produce the best S/A binder with respect to aggregate coating, mix spreading, workability and compaction.

Marshall stability tests conducted by Gulf Oil Canada Limited indicated that S/A mixes are superior to conventional asphalt-concrete mixes. The following conclusions were drawn relative to stability:

1. S/A stabilities are higher than those for conventional asphalt mixes.
2. Stability increased with an increase of sulfur content.
3. No significant loss in flow or properties at 140°F was noted.

Table 1.3. PHYSICAL PROPERTIES OF S/A BINDERS [7]

Sample Description	100	90 10	80 20	70 30	60 40	55 45	50 50	40 60	100
Blend of 85-100 pen Asphalt Elemental sulphur	100	10552	1.1200	1.1828	1.2320	1.2854	1.3442	1.4337	1.9556*
Gravity, specific, 60°F	1.0268								
Softening point, °F ASTM D36	112 112	101 104	103 105	107 107	108 110	109 ---	111 110	134 ---	
Penetration, 77°F, 100 g, 5 sec ASTM D5	92 92	171 145	176 156	181 153	183 165	168 ---	70 75	72 ---	
Ductility, 77°F, ASTM D113	150+	142	101	29	25	47	44	23	
Flash Point, COC, °F ASTM D92	560	360	345	345	335	330	320	325	
Fraas Break Point, °C, IP80	-16	-14	-15	-12	-13	-14	---	---	

*Data point from literature.

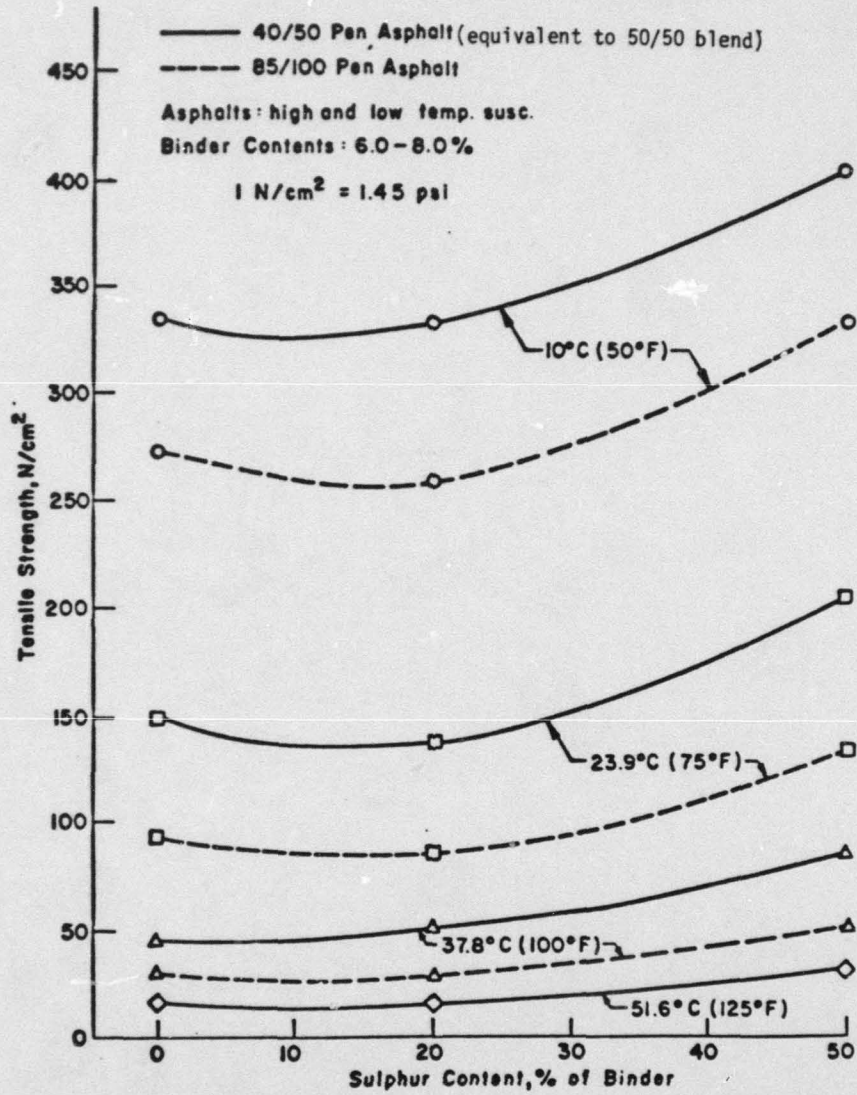


Figure 1.3. RELATIONSHIPS BETWEEN TENSILE STRENGTH AND SULFUR CONTENT [8]

4. Poorly graded and low quality aggregates can be effectively stabilized with S/A binder.
5. Stability of S/A mixes was not affected after water soaking.
6. Various types of asphalt can be utilized with sulfur to produce good S/A binder.

As a result of these preliminary laboratory results, Austin Research Engineers of Texas was retained by Gulf Oil Canada Limited to carry out engineering evaluation and experimental design. The goals established for Austin Research were (1) whether or not S/A mixtures exhibit better engineering characteristics than conventional mixtures, and (2) the nature of the effects produced by various S/A mixture and testing variables.

The basic tests utilized in this engineering evaluation were static and repeated-load indirect tensile tests to obtain an estimate of tensile strength, resilient modulus and fatigue life. The major variables evaluated were penetration, temperature susceptibility, binder content, sulfur - asphalt ratios, tensile stress and test temperature.

Tensile strengths of S/A mixes were found to be higher than those of conventional asphalt mixtures. Tensile strength values were very dependent upon sulfur-asphalt ratio, consistency or penetration value of the asphalt cement, and test temperature (see Figures 1.3 and 1.4). As illustrated by Figure 1.5, tensile strength was only slightly dependent upon binder content.

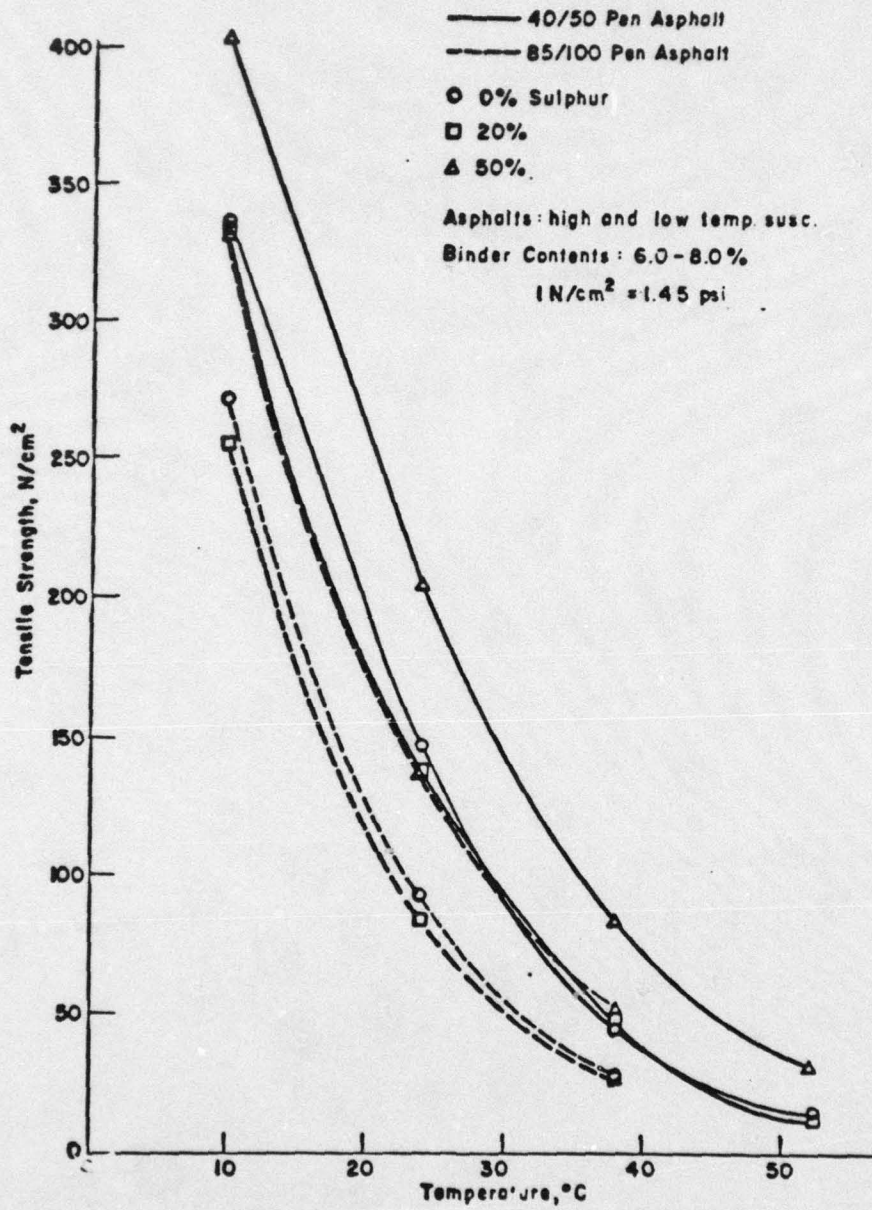


Figure 1.4. RELATIONSHIPS BETWEEN TENSILE STRENGTH AND TEMPERATURES [8]

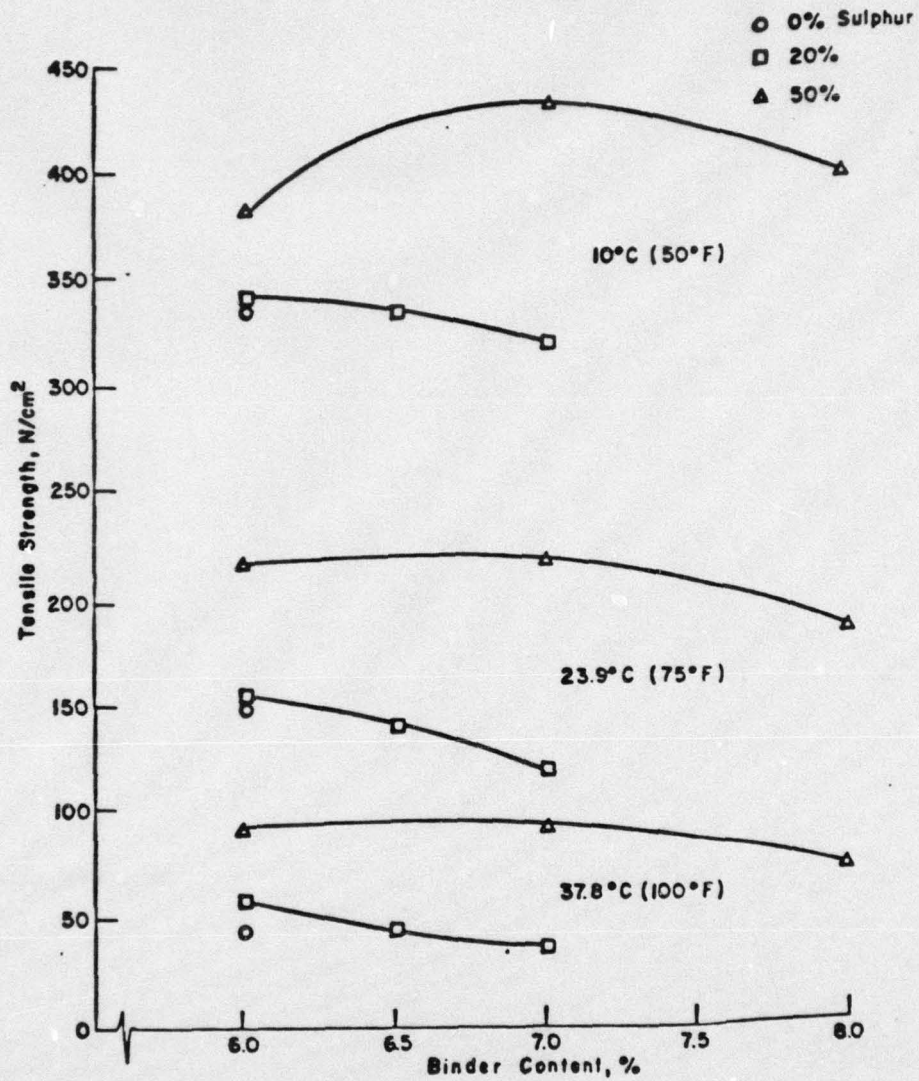


Figure 1.5. RELATIONSHIP BETWEEN TENSILE STRENGTH AND BINDER CONTENT FOR SULFUR-ASPALT MIXTURES WITH 40/50 PEN ASPHALT [8]

The following conclusions can be drawn upon examination of Figures 1.3 and 1.4:

1. As the asphalt cement (AC) penetration ratio increases, tensile strength increases.
2. As the S/A ratio increases over 20 per cent and up to 50 per cent, tensile strength increases.
3. As temperature decreases, strength increases.
4. The effect of adding 50 per cent sulfur to 85/100 penetration asphalt is the same as decreasing penetration to 40/50.

The resilient modulus/stiffness of S/A mixes was generally higher than that of conventional asphalt mixtures. The stiffness was dependent upon the S/A ratios, penetration value of the asphalt cement and the test temperature (see Figures 1.6 and 1.7). Just as with tensile strength, resilient modulus was only slightly dependent upon binder content (see Figure 1.8). Consistent with tensile strength, little variation in stiffness was noted up to 20 per cent sulfur, but significant changes in stiffness were noted up to 50 per cent sulfur.

Fatigue life was most dependent upon S/A ratios, penetration of asphalt cement and test temperature. As was the case with tensile strength and resilient modulus, binder content had little effect upon fatigue life.

The following conclusions were reached with respect to fatigue life:

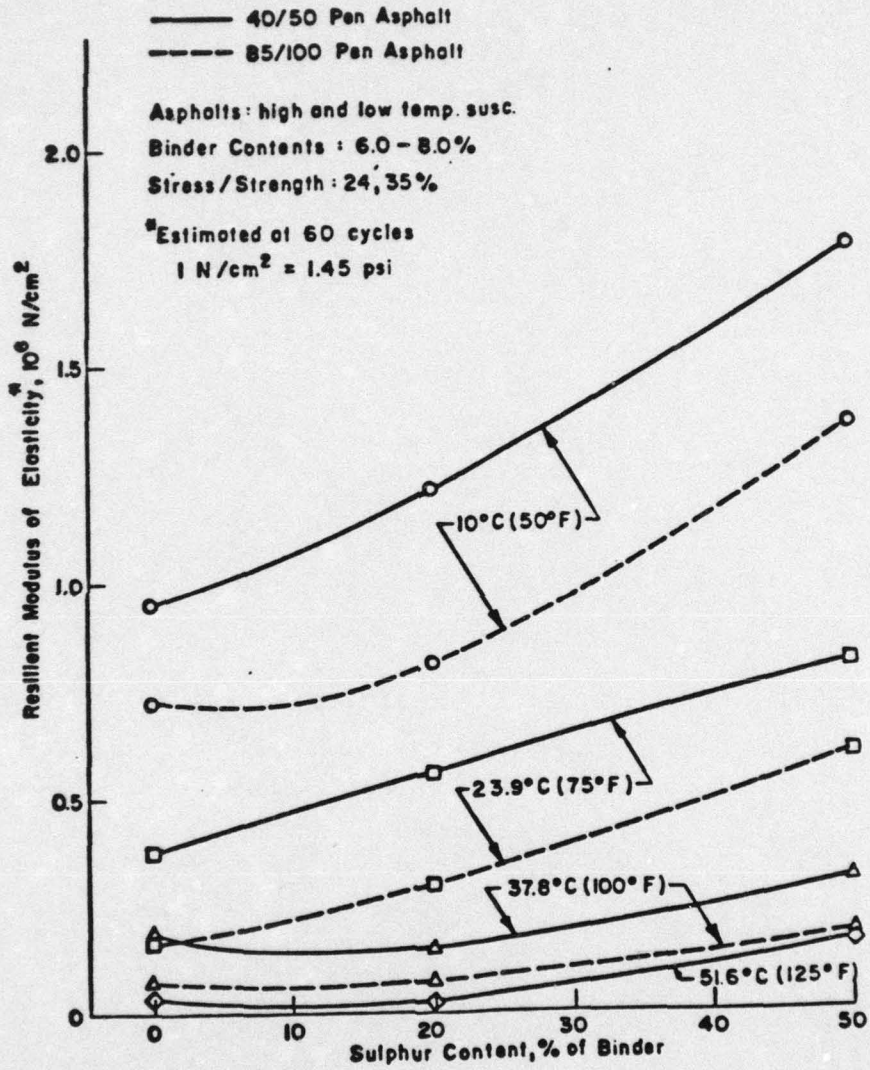


Figure 1.6. RELATIONSHIPS BETWEEN RESILIENT MODULUS AND SULFUR CONTENT [8]

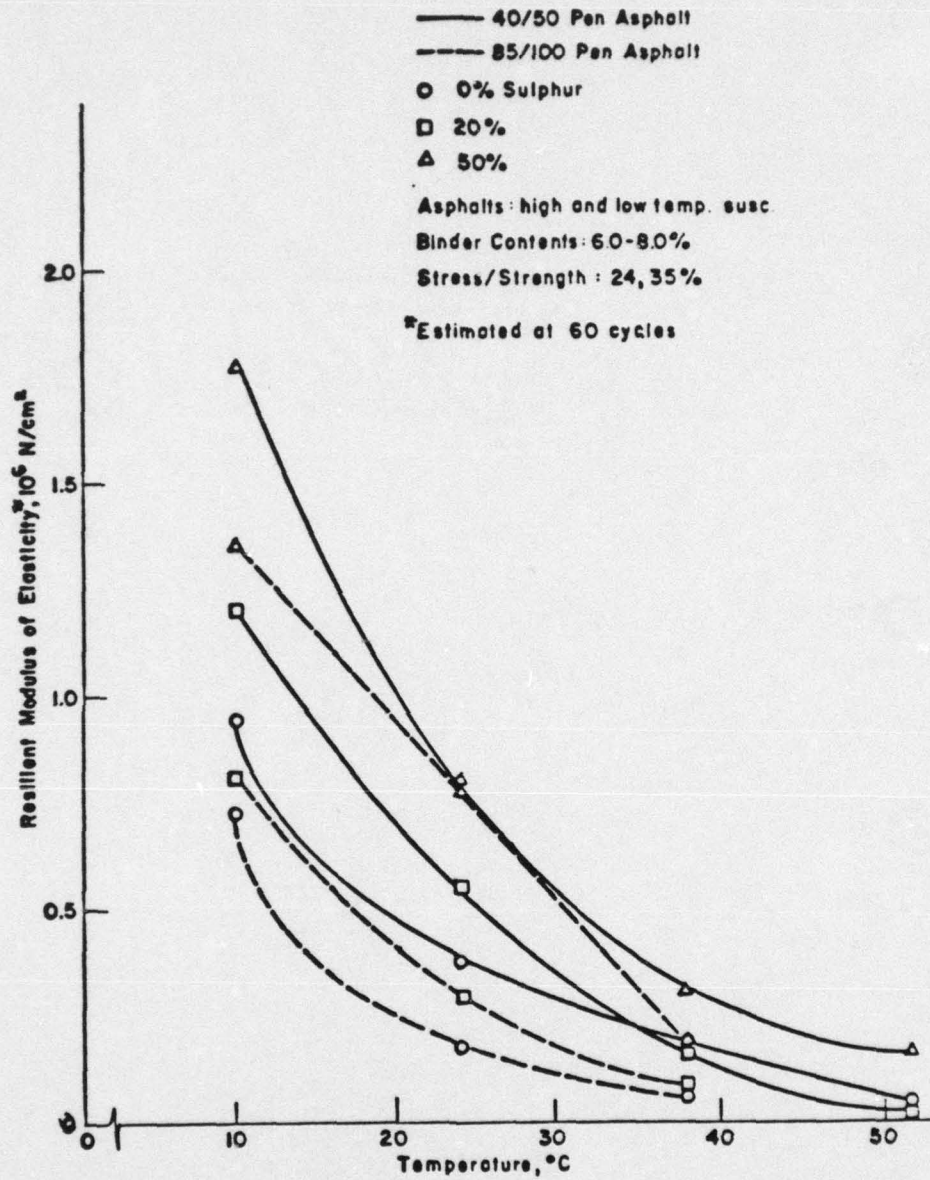


Figure 1.7. RELATIONSHIPS BETWEEN RESILIENT MODULUS OF ELASTICITY AND TEMPERATURE FOR SULFUR-ASPHALT MIXTURES [8]

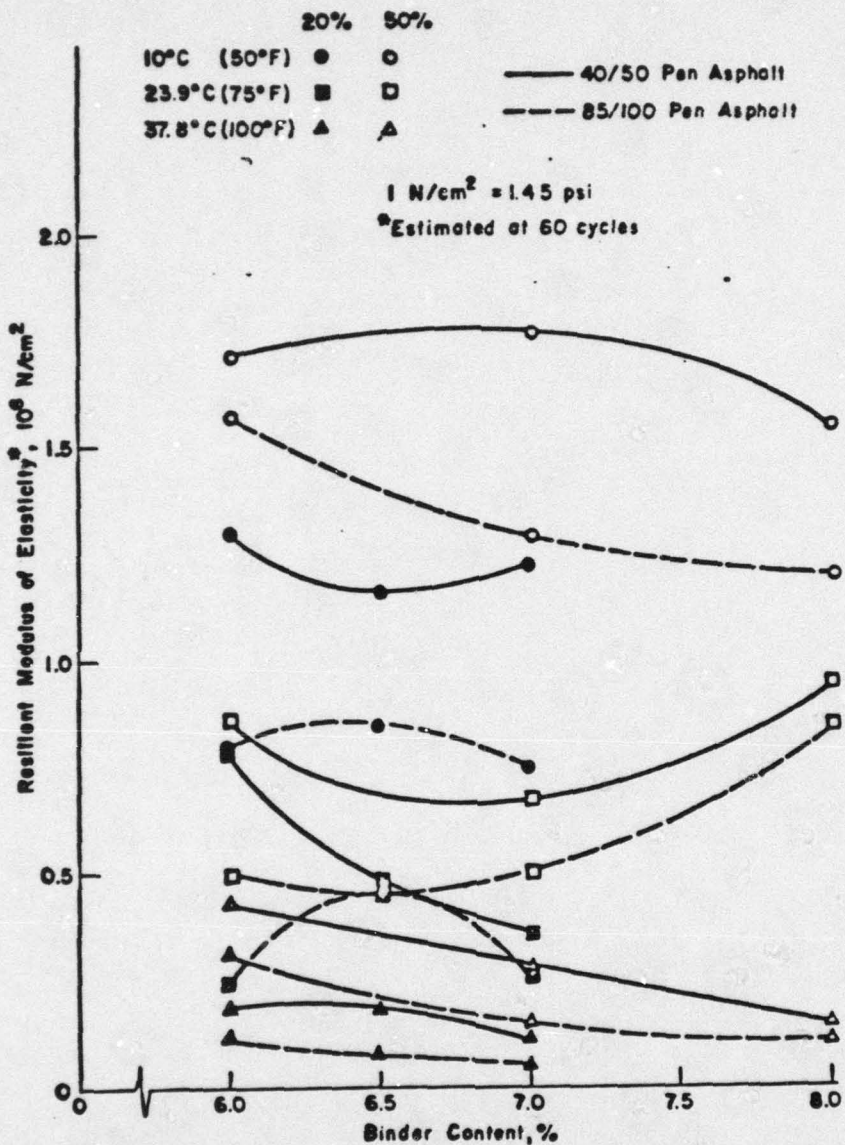


Figure 1.8. RELATIONSHIPS BETWEEN RESILIENT MODULUS OF ELASTICITY AND BINDER CONTENT FOR SULFUR- ASPHALT MIXTURES [7]

1. The optimum binder content for maximum fatigue life is higher than the optimum for maximum strength.
2. As the S/A ratio increases over 20 per cent and up to 50 per cent, fatigue life increases.
3. Fatigue life increases with a decrease in AC penetration.
4. Fatigue life increases with a decrease in temperature.

The Gulf Oil Canada Limited sulfur asphalt system concludes that S/A binders have slightly superior engineering properties than conventional asphalt binders, but the real advantage is in the economic savings realized from the partial replacement of asphalt. The research done for Gulf by Austin Research Engineers of Texas indicated that the most significant improvement of S/A mixtures over conventional mixtures was observed with the addition of 50 per cent sulfur.

The Societe National Elf-Aquitaine (SNEA) Sulfur Asphalt System

In the SNEA process liquid sulfur is dispersed in molten asphalt to produce sulfur-asphalt binder. The advantages of this technique are (1) that up to 30 per cent of the asphalt by weight can be replaced by sulfur, while the absolute binder content is held constant; (2) there is an energy savings in the preparation and compaction of the S/A mixture; and (3) because of improved engineering properties of the mixture due to the sulfur utilization, poorer quality aggregates or thinner pavements can be utilized while still maintaining the same performance characteristics as a conventional asphaltic concrete pavement.

This process is patented and many aspects of the system are not readily available. Liquid sulfur is dispersed into molten asphalt at 240°F (120°C) resulting in very fine sulfur particles (less than 5 μ). An undisclosed special stabilizing agent is introduced into the binder 10 hours after the dispersion of liquid sulfur.

The results of the SNEA study are as follows:

1. S/A mixtures prepared by the SNEA method can be utilized in pavements for maintenance and new construction.
2. When using similar aggregates, up to 30 per cent of asphalt can be replaced by sulfur.
3. S/A mixtures can be produced and paved using conventional equipment with only minor modifications.
4. S/A mixtures are prepared at lower temperature (30°C lower) than conventional mixtures with resultant energy savings.
5. The use of S/A binders allows utilization of low quality aggregates which would not normally be acceptable for conventional asphalt concrete.
6. S/A mixtures permit thinner pavement for a given set of environmental and load conditions.

The Pronk Sulfur- Asphalt System

This process was developed by Frank E. Pronk with the support of the Sulfur Development Institute of Canada (SUDIC). Work began in 1973. The process is very similar to the Gulf Oil Canada Limited

process, with the exception that Pronk adds a small amount (approximately .001 per cent) of organosiloxane polymers as a stabilizer. The S/A ratio of a typical mixture is 30-40 per cent by weight, with a mixing temperature of 130-150°C. Though the mixture can be prepared by direct combination of the ingredients in the plant pugmill, SUDIC recommends that the sulfur asphalt and stabilizing agent be emulsified by use of an in-line mixing blender prior to their coming in contact with the aggregate.

Pronk illustrated the stabilizing effect of this particular polymeric organosiloxane with two identical emulsions of sulfur and asphalt prepared at 137°C, the only difference between the two emulsions being the addition of the stabilizing agent to one. The samples were stored at 130°C and gently agitated with a propellor-type stirrer [11]. The emulsions were sampled periodically over a 72-hour period and the specific gravity at the top was compared to the specific gravity at the bottom of each sample. The results are shown in Table 1.5. Table 1.4 gives specific gravities for given S/A ratios [9, 10] with uniform dispersion of sulfur and asphalt.

The particular class of polymeric organosiloxanes favored by Pronk has previously been used in conventional asphaltic hot mixes primarily to eliminate foaming in the presence of moisture and to alleviate tearing problems encountered when placing certain types of hot mixes [9, 10]. The tearing problem was attributed to the presence of moisture and/or air bubbles at the mix surface [5]. The

Table 1.4. SPECIFIC GRAVITY OF SULFUR-ASPHALT BINDERS (From: Kennepohl, 1975 [7].)

Sample Description	Composition, % wt.								
	100	90 10	80 20	70 30	60 40	55 45	50 50	40 60	100
Blend of 85/100 per Asphalt Elemental Sulphur									
Gravity, Specific 60°F (16°C)	1.0268	1.0552	1.1200	1.1828	1.2320	1.2854	1.3442	1.4337	1.9556

Table 1.5. EMULSION STABILITY (From: Pronk et al., 1975 [39])

Sample*	½h		5h		24h		48h		72h	
	Top	Bottom	Top	Bottom	Top	Bottom	Top	Bottom	Top	Bottom
X	1.19	1.18	1.05	1.80	1.04	1.75	1.05	1.62	1.05	1.23
Y	1.19	1.19	1.10	1.21	1.05	1.23	1.14	1.21	1.15	1.20

Relative Densities (g cm⁻³)

* X = S:A, 37.5:62.5 by wt. No additive.

Y = S:A, 37.5:62.5 by wt. + additive.

NOTE: Specific gravity of 37.5:62.5 emulsion is 1.19.

siloxane improves the placement characteristics through two possible effects, suppression of bubble formation and screed lubrication.

There is some evidence that the stabilizing agent tends to reduce the amount of hydrogen sulfide emitted during production. Table 1.6 shows typical air emission data for a Pronk sulfur asphalt trial.

The U.S. Bureau of Mines Sulfur-Asphalt System

The U.S. Bureau of Mines study of utilization of elemental sulfur in asphaltic mixtures was oriented toward development of a simplified procedure for preparing and utilizing the sulfur-asphalt binder. In an effort to utilize sulfur as an extender for asphalt, the U.S. Bureau of Mines' scientists, headed by McBee and Sullivan, directed their studies toward the direct combination of sulfur and asphalt within the mixer without premixing them as required in the Gulf, Pronk and SNEA processes.

McBee and Sullivan, in their extensive studies of the French and Canadians' sulfur-asphalt emulsions, were unable to discern any appreciable differences between the emulsified and the non-emulsified SEA binders. Based upon their laboratory data and the fact that sulfur is highly soluble (20 per cent or more) in most grades of asphalt at the commonly acceptable mixing temperature of 248°F (120°C) to 302°F (150°C) and the high shear energy developed in mixing the binder and aggregates, McBee and Sullivan concluded that hot-mix plant pugmills could be used as the principal mixing

Table 1.6

TYPICAL AIR EMISSION DATA FOR A PRONK SULFUR ASPHALT TRIAL [11]

	Plant	Paving Site	
		A	B
Particulate sulfur, mg/m ³	.7	.3	.2
	1.5		.7
	9.6		
	3.0		
	.4		
H ₂ S, μg/m ³ *	455	925	75
	2125	10	530
	30	610	135
	10	650	610
SO ₂ , μg/m ³ *	430	200	60
	170	260	370
	115	230	170
	115	340	170
	115		

*Note: data are not corrected for temperature and pressure.

mechanism for sulfur and asphalt.

A test program to determine the effectiveness of substituting sulfur for asphalt in pavement mixes and the results of these tests were compared to those of conventional paving mixtures.

Field testing was done first with small patch tests and then by constructing a full scale road test on a section of U.S. Highway 93 near Boulder City, Nevada. The results of the laboratory and post-construction data of the field tests show that sulfur asphalt mixes prepared by the direct addition procedure were equivalent to conventional asphalt concrete in all respects of performance and superior with respect to ease and amount of required compaction.

Laboratory Analysis:

Two types of aggregate were utilized in McBee and Sullivan's laboratory analysis (limestone and volcanic). Marshall design properties were the primary evaluation tools, but a temperature sensitivity study and fatigue testing were also performed. Five different percentiles of asphaltic replacement by sulfur (15, 25, 35, 50, and 75 per cent) were examined.

Materials:

The sulfur used was a commercial grade (99.9 per cent pure). The aggregates as previously mentioned were crushed limestone and volcanic rock, each further blended with 25 per cent by weight construction sand and 15 per cent by weight desert sand to meet Type 2 State of Nevada gradation specifications (see Figure 1.9).

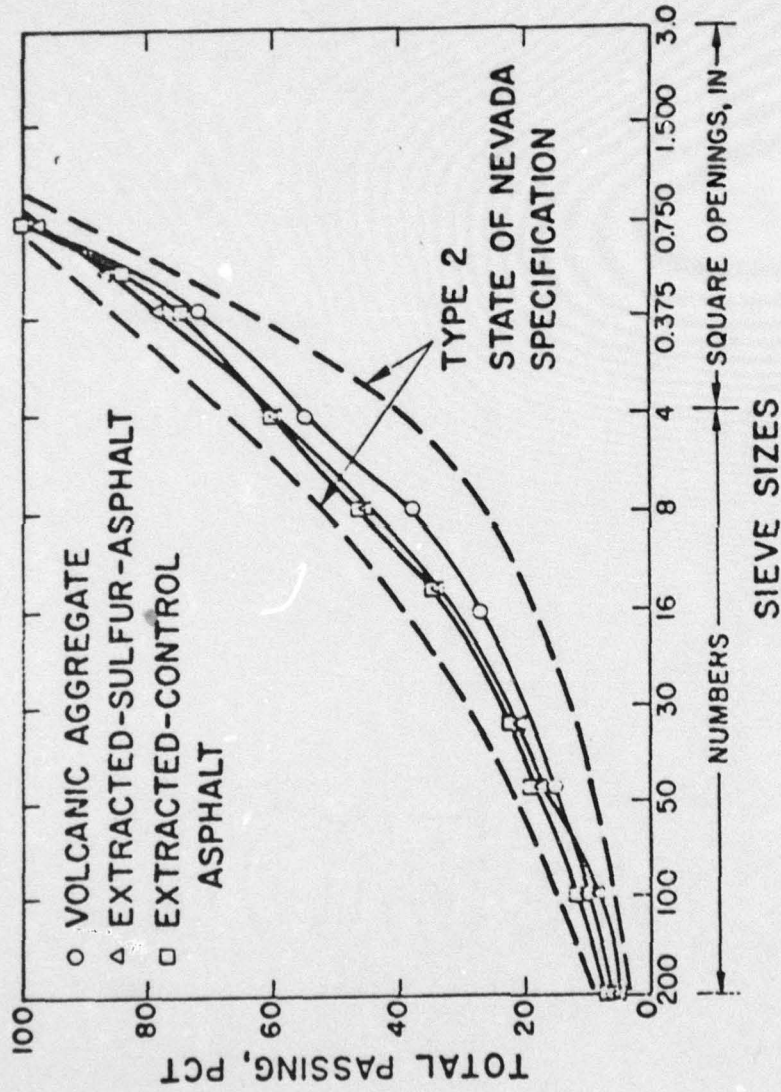


Figure 1.9. SIZE GRADATION FOR AGGREGATE MATERIALS [40]

Results of Laboratory Analysis:

Laboratory tests based upon Marshall properties indicated that the optimum asphalt binder contents were 5.7 and 7.0 per cent by weight for the limestone and volcanic aggregates, respectively. Table 1.7 shows the properties of the different aforementioned sulfur -asphalt ratios. This table shows increasing stability and increasing dynamic stiffness with increasing percentage of sulfur in the binder. Figure 1.10 shows the viscosity versus temperature and indicates a reduction of viscosity with the addition of sulfur up to 35 per cent by volume. This lowering of viscosity increases the efficiency of mixing and the placement of the mixtures. The researchers concluded that the decrease in viscosity further substantiates their conclusion that the sulfur and asphalt could be added directly to the aggregate without premixing.

Scanning electronic microscopic analysis of the mixes showed that the sulfur and asphalt constituents of the binders were uniformly distributed. Microscopic analysis further showed that no large concentrations of sulfur occurred between aggregate particles and the binder. This indicated that the sulfur was either initially dissolved or evenly dispersed in the binder and remained so during and after crystallization of the sulfur.

Fatigue analysis was conducted by the Texas Transportation Institute, Texas A & M University, utilizing both aggregate types. Third point flexural fatigue tests were conducted at five constant stress amplitudes. The results are shown in Figures 1.11 and 1.12.

Table 1.7. MARSHALL DESIGN DATA COMPARISON

Composition ¹		Asphalt		Specific Gravity	Voids pct	Marshall		Dynamic ² Stiffness psi x 10 ⁶
Sulphur Vol- pct	Wt- pct	Vol- pct	Wt- pct			Stability, lb	Flow, 0.01 in	
Limestone Aggregate								
0	0	100	5.7	2.411	2.3	2,140	10	0.599
15	1.8	85	5.1	2.427	1.8	2,325	10	1.466
25	2.9	75	4.5	2.425	2.5	2,530	10	1.639
35	4.1	65	3.9	2.423	3.2	3,750	8	2.364
50	5.8	50	2.9	2.437	3.5	7,350	8	---
75	8.6	25	1.5	2.433	4.9	10,615	8	---
Volcanic Aggregate								
0	0	100	7.0	2.288	2.4	2,580	12	0.653
15	2.0	85	5.9	2.300	2.8	2,230	10	0.980
25	3.4	75	5.2	2.307	3.2	3,085	11	1.542
35	4.7	65	4.4	2.321	3.2	5,520	10	2.040
50	6.7	50	3.4	2.320	4.4	9,605	12	---
75	9.9	25	1.7	2.343	4.9	9,910	6	---

¹Vol- pct refers to the volume percent in the binder

²Wt- pct refers to the weight-percent of the total mix

³Determined using the Schmidt method [41] at ambient temperature [40]

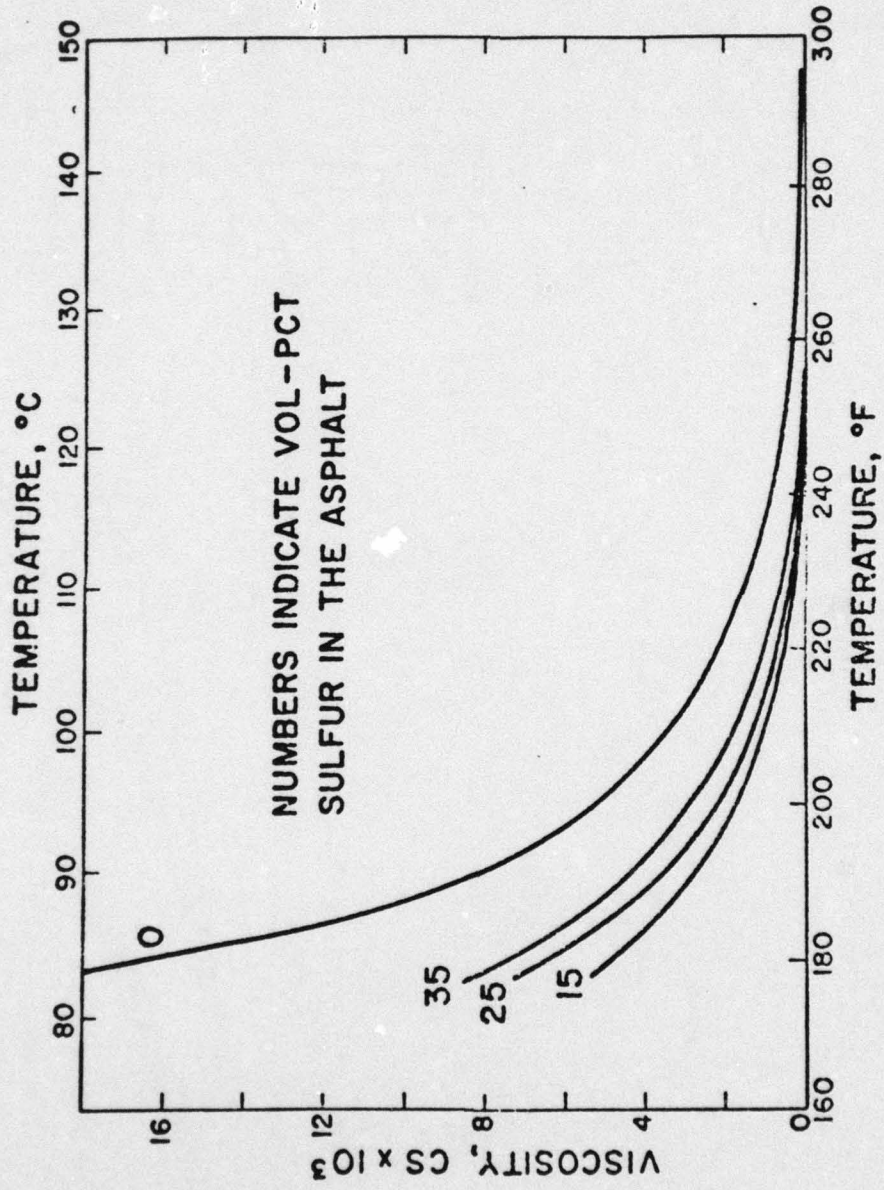


Figure 1.10. VISCOSITY OF SULFUR-ASPHALT BINDER VERSUS TEMPERATURE [40]

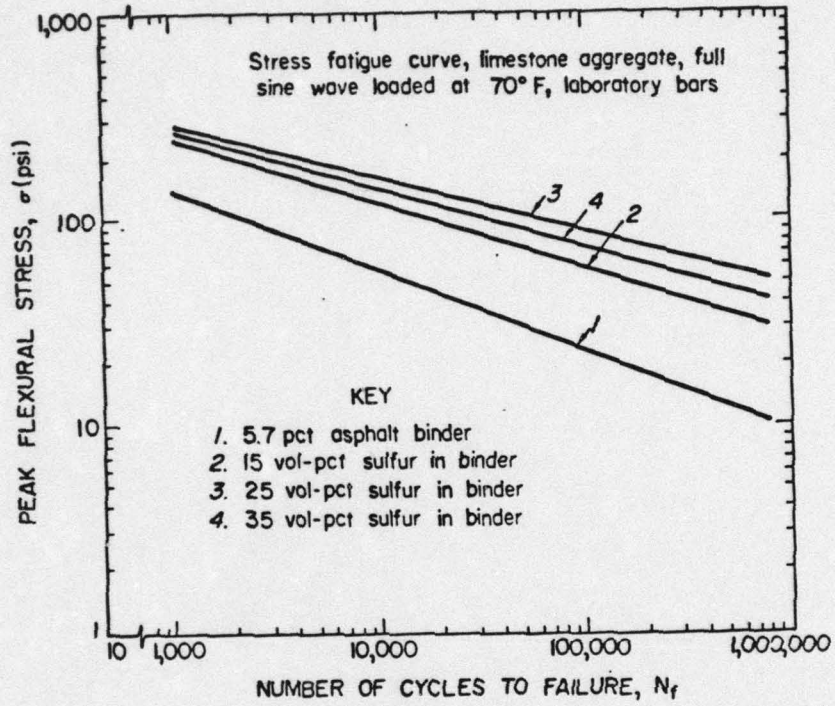


Figure 1.11. STRESS FATIGUE CURVE, LIMESTONE AGGREGATE [40]

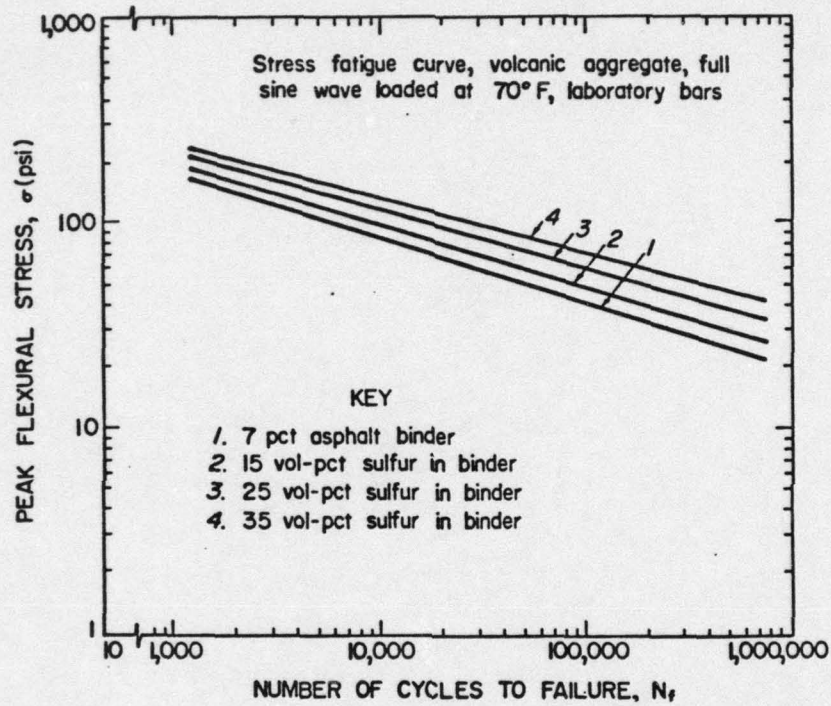


Figure 1.12. STRESS FATIGUE CURVE, VOLCANIC AGGREGATE [40]

Examination of these curves shows that the fatigue life of these beams is a function of the sulfur content. Conventional asphalt mixes showed a fatigue life of one million cycles at 10-20 psi constant stress, while the sulfur asphalt mixes showed the same fatigue life but required a 30-40 psi constant stress. These results indicate that the performance characteristics of conventional asphalt concrete can be improved with the addition of sulfur, which will result in more durable pavements and even possibly thinner pavement requirements for a given expected loading.

Conclusions:

The Bureau of Mines concluded that there are no advantages to be gained by the premixing of sulfur and asphalt; in fact, it is probably more energy cost-effective not to do so. The Bureau of Mines laboratory results indicate that the material properties resulting from direct addition are compatible with those resulting from the Gulf, Pronk and SNEA procedures.

CHAPTER II

CURRENT U.S. FIELD TESTS

Introduction

As can be imagined, vast amounts of laboratory data have been generated by various research organizations. The laboratory work has indicated that sulfur asphalt concretes perform as well as or better than conventional pavements [7, 12, 13, 15, 16, 17, 18, 19]. In conjunction with this laboratory research, numerous field tests have been conducted in Canada, Europe, the Middle East and the United States. Table 2.1 is a summary of the known field trials to date.

The two field trials that are the most applicable to the University of Washington's (UW) study of repetitive wheel load testing at the Washington State University's (WSU) test track are the two-lane test section on U.S. 69 in Angelina County, Texas (hereafter referred to as the LUFKIN TEST) and the test section constructed by the Nevada Highway Department at the junction of U.S. Highways 93 and 95 near Boulder City, Nevada (hereafter referred to as the BOULDER CITY TEST).

Lufkin Field Trial

Layout

This project was constructed during September, 1975, through the efforts of the State Department of Highways and Public Transportation, the Federal Highway Administration, SNEA, the U.S. Bureau of Mines, Texas Gulf, Inc. and Moore Brothers Construction Company [20].

Table 2.1. SURVEY OF SULFUR-ASPHALT FIELD TRIALS [19]

Location	Length, Miles	Type of Test	Year	Process
U.S.A.				
Texas	0.6	Full Depth	1975	SNEA
Texas	0.6	Full Depth	1977	Shell
Texas	0.5	Full Depth	1978	SNEA
Nevada	0.4	Base, Surfacing, Full Depth	1977	U.S. Bureau of Mines
Michigan	1.0	Resurfacing	1977	Gulf
Louisiana	0.3	Full Depth	1977	Shell
Canada				
Alberta	0.4	Full Depth	1974	Gulf
Alberta	1.0	Resurfacing	1974	Gulf
Alberta	1.3	Full Depth	1977	Gulf
Ontario	4.0	Full Depth	1975	Gulf
Ontario	2.0	Full Depth	1977	Gulf
Ontario	0.8	Resurfacing	1964	Shell
Ontario	1.0	Full Depth	1972	Shell
British Columbia	0.2	Full Depth	1970	Shell
Quebec	0.2	Full Depth	1972	Shell

Table 2.1 (continued)

Location	Length, miles	Type of Test	Year	Process
Europe				
France	0.6	Full Depth	1973	SNEA
France	3.3	Resurfacing and Full Depth	1974	SNEA
France	3.7	Resurfacing	1975	SNEA
France	8.3	Resurfacing	1976	SNEA
France	3.0	Resurfacing	1976	SNEA
France	2.0	Full Depth	1977	SNEA
Spain	1.8	Resurfacing	1976	SNEA
Finland	1.5	Resurfacing	1976	SNEA
Belgium	1.5	Full Depth	1977	SNEA
Middle East				
Iraq	0.6	Full Depth	1977	SNEA
Iraq	0.6	Full Depth	1977	SNEA
Kuwait	1.0	Full Depth	1977	SNEA

1 mile = 1.6 km

This 1113-meter test section was divided into ten subsections which were composed of various conventional and experimental SEA mixtures (see Figure 2.1, a schematic of the test sections). There were two depths of base course utilized. The 7-inch (178 mm) bases were designed to accommodate traffic in accordance with state highway specifications. The 5-inch (127 mm) bases were intentionally under-designed to induce early failure.

Materials

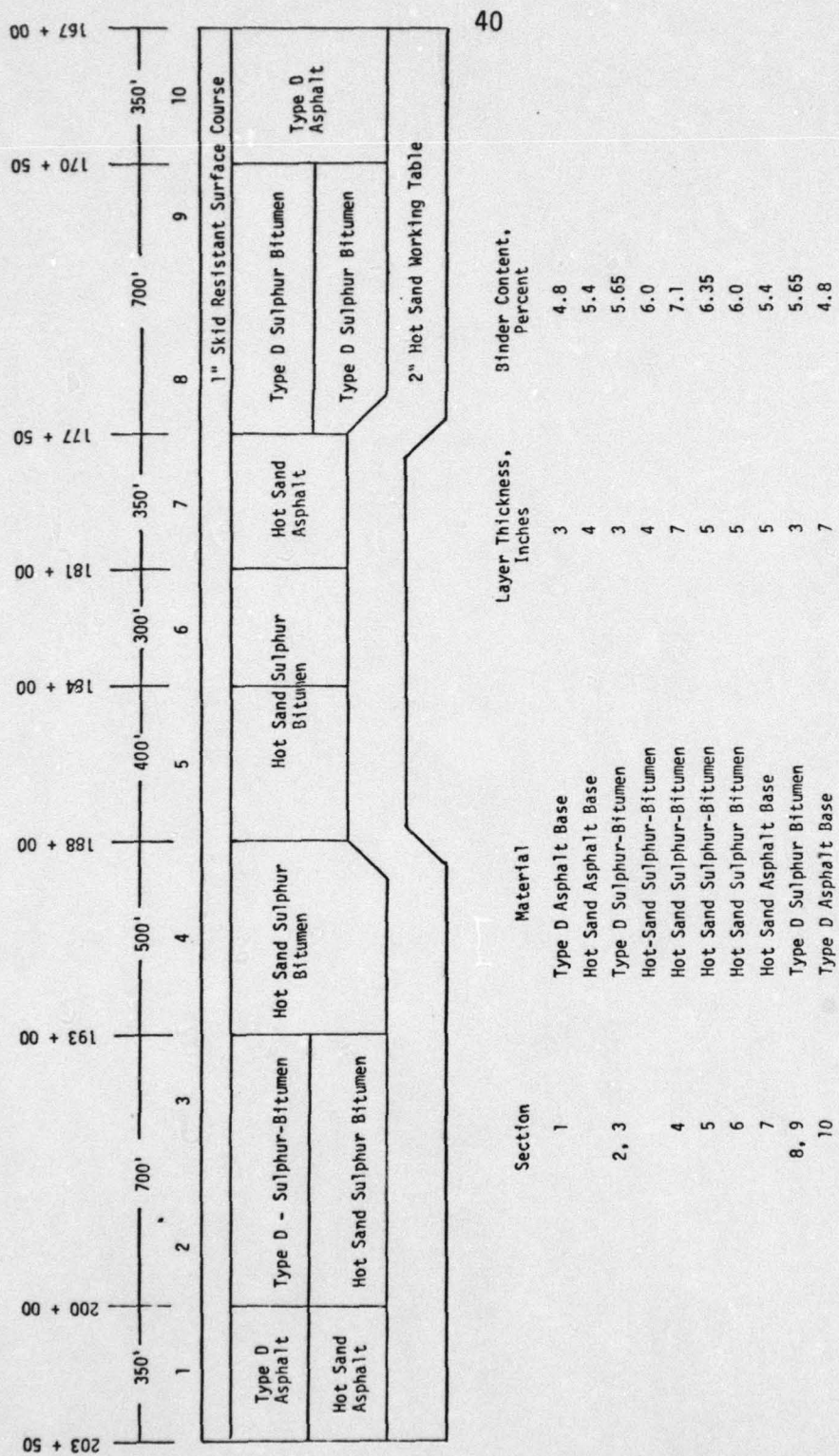
The sulfur-asphalt mixtures were prepared with a 30/70 sulfur-asphalt emulsion prepared from industrial sulfur and Texaco AC-20 asphalt. The binder contents of the SEA mixtures varied between 5.3 and 7.1 per cent by weight.

The conventional sections also consisted of mixes prepared with Texaco AC-20. The binder content for the conventional sections varied between 4.5 and 6.0 per cent by weight.

The aggregate used in both conventional and SEA mixes was a blend of pea gravel and Lufkin area dune sand. The gradation of these aggregates is given in Figure 2.2 [20].

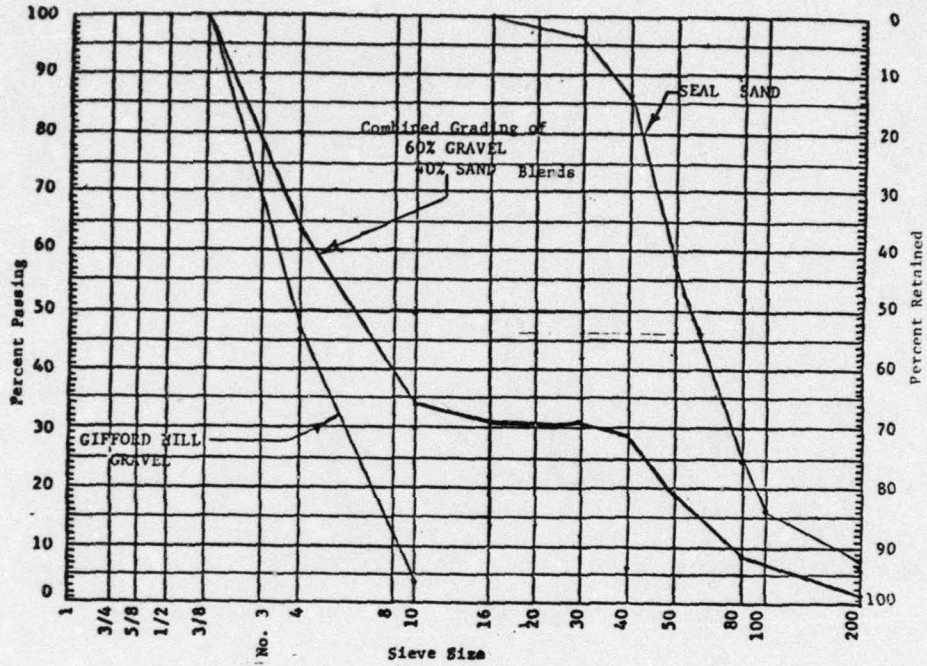
Equipment and Methods

The field test section was located approximately 15 miles from the hot mix plant. The sulfur-asphalt emulsions were prepared in a colloid mill furnished by SNEA and is illustrated in Figure 2.3 [20].



1 ft. = 0.3 m
 1 in. = 25.4 mm

Figure 2.1. LAYOUT OF SNPA SULFUR BITUMEN BINDER PAVEMENT TEST - U.S. HIGHWAY 69, LUFKIN, TEXAS [20]



Specific Gravity of:

Gifford-Hill Gravel

Retained on No. 4 sieve: 2.556
 Passing on No. 4 sieve: 2.564

Combined: 2.560

Seal Sand

Retained on No. 80 sieve: 2.533
 Passing on No. 80 sieve: 2.582

Combined: 2.560

Figure 2.2. AGGREGATE GRADATIONS FOR LUFKIN FIELD TRIALS [19]

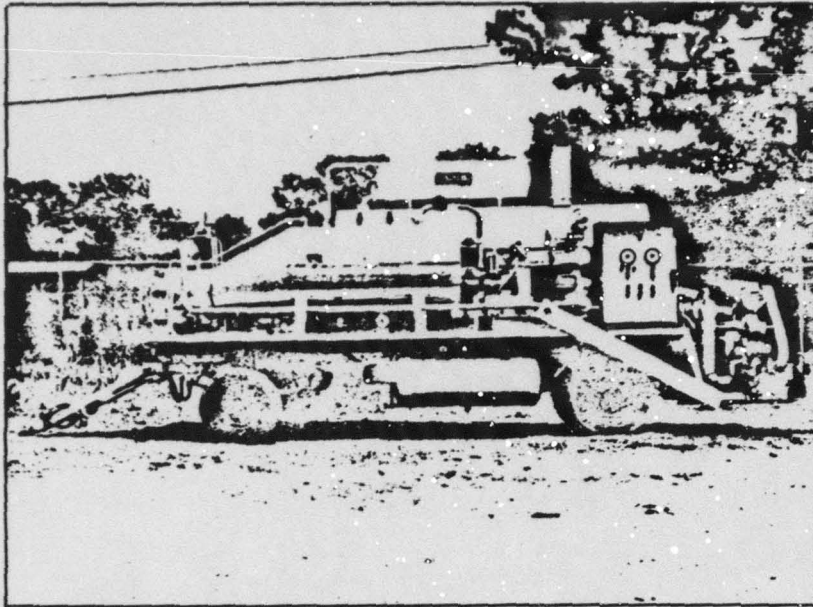


Figure 2.3. COLLOID MILL FURNISHED BY SNPA
FOR PREPARATION OF SULFUR-
ASPHALT EMULSIONS [20]

A schematic of the SEA production operation is shown in Figure 2.4 [20].

A 2-inch (9 cm) "Hot-Sand" working platform consisting of a SAS mixture was placed over a 6-inch (15.2 cm) lime-stabilized subgrade prior to paving with the various SEA and conventional mixes [19, 20]. The aggregate for the working platform was dune sand obtained from a Seal Pit in the Lufkin area (see Figure 2.2 for gradation). The working platform was laid without compaction other than that provided by the screed from the Barber-Green Series 100 paver. This paver was used for paving both the working platform and the other test section layers.

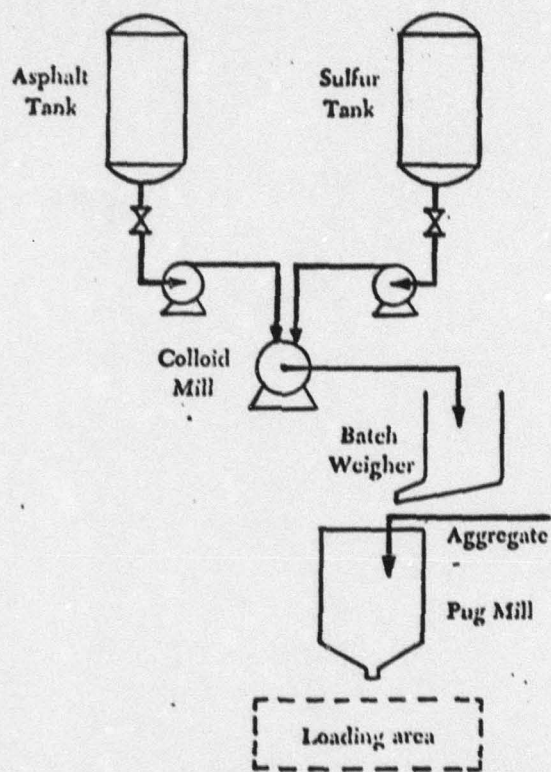


Figure 2.4. SCHEMATIC DRAWING OF SULFUR-ASPHALT MIXING STATION

The actual test sections were compacted with a Hyster C-615A vibratory steel roller. The roller was used in the vibratory mode to achieve initial compaction and in the nonvibratory mode for final compaction.

Quality Control and Initial Testing

Initial test data indicated that S/A mixtures have Hveem stabilities 35 to 45 per cent higher than conventional asphalt mixes. The testing also indicated that the stability of pure asphalt mixtures decreased with increasing binder content and that the S/A mixtures' stabilities remained essentially constant with increasing binder content. This characteristic was applicable to both the SAS working platform and the base courses [19].

Data Analysis

Field cores were a primary means of data collection. During the Lufkin test, cores were taken initially after construction, 12 months after construction (6 months after opening to traffic) and at 6-month intervals thereafter until the 36th month after construction. The final set of cores was obtained 48 months after construction. The last data for the last cores are not available at this writing.

The Texas Transportation Institute at College Station, Texas tested these cores for various physical properties. These tests include maximum specific gravity, bulk specific gravity, Marshall stability and flow, Hveem stability, resilient modulus at 69°F (20°C), and indirect tensile strength at 68°F (20°C). For a discussion of

these tests, the reader is directed to reference number 19, Chapter IV.

It was noted that the bulk density generally increases with age. The assumed reason for this change is that the road traffic provided additional compaction after the placement of the material [19].

As the pavement ages the per cent of air voids decreases. This was to be expected because the bulk density of all of the mixtures was increasing with time. The 4.8 per cent SEA mixture shows a consistently higher percentage of air voids than the other two mixtures, 6 to 11 per cent. The 4.8 per cent AC mixture has a range of 5 to 10 per cent air voids. A range of 4 to 9 per cent air voids was noted for the SEA mixture [19].

Figure 2.5 shows that Hveem stabilities for all of the SEA and conventional mixtures increase with time and tend to level off at about 28 to 30 per cent. This was attributed to the stiffening of the binder and a reduction in air voids.

It appears that with time, the 4.8 per cent SEA mixture maintained a slightly lower Hveem stability level than the other two mixtures, 4.8 per cent AC and 5.65 per cent SEA. Summarizing Figure 2.5, we can say that:

1. The 4.8 per cent SEA levels off at approximately 27 per cent increase in Hveem stability.
2. The 4.8 per cent AC mixture has ranged between 21 to 32 per cent.

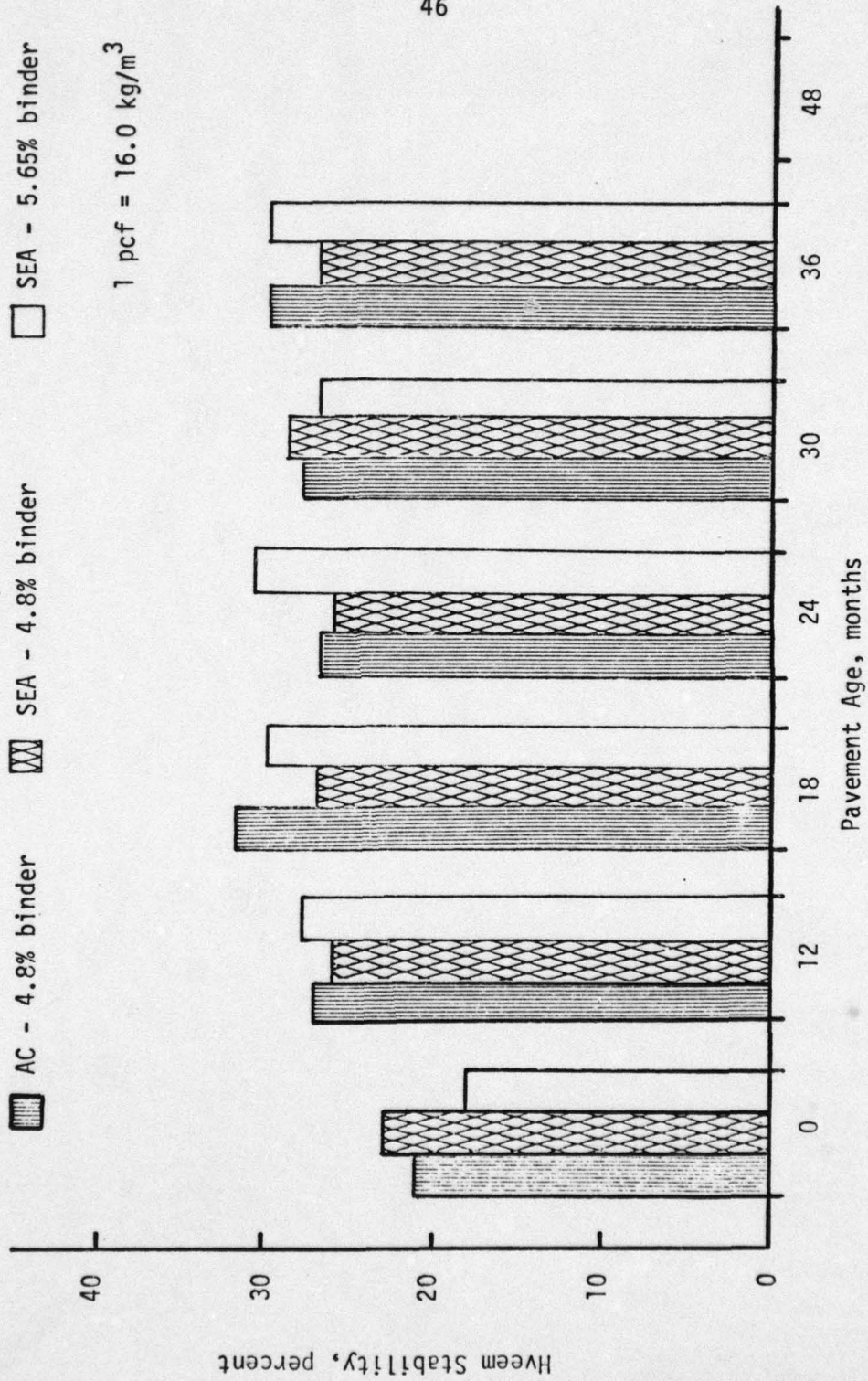


Figure 2.5. HVEEM STABILITY VERSUS PAVEMENT AGE FOR HMA MIXTURES, U.S. 69 [19]

3. The 5.65 per cent SEA mixture had a range of 18 to 31 per cent [19].

These values are about 10 per cent lower than the laboratory predicted results for SEA mixtures. The laboratory results had shown that for equivalent volumes of conventional and 30/70 SEA mixtures, the SEA mixtures would have a higher Hveem stability [21]. The 4.8 per cent by weight AC mixture and the 5.65 per cent by weight SEA mixture are of equal binder by volume. The difference in binder content by weight is due to the different specific gravity of sulfur in comparison to asphalt. After 36 months the 4.8 per cent AC and the 5.65 per cent SEA mixtures had approximately equivalent Hveem stabilities.

Figure 2.6 shows that the Marshall stability of the SEA and conventional mixes increases with the age of the paving material even though it is apparent that there is a high degree of data scatter. This increase of Marshall stability with age is indicated by:

1. The 4.8 per cent AC mixture levels out at 1190 lbs. (5360 N).
2. Even though the 4.8 per cent SEA mixture experiences the most severe scattering, when compared to the other two materials, it still has the lowest stability values. The last four test periods have an average Marshall stability of 850 lbs. (3830 N).

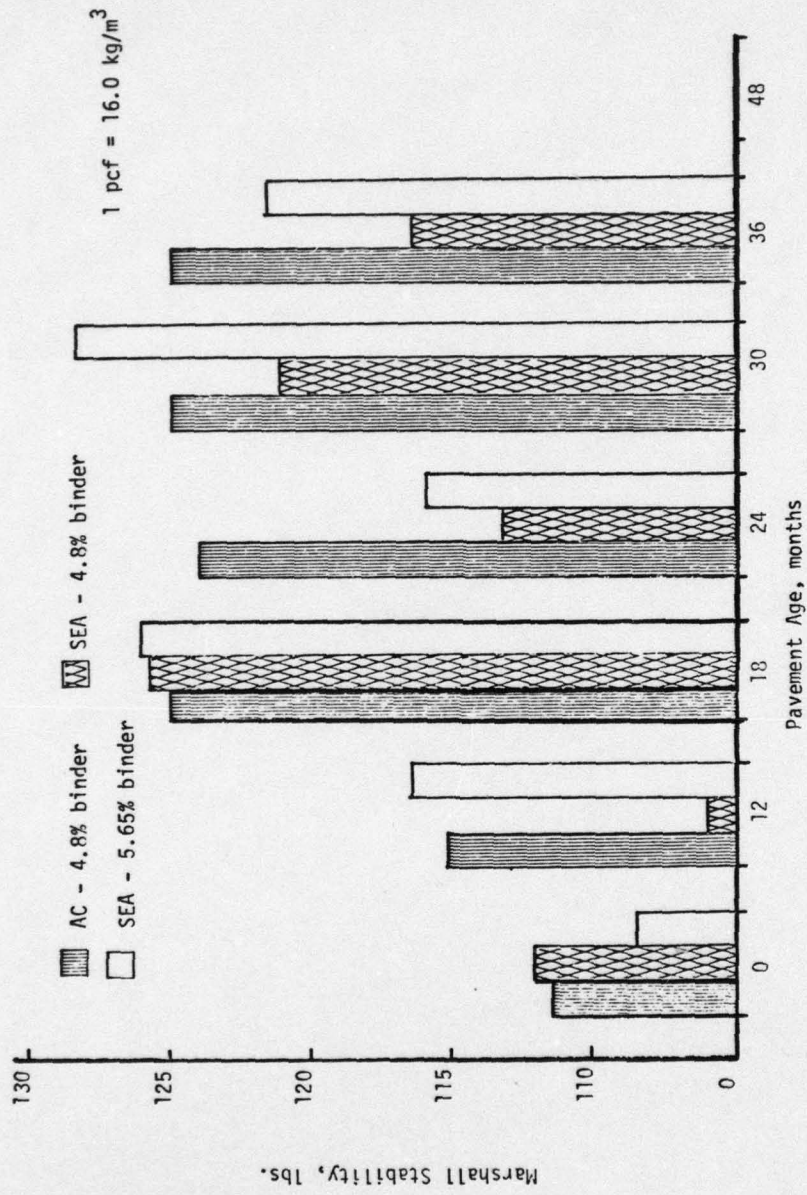


Figure 2.6. MARSHALL STABILITY VERSUS PAVEMENT AGE FOR HMAC MIXTURES, U.S. 69 [19]

3. The 5.65 per cent SEA material shows a general tendency to increase with age. The last four test periods have an average Marshall stability of 1080 lbs.

The Marshall flow of the conventional and S/A mixtures decreased as the materials stiffened with age. The flow values for all materials leveled off at around 14 (3.6 mm).

The splitting tensile strengths of all three mixtures increased with pavement age. As in the Marshall stability test, the 4.8 per cent SEA mixture seems to have the lowest strength of the three materials. A comparison of the three materials in relation to splitting tensile strength follows:

1. The 4.8 per cent SEA mixture appeared to have lowest splitting tensile strength, which was 30 psi (200 k Pa) initially and increased to 140 psi (1000 k Pa) after 36 months.
2. The 5.65 per cent SEA mixture had the next higher splitting tensile strength, nearly equal to that of the 4.8 per cent AC mixture, with a value of 30 psi (200 K Pa) initially and increasing to 170 psi (1170 k Pa) after 36 months.
3. The 4.8 per cent AC mixture had the highest splitting tensile strength. Initially the splitting tensile strength was 50 psi (350 k Pa) increasing to 180 psi (1240 k Pa).

Newcombe attributes the increase in splitting tensile strength to two factors. As with the Marshall stability, the increase in splitting tensile strength reflects a stiffening of the pavement material with time due to hardening of the binder and the added compaction due to traffic [19].

The resilient modulus of the three mixes increased with time, as illustrated by Figure 2.7. Newcombe questioned the validity of the 12-month data point for the 4.8 per cent SEA mixture, but had no explanation for it. There is no one mixture that showed a consistently higher resilient modulus than the other two. It must be noted that the resilient moduli were only examined at one temperature, 68°F.

Boulder City Field Test

Layout

This project was completed in January 1977 through the efforts of the Nevada Highway Department, the U.S. Bureau of Mines, the Federal Highway Administration, the Sulfur Institute and Frehner Construction Company. Previous trials with sulfur-extended asphalt had used high shear mixing equipment to preblend the sulfur and asphalt prior to mixing with the aggregates. This trial demonstrated a simplified SEA technology developed by the U.S. Bureau of Mines, wherein the sulfur and asphalt are added directly to the aggregate while in the pugmill.

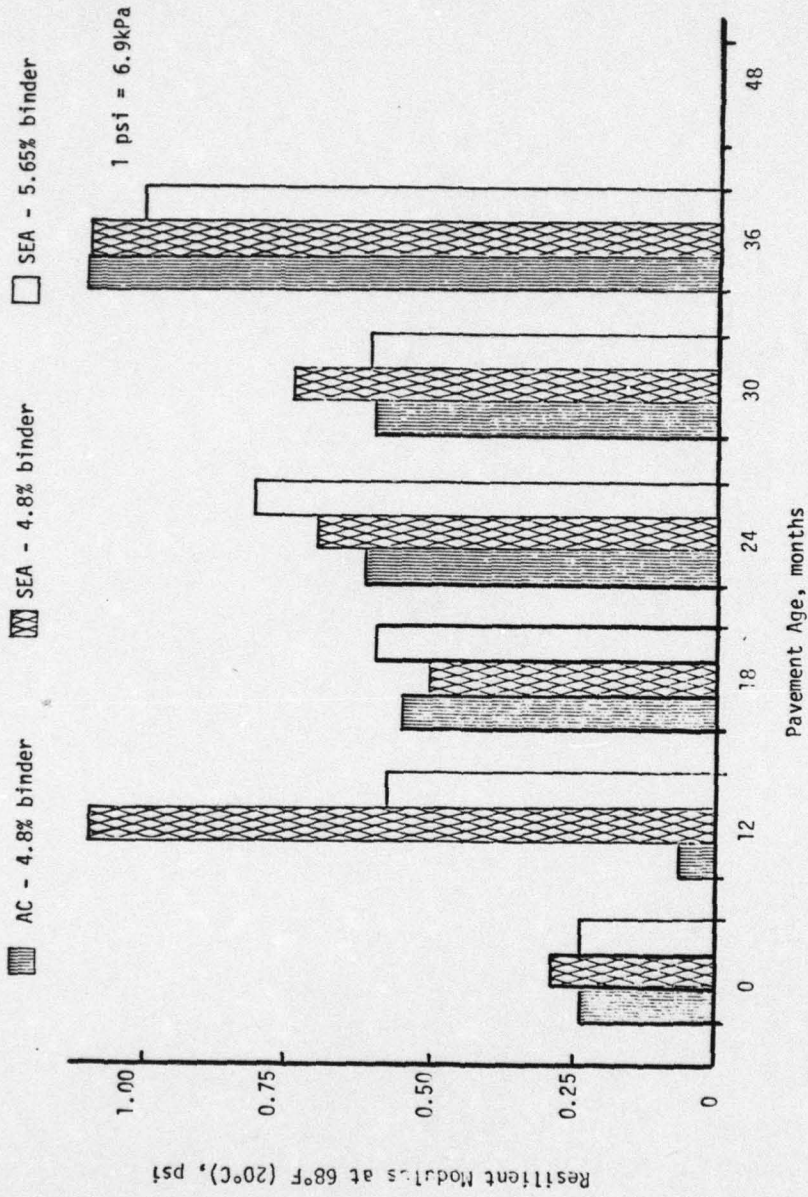


Figure 2.7. RESILIENT MODULUS AT 68°F (20°C) VERSUS PAVEMENT AGE FOR HMA MIXTURES, U.S. 69 [19]

Sulfur replaced about 30 per cent of the asphalt in the control sections. Approximately 1,000 tons (900×10^3 kg) of SEA paving mixture were prepared and used as base course, surface course and as full depth paving material for a total of 1,600 feet (488 meters) of 28-foot (8.5 meter) wide pavement. The trial is located at the junction of U.S. Highway 93 and 95 between engineering stations RI 0+00 and RI 21+00 on the W to E right traffic lanes.

The field trial was designed to test three different combinations of S/A and conventional mixes as illustrated in Figures 2.8 and 2.9. An open-graded function course was placed over the test and control sections to assist in skid resistance.

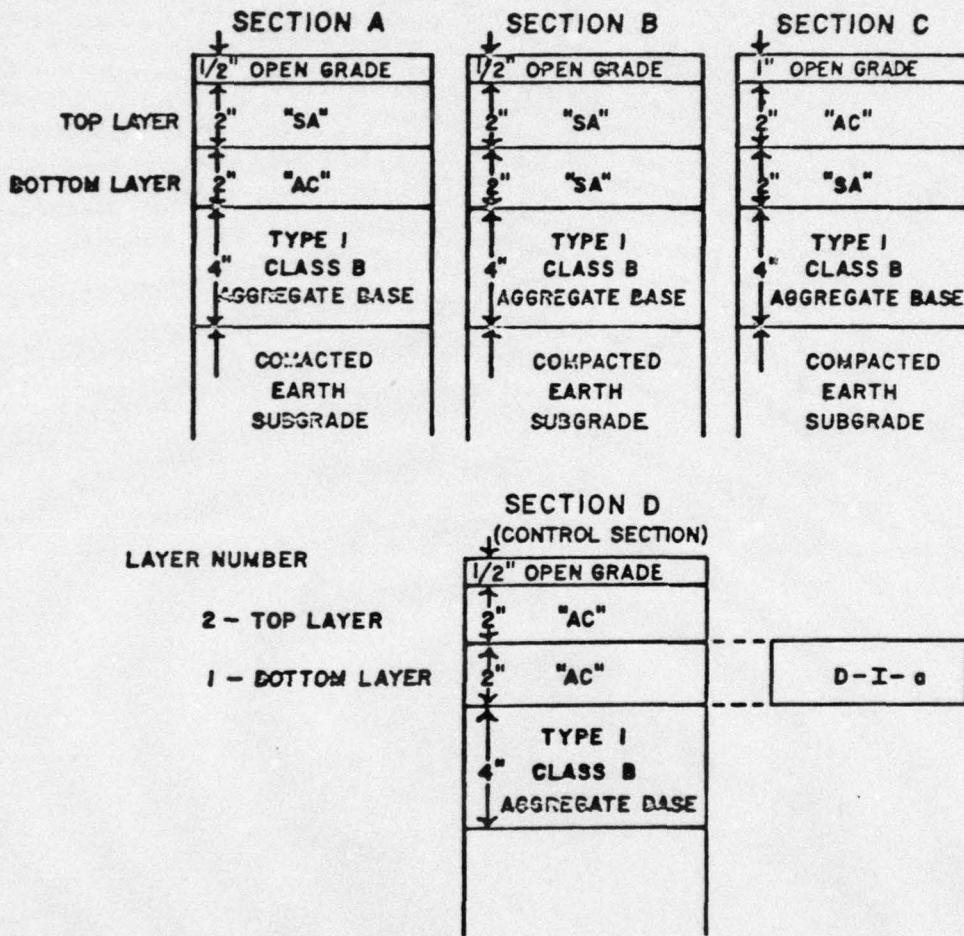
Materials

The control section and asphalt concrete sections were constructed with 6.3 per cent binder by weight. The SEA mixtures, on the other hand, consisted of 6.8 per cent by weight binder (1.8 per cent sulfur and 5.0 per cent asphalt for a S/A ratio of 26/74). The sulfur was more than 99.83 per cent pure by weight. The asphalt was AR-4000 (approximately equivalent to AC-20). AC-20 was also used in the Lufkin field test.

The aggregate gradation used in both the SEA and conventional mixes is shown in Figure 2.10 [22].

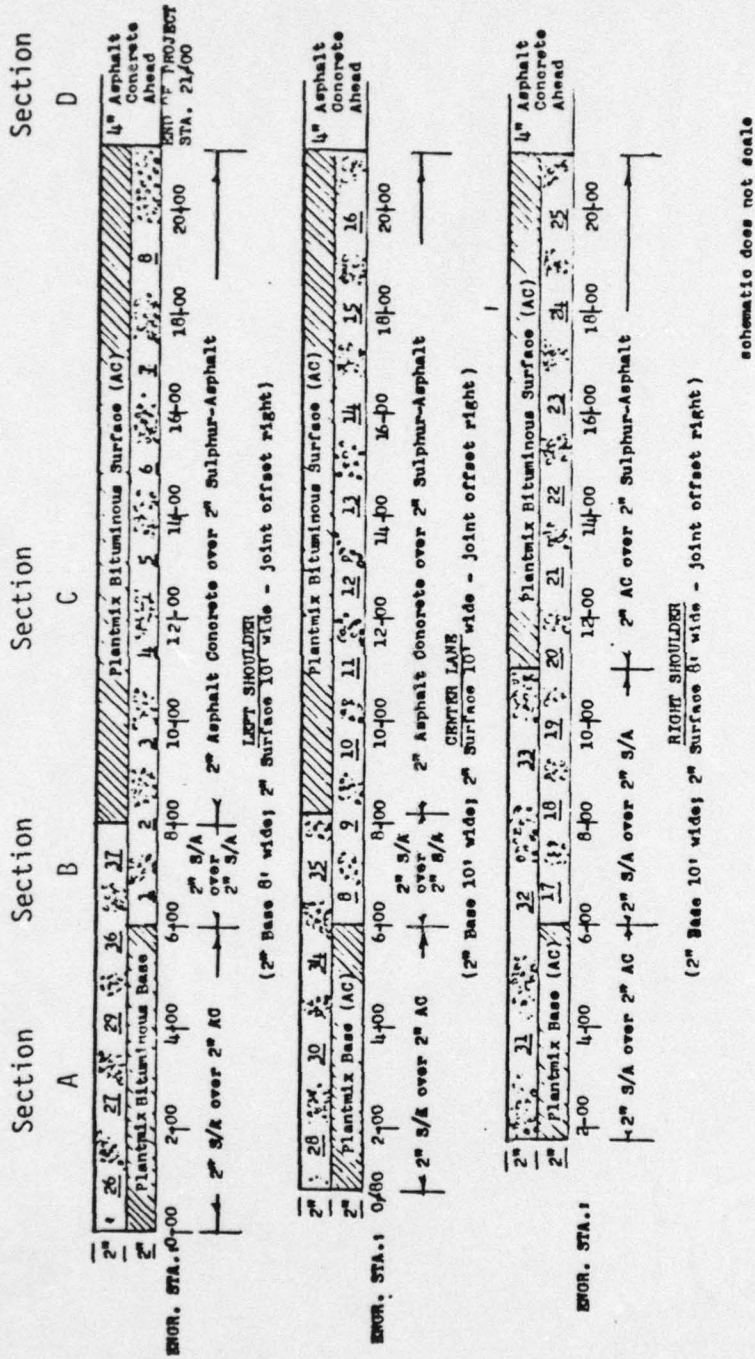
Equipment and Method

The construction was accomplished with conventional mixing, hauling and paving equipment, and with no equipment problems or need for



Ex: D-I-a reads section D, sample I, bottom layer (b is top layer).

Figure 2.8. PROFILE OF SULFUR-ASPHALT (SA) CONCRETE AND ASPHALT CONCRETE (AC) TEST SECTIONS AND SPECIMEN IDENTIFICATIONS [3]



schematic does not scale

Figure 2.9. SEA EXPERIMENTAL PROJECT SCHEMATIC OF TEST ITEMS [22]

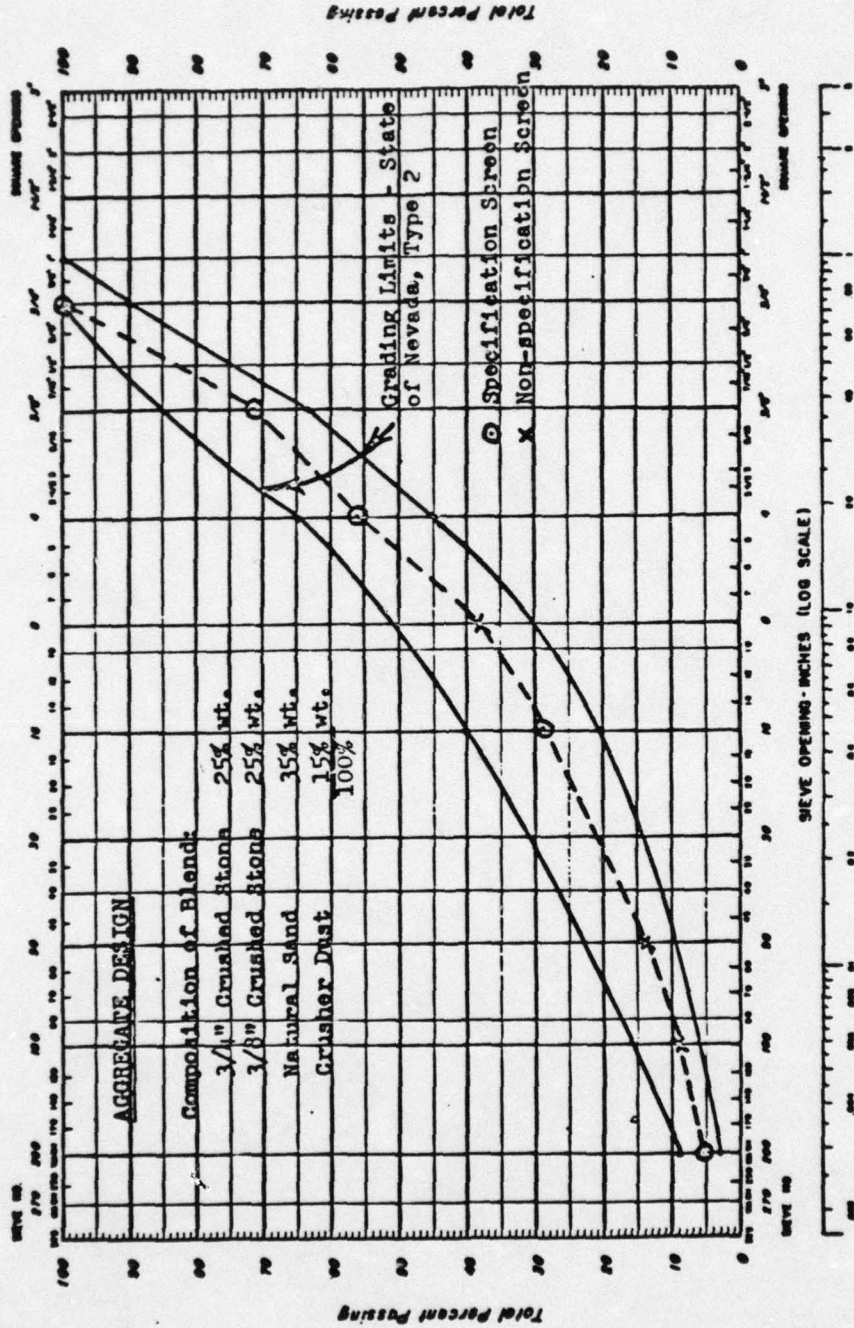


Figure 2.10. AGGREGATE GRADATION CHART SHOWING THE GRADING LIMITS AND COMPOSITION OF BLEND [22]

modification. Figure 2.11 [22] illustrates the S/A system instituted at the mixing plant.

Air Quality

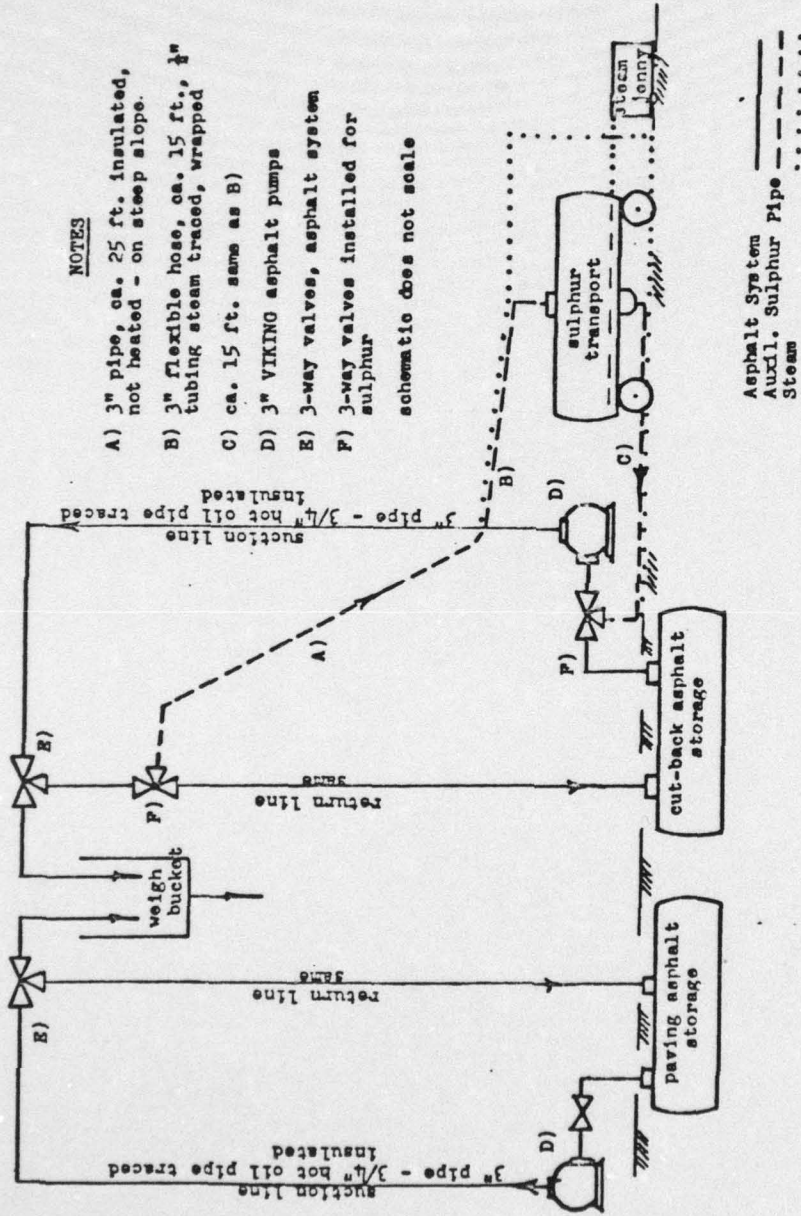
Monitoring of H_2S and SO_2 was carried on throughout the construction and is summarized below:

<u>Location</u>	<u>H_2S (ppm)</u>	<u>SO_2 (ppm)</u>
Asphalt plant pugmill	< 0.5	0
Asphalt paver (driver level)	0.0 - 0.2	0
Behind the paver (just above freshly paved surface)	0.0 - 0.5	0
Paver hopper (as material was dumped)	1 - 20	0

These are well within acceptable limits when compared with Table 2.2. The only potentially dangerous concentration noted was a momentarily high concentration in the paving hopper as the material was dumped [3].

In Situ Testing

The approach to in situ testing was to measure the surface deflection of the four test sections described in Figures 2.8 and 2.9. From these deflections, an estimate was made of the elastic moduli of each layer. Elastic layer theory was then applied to estimate the stresses and strains in the pavements. The deflections experienced are depicted in Figures 2.12 and 2.13. These deflections were measured with the Dynaflect.



NOTES

- A) 3" pipe, ca. 25 ft. insulated, not heated - on steep slope.
- B) 3" flexible hose, ca. 15 ft., 1/4" tubing steam traced, wrapped
- C) ca. 15 ft. same as B)
- D) 3" VIKING asphalt pumps
- E) 3-way valves, asphalt system
- F) 3-way valves installed for sulphur

schematic does not scale

Figure 2.11. SCHEMATIC OF S/A SYSTEM [22]

Table 2.2. TOXICITY OF HYDROGEN SULFIDE GAS [43]

<u>H₂S Concentration</u>	<u>Environmental Impact</u>
.02 ppm	Odor Threshold Value
5-10 ppm	Suggested MAC*
20 ppm	MAC
70-150 ppm	Slight symptoms after exposure of several hours
170-300 ppm	Maximum concentration that can be inhaled for one hour without serious consequences
400-700 ppm	Dangerous after continuous exposure of 30 min - 1 hr
600 ppm	Fatal with exposure greater than 30 min.

*Maximum allowable concentration

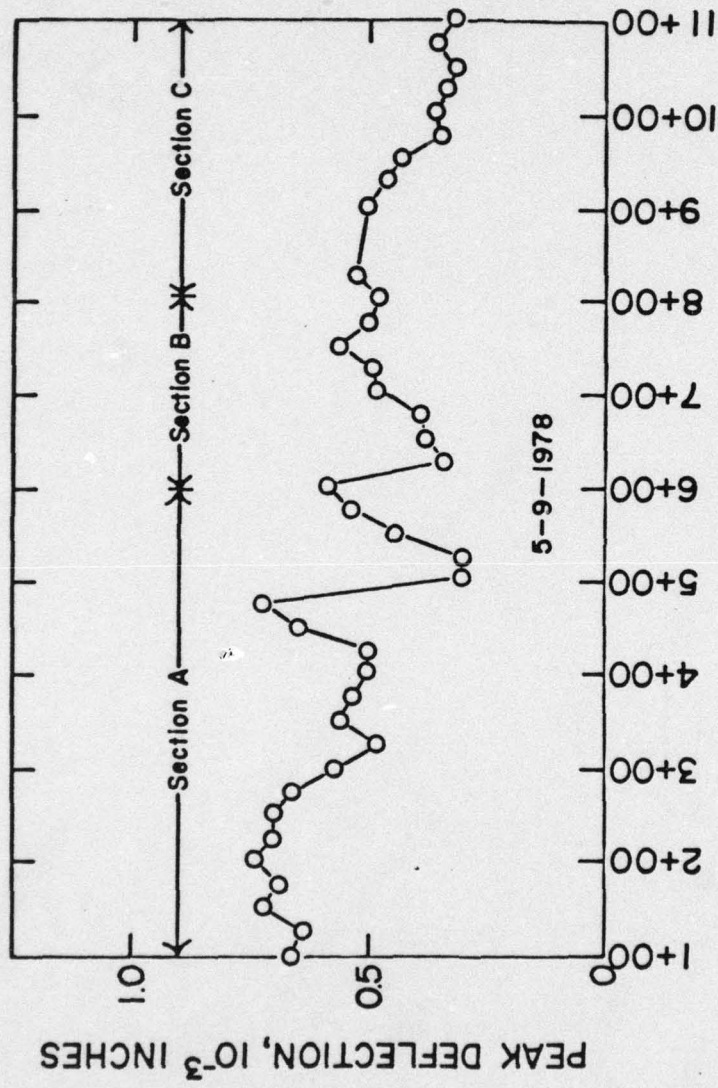


Figure 2.12. PEAK DEFLECTION PROFILE DUE TO DYNAFLECT LOADING FOR THE VARIOUS TEST SECTIONS OF U.S. 93-95, BOULDER CITY, NEVADA (SLOW LANE 0-W-P) [3]

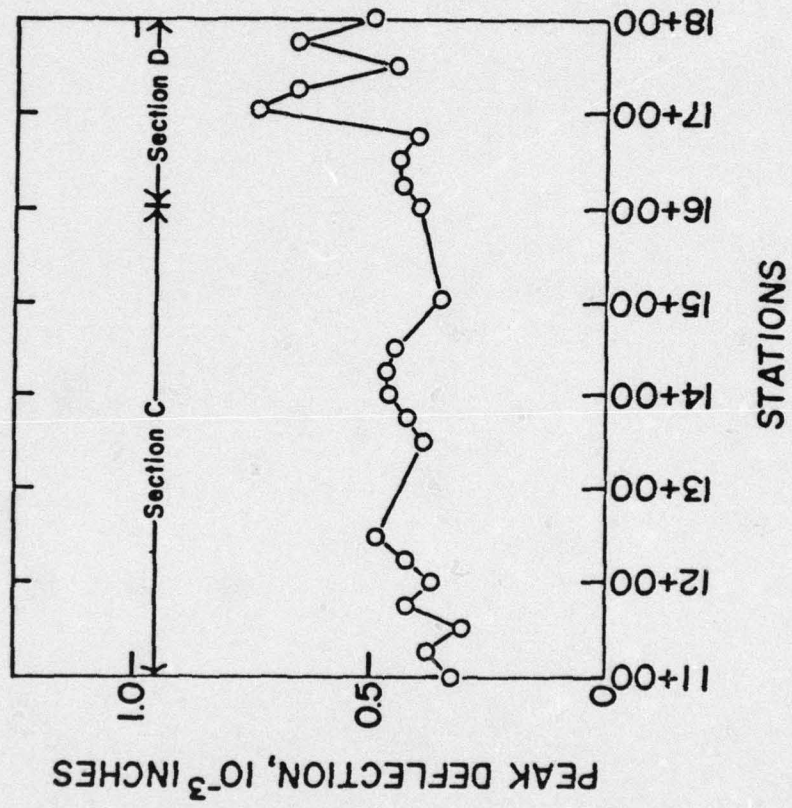


Figure 2.12. Continued

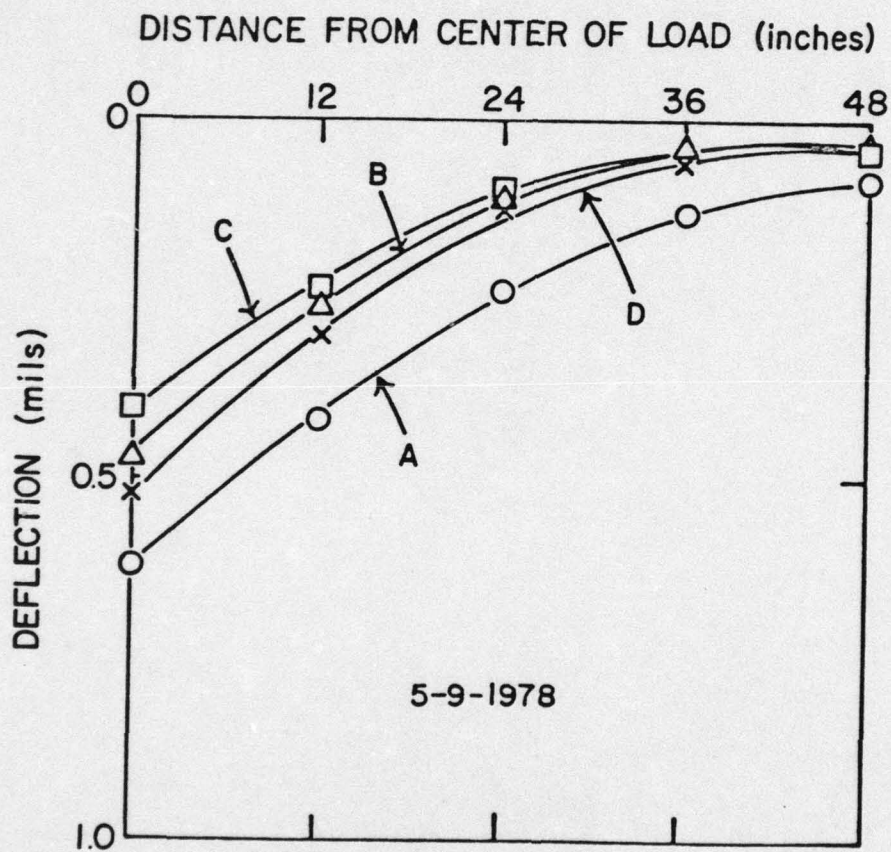


Figure 2.13. DEFLECTION BASINS FROM THE AVERAGE OBSERVATIONS FOR THE VARIOUS TEST ITEMS OF U.S. 93-95, BOULDER CITY, NEVADA (SLOW LANE O-W-P) [3]

Laboratory Testing of Cored Samples

Coring was accomplished on 13 June 1978 with a total of 12 cores being taken, three from each section. The cores were shipped to the University of Washington where testing was performed on them.

Marshall flow and stability tests were run and Table 2.3 shows the results and variations experienced with each test. As can be seen from these tables, S/A concrete Marshall stabilities are higher than their AC counterparts. In each test the top layer had higher Marshall stabilities than the bottom layer. This could be the result of two factors -- the additional compaction from traffic and the more rapid aging of the upper layer due to higher temperatures and possible exposure to the air.

The resilient modulus as well as Poisson's ratio were evaluated with respect to temperature. Testing was conducted at three temperatures, 5°C, 25°C and 40°C, utilizing the Schmidt apparatus. Figure 2.14 illustrates graphically the average M_R 's determined for each section. Each data point is the mean of six replicate tests. It can be concluded that the M_R 's for the S/A mixtures were higher than that for AC.

At the time of the test the pavements had been in use for more than 18 months and the resilient properties of the different sections showed that in terms of M_R , Sections B and C are superior to Sections A and D.

Poisson's ratio was also determined during this testing sequence. Poisson's ratios were determined on all samples at

Table 2.3. VARIATIONS IN MARSHALL STABILITIES, TEST RESULTS AT 60°C WITHIN EACH LAYER FOR VARIOUS TEST ITEMS OF U.S. 93-95, BOULDER CITY, NEVADA, SECTIONS A, B, C, AND D [3]

Mix Type	Measure of Dispersion	Marshall	
		Stability (lbs.)	Flow (0.01 in.)
"AC" Section A (Bottom Layer)	Mean	1385	14.3
	Std. Dev.	222	1.3
	C.V., %	16.0	9.0
"SA" Section A (Top Layer)	Mean	2708	13.8
	Std. Dev.	255	2.3
	C.V., %	9.0	16.0
"SA" Section B (Bottom Layer)	Mean	1793	16.7
	Std. Dev.	505	3.4
	C.V., %	28.0	20.0
"SA" Section B (Top Layer)	Mean	2158	15.8
	Std. Dev.	211	0.6
	C.V., %	10.0	4.0
"SA" Section C (Bottom Layer)	Mean	2113	16.2
	Std. Dev.	150	0.6
	C.V., %	7.0	4.0
"AC" Section C (Top Layer)	Mean	2461	18.5
	Std. Dev.	196	1.5
	C.V., %	8.0	8.0
"AC" Section D (Top Layer)	Mean	1452	13.2
	Std. Dev.	323	1.8
	C.V., %	22.0	14.0
"AC" Section D (Bottom Layer)	Mean	1217	15.5
	Std. Dev.	245	1.8
	C.V., %	20.0	11.0

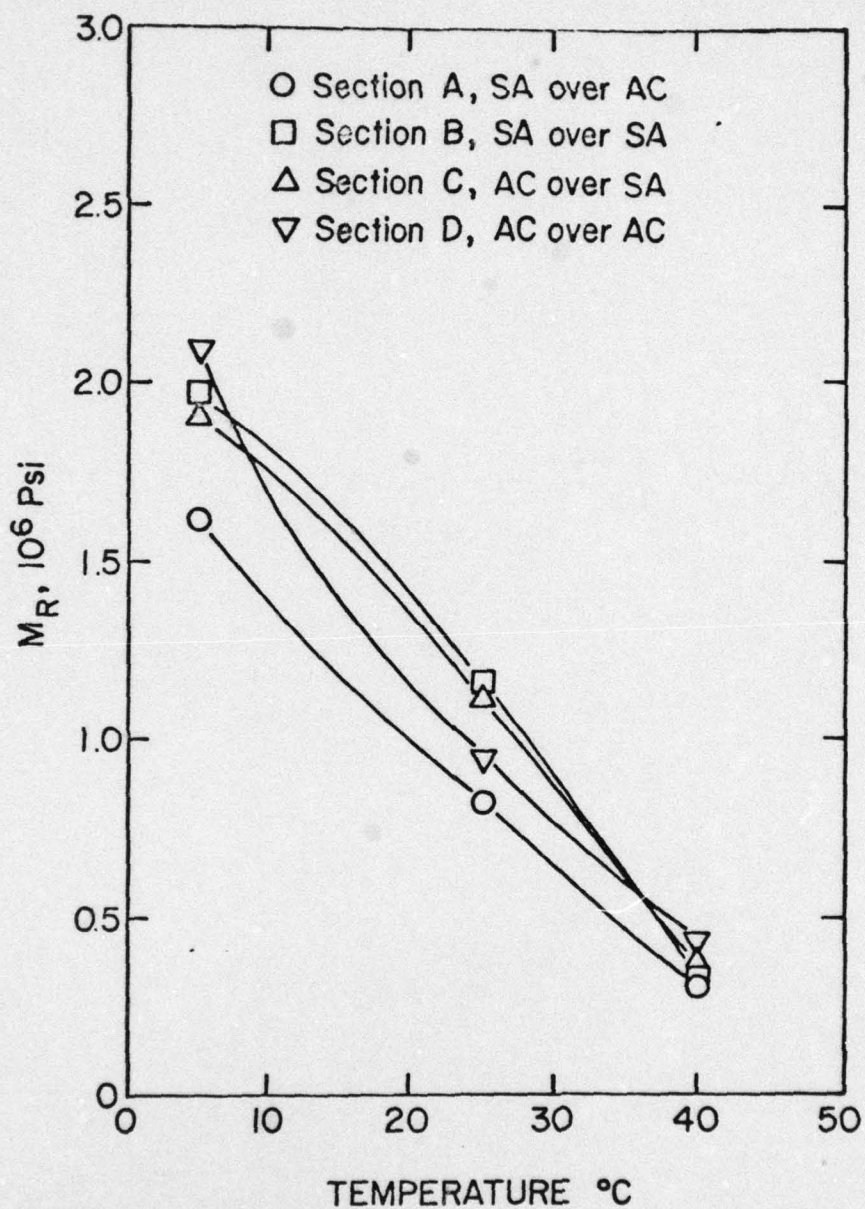


Figure 2.14. RELATIONSHIP BETWEEN THE AVERAGE RESILIENT MODULUS AND TEMPERATURE FOR EACH SECTION OF U.S. 93-95, BOULDER CITY, NEVADA [3]

each of the three temperatures. There was very little variation in Poisson's ratio and its range was between .31 and .33 [3].

CHAPTER III
MIX DESIGN AND RESILIENT MODULUS EVALUATION
OF SULFUR-EXTENDED ASPHALT PAVEMENTS

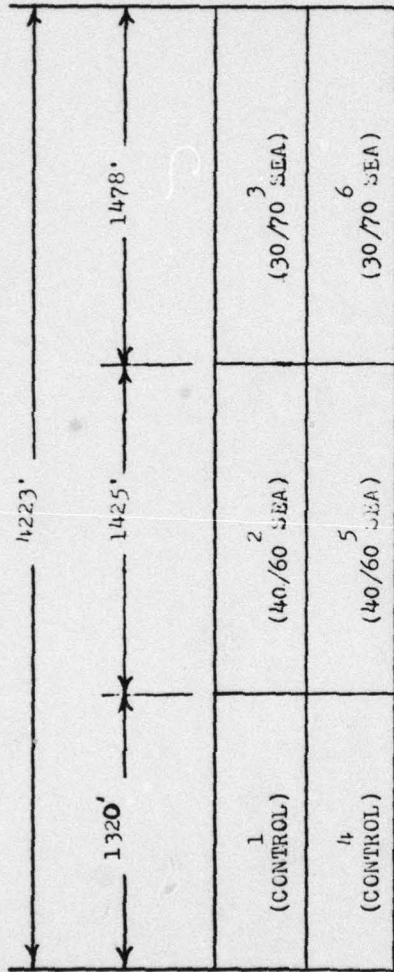
Background

As has been previously mentioned, a number of laboratory-analytical studies have been conducted to investigate the effect of combining sulfur, asphalt and various aggregates in paving mixtures. Several full-scale experimental highway projects have been built as discussed in Chapter II.

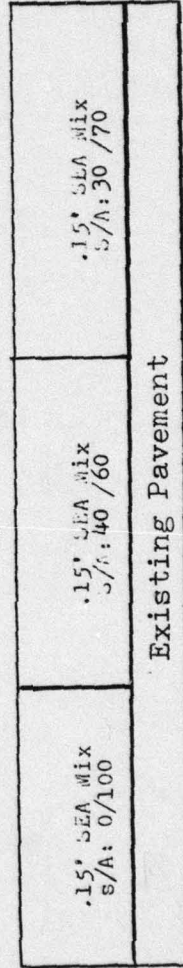
The results of laboratory work have indicated that SEA binders are equivalent to or perhaps even superior to conventional pavements. The final results of the full-scale highway projects are still in progress and are somewhat inconclusive.

The University of Washington is performing a study sponsored by the Washington State Department of Transportation to plan, construct, monitor and evaluate a sulfur-extended asphalt project. This project, through the utilization of repetitive wheel load testing at the Washington State University test track, is intended to bridge the gap between laboratory-analytical studies and the full-scale highway projects. Further details on the test track and its construction will be presented in Chapter IV.

In addition to the test track sections, a 1287 meter (4223 foot) segment of SR 270, located near Pullman, Washington, was overlaid with the same materials as utilized at the test track. Figure 3.1 shows



Top View



Longitudinal Cross Section

Figure 3.1. PLAN AND CROSS-SECTIONAL VIEW OF SR 220

a plan and typical cross-sectional view of SR 270 as finally constructed. An evaluation of SR 270 is beyond the scope of this report and will be covered in subsequent reports [23].

This project affords a unique opportunity to concurrently construct both the test track and the experimental highway from the same materials and with the same central batch plant. Later comparisons of the behavior of the materials on the test track and those on the actual highway should be very informative.

Prior to construction of the test track and highway sections, extensive testing of the characteristics of the materials and a mix design to find the optimum binder content of the different mixes were undertaken at the University of Washington. The remainder of this chapter will be devoted to the results of these tests, the mix design results, and the determination of resilient modulus.

Materials Characteristics

The aggregate, a crushed columnar basalt, was obtained from a quarry adjacent to the WSU test track in Pullman, Washington. The specific gravity is 2.74 and the absorption is 2.29%. The test for specific gravity and absorption were conducted in accordance with ASTM C 127 [24]. The quarry is owned by United Paving.

The asphalt cement was also provided by United Paving. The asphalt, an AR-4000, was produced by Husky Oil Company and was tested in accordance with ASTM D 70 [25] for its specific gravity, which was found to be 1.024. The sulfur was an 80-mesh ground

sulfur from the Montana Sulfur and Chemical Company, Billings, Montana. The sulfur was not tested for purity due to attested purity claimed by the producer and available literature statements that small variances of impurity have little impact on SEA mixtures [3].

Sample Preparation

A total of 90 samples were prepared (45 samples for a Marshall mix design and 45 samples for a Hveem mix design). These 90 samples were further subdivided into 6 sets of 15 samples, sets A through F. Sets A, B and C were prepared by the Marshall method and D, E and F were prepared by the Hveem method. Sets A and D had a S/A ratio of 0/100, B and E had a S/A ratio of 50/50, and C and F had a S/A ratio of 30/70.

Each mix design method had triplicate samples made at the following binder contents: 4.5, 5.0, 5.5, 6.0, and 6.5 per cent by weight of the mix. However, since sulfur and asphalt do not have the same specific gravity (asphalt is approximately half that of sulfur), appropriate adjustments were made to the sulfur/asphalt binder contents to equate them at equal volumes when preparing them for comparison to conventional asphalt binders. Table 3.1 illustrates the relative density of S/A binders.

The per cent of binder by weight in the samples had to be adjusted to have equivalent amounts of binder by volume. They were adjusted as illustrated in Table 3.2.

Table 3.1
RELATIVE DENSITY OF VARIOUS S/A BINDERS [7,11]

% AR 4000 / 85/100 Penetration Asphalt	100	90	80	70	60	55	50	40	0
% Elemental Sulfur	0	10	20	30	40	45	50	60	100
Relative Density at 16°C (61°F)	1.0268	1.0552	1.0552	1.1828	1.2320	1.2854	1.3442	1.4337	1.9556

Table 3.2
EQUIVALENT BINDER CONTENT FOR 30/70 AND 50/50 S/A BINDERS COMPARED TO CONVENTIONAL 0/100*

S/A Ratio	Per Cent by Weight				
0/100	4.5	5.0	5.5	6.0	6.5
30/70	5.3	5.9	6.5	7.1	7.7
50/50	6.1	6.7	7.4	8.1	8.8

*Henceforth, actual binder content by weight will be presented inside parentheses () and the equivalent 0/100 will be presented as well; e.g., for S/A ratio 30/70, 4.5% (5.3%).

Table 3.3
 AGGREGATE GRADATION WSDOT CLASS B [26]

Sieve Size	% Retained	% Passing Cumulative	Specification Limits
5/8	0	100	100
1/2	7	93	90-100
3/8	16	77	75-90
1/4	19	58	55-75
No. 10	24	34	32-48
No. 40	18	16	11-24
No. 80	6	10	6-15
No. 200	5	5	3-7
- 200	5	0	0

The aggregate gradation used was in accordance with Washington State Department of Transportation Class B specifications (see Table 3.3).

Figure 3.2 illustrates the gradation used in this study compared to the gradation specification limits prescribed by Class B gradation requirements of WSDOT. It should be noted that the gradation utilized tends to be on the coarse side of the Class B specification. This was intentionally done because previous studies done at the University of Washington indicated that unusually low air void contents resulted from mixtures with a gradation in the middle of the band [27,28].

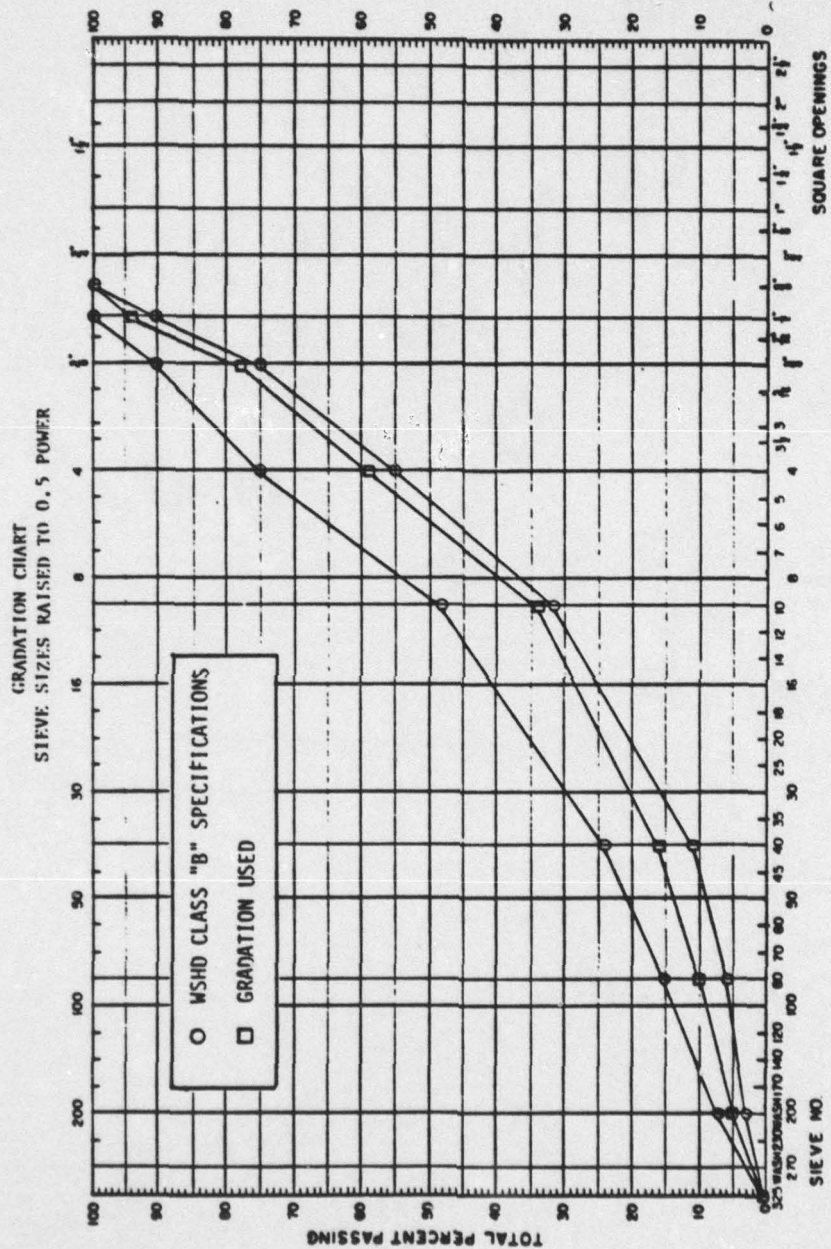


Figure 3.2. AGGREGATE GRADATION, WSDOT CLASS "B"

For the Marshall mix design method, the samples were prepared in accordance with ASTM D 1559 [29] with modifications made by Pronk [30]. These modifications are as follows:

- the blending of sulfur and asphalt with a drink mixer at medium speed
- the addition of .001% siloxane polymer in the form of Dow Corning 200 to facilitate the dispersion of the sulfur and improve the stability of the emulsion

For the Hveem mix design method, the samples were prepared identically to those of the Marshall method except that compaction was accomplished with a pneumatic kneading device rather than the drop hammer employed with the Marshall method. Figure 3.3 shows the preparation sequence of the 90 samples (i.e., both Hveem and Marshall samples).

Sample Testing

Sets A, B and C (45 samples) were then tested for resilient modulus, bulk specific gravity, Marshall stability and flow, and maximum specific gravity. Sets D, E and F were tested for resilient modulus, bulk specific gravity, Hveem stability, indirect tensile strength, and maximum specific gravity (see Figures 3.4 and 3.5).

The testing was done in accordance with established testing procedures as indicated:

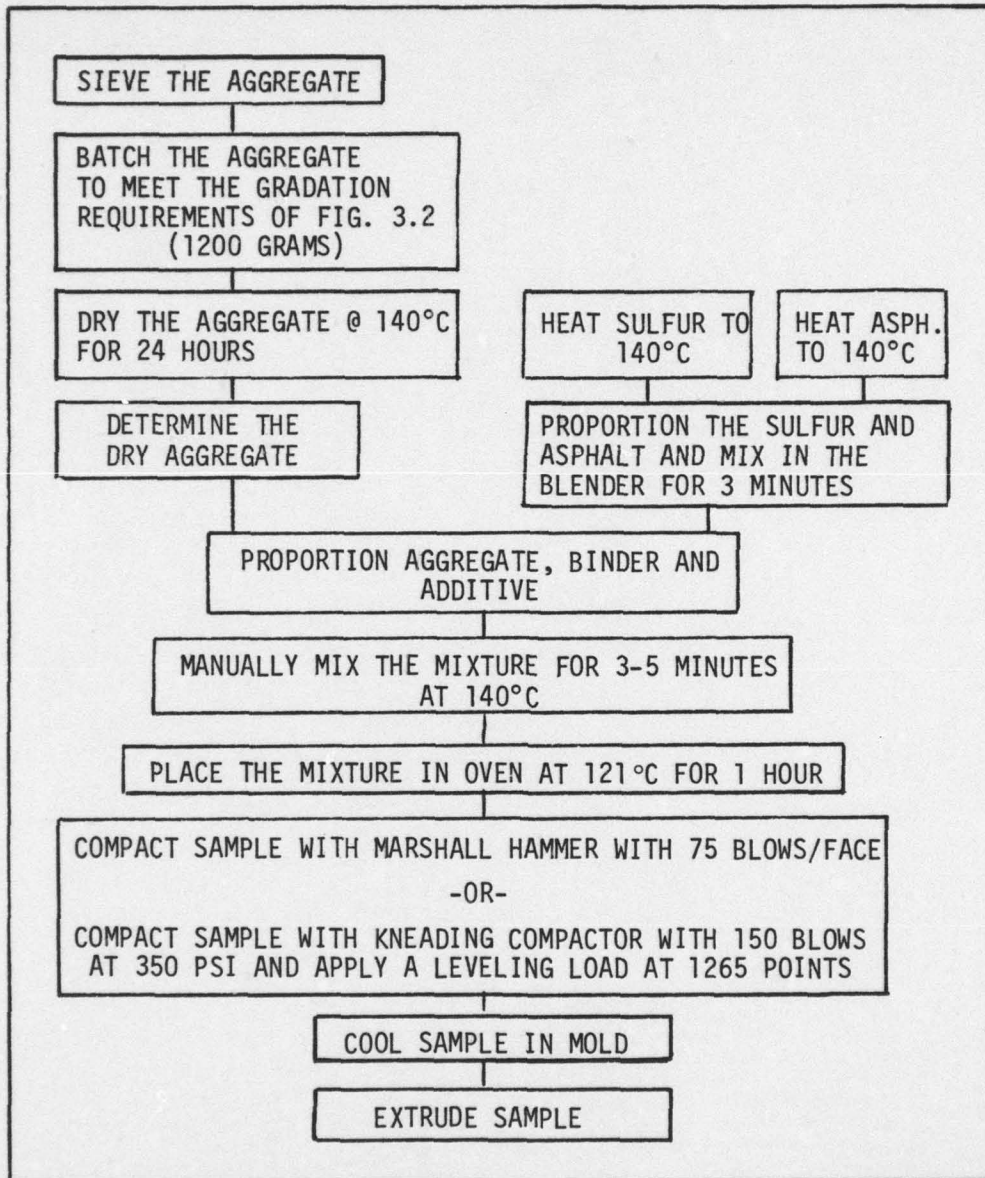


Figure 3.3. HVEEM AND MARSHALL SAMPLE PREPARATION

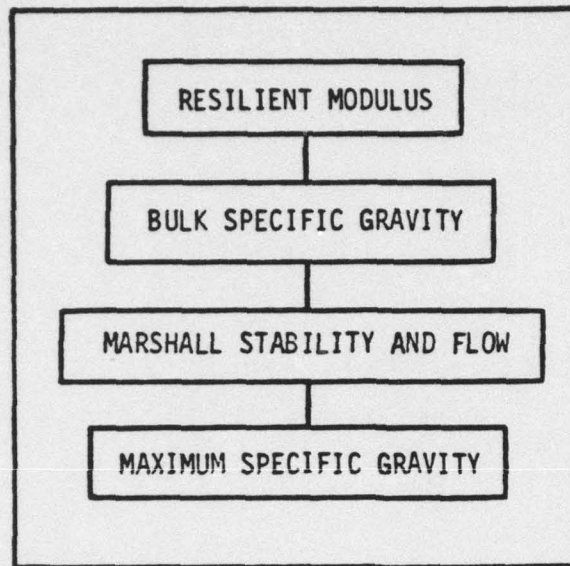


Figure 3.4. MARSHALL SAMPLE TESTING SEQUENCE

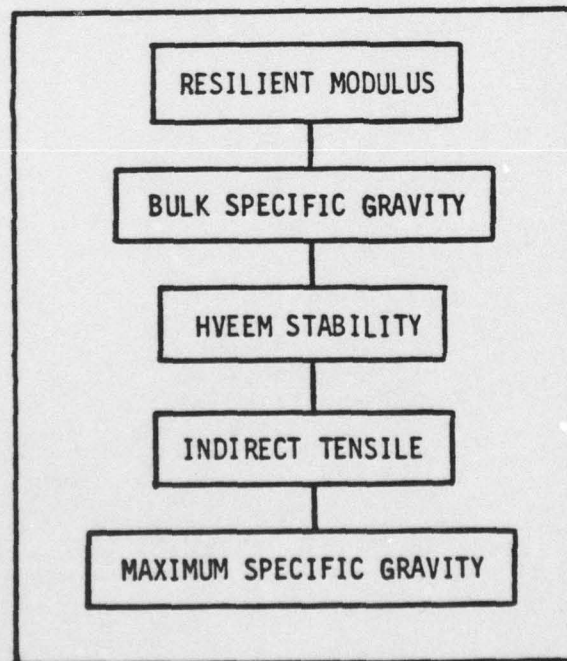


Figure 3.5. HVEEM SAMPLE TESTING SEQUENCE

MARSHALL SAMPLES (Sets A, B, C)

Test -	Procedure Reference
Resilient Modulus -	Proposed ASTM "Indirect Tensile Test Method for Resilient Modulus of Bituminous Mixtures" [26]
Bulk Specific Gravity -	WSDOT Test Method 704 [31]
Marshall Stability & Flow -	ASTM Test Designation D1559 [29]
Maximum Specific Gravity -	WSDOT Test Method 705 [32]

HVEEM SAMPLES (Sets D, E, F)

Test -	Procedure Reference
Resilient Modulus -	Same as for Samples A, B, C
Bulk Specific Gravity -	Same as for Samples A, B, C
Hveem Stability -	WSDOT Test Method 703 [33]
Indirect Tensile Strength -	ASTM Designation C46 [34]
Maximum Specific Gravity -	Same as for Samples A, B, C

Further details on each test procedure are available in Reference 26 including a copy of the proposed ASTM Standard for Resilient Modulus Testing (Appendix A of Reference 26).

Results of the Marshall Mix Design

The results of the Marshall testing should be compared to the standard Marshall criteria shown in Table 3.4. The optimum binder content is determined by graphing the results and comparing them to Table 3.4. Consideration is given in particular to the graphic

Table 3.4
MARSHALL DESIGN CRITERIA [35]

Traffic category	Heavy	
Number of compaction blows each end of specimen	75	
	Minimum	Maximum
Stability, lb.	750	
Flow, .01-in.	8	16
Per cent air voids:		
surface course	3	5
base course	3	8
Per cent voids in mineral aggregate	14	

results of maximum Marshall stability, maximum unit weight, and the median of the limits given in Table 3.4 for air voids. The optimum is then the numerical average of these three binder contents.

The tabular and graphic results of Marshall mix design testing conducted on sample sets A, B and C are shown in Tables 3.5 - 3.7 and Figures 3.6 - 3.8.

Table 3.5. MARSHALL MIX DESIGN DATA
100/0 ASPHALT/SULPHUR RATIO

BINDER CONTENT (%) BY WEIGHT	SAMPLE	WEIGHT IN AIR (GRAMS)	WEIGHT IN WATER (GRAMS)	BULK SPECIFIC GRAVITY	UNIT WEIGHT	MAXIMUM SPECIFIC GRAVITY	VMA	% AIR VOIDS	STABILITY		FLOW
									MEASURED	ADJUSTED	
4.5	A1	1231.0	726.0	2.437	152.3	2.514			3700	3552	19
	A2	1225.5	723.5	2.441	152.3	2.506			3450	3312	19
	A3	1227.5	725.0	2.444	152.3	2.575	16.8	3.6	3150	3150	19
				2.440	152.3	2.532				3338	19.0
5.0	A4	1232.5	735.0	2.477	154.8	2.595			3400	3876	17
	A5	1239.0	741.0	2.487	155.4	2.591			3840	4186	17
	A6	1246.5	748.0	2.500	156.0	2.597			3780	4120	18.1
				2.488	155.4	2.594	15.5	4.0		4061	17.4
5.5	A7	1243.0	739.5	2.468	154.1	2.564			3560	3560	19
	A8	1233.5	731.0	2.454	153.5	2.558			3600	3600	19
	A9	1247.0	741.0	2.464	153.5	2.542			3780	3780	24
				2.462	153.7	2.555	16.9	3.6		3647	20.7
6.0	A10	1242.0	744.0	2.494	155.4	2.539			3460	3598	20
	A11	1238.0	738.0	2.476	154.8	2.519			3200	3328	23
	A12	1255.0	745.0	2.460	153.5	2.530			2900	2900	18
				2.476	154.6	2.529	16.9	2.1		3275	20.3
6.5	A13	1251.0	751.5	2.504	156.0	2.508			3080	3203	22
	A14	1248.0	750.0	2.506	156.6	2.518			3450	3450	23
	A15	1254.0	752.0	2.498	156.0	2.529			3300	3168	20
				2.502	156.2	2.518	16.4	0.6		3274	21.7

Table 3.6. MARSHALL MIX DESIGN DATA
70/30 ASPHALT SULPHUR RATIO

BINDER CONTENT (%) BY WEIGHT	SAMPLE	WEIGHT IN AIR (GRAMS)	WEIGHT IN WATER (GRAMS)	BULK SPECIFIC GRAVITY	UNIT WEIGHT	MAXIMUM SPECIFIC GRAVITY	VMA	% AIR VOIDS	STABILITY		FLOW
									MEASURED	ADJUSTED	
4.5 (5.3)	C1	1249.0	738.5	2.447	152.9	2.687			4450	4851	17.8
	C2	1249.5	739.0	2.448	152.9	2.639			4780	5210	18.0
	C3	1249.5	734.5	2.426	151.6	2.695	16.7	8.6	4700	5123	19.3
				2.440	152.5	2.674				5061	18.4
5.0 (5.9)	C4	1261.5	749.5	2.464	153.5	2.665			5310	5788	19.7
	C5	1262.0	752.0	2.475	154.1	2.633			4660	5079	17.5
	C6	1261.5	750.5	2.469	154.1	2.667	16.3	7.0	4920	5363	19.1
				2.469	153.9	2.652				5410	18.8
5.5 (6.5)	C7	1258.0	755.0	2.501	156.0	2.623			4050	4415	20.0
	C8	1245.0	742.5	2.478	154.8	2.625			3980	4338	19.2
	C9	1265.0	757.0	2.490	155.4	2.621	16.0	5.1	3140	3423	21.2
				2.490	155.4	2.623				4059	20.1
6.0 (7.1)	C10	1254.0	748.5	2.481	154.8	2.612			2850	3249	20.6
	C11	1257.5	750.0	2.478	154.8	2.611			3600	4104	24.2
	C12	1254.0	750.0	2.488	155.4	2.608	16.6	4.9	3600	3924	22.7
				2.482	155.0	2.610				3759	22.5
6.5 (7.7)	C13	1261.5	753.0	2.481	154.8	2.600			3370	3673	28.9
	C14	1235.0	736.0	2.475	154.1	2.600			3200	3648	25.8
	C15	1253.0	748.0	2.481	154.8	2.592	17.3	4.7	2770	3019	26.3
				2.479	154.6	2.597				3447	27.0

Table 3.7. MARSHALL MIX DESIGN DATA
50/50 ASPHALT/SULPHUR RATIO

BINDER CONTENT (%) BY WEIGHT	SAMPLE	WEIGHT IN AIR (GRAMS)	WEIGHT IN WATER (GRAMS)	BULK SPECIFIC GRAVITY	UNIT WEIGHT	MAXIMUM SPECIFIC GRAVITY	VMA	% AIR VOIDS	STABILITY		FLOW
									MEASURED	ADJUSTED	
4.5 (6.1)	B1	1226.5	734.5	2.493	155.4	2.541			10,900	11,881	18.8
	B2	1253.0	751.0	2.496	156.0	2.667			11,040	12,034	24.0
	B3	1242.0	744.0	2.494	155.4	2.660	15.0	5.0	8,610	9,815	23.0
				2.494	155.6	2.623				11,243	22.0
5.0 (6.7)	B4	1261.0	758.0	2.507	156.6	2.644			11,260	12,273	29.0
	B5	1252.5	749.0	2.488	155.4	2.632			9,800	10,682	30.0
	B6	1255.0	752.5	2.496	156.0	2.611	15.2	4.9	9,650	10,519	29.0
				2.497	156.0	2.629				11,158	29.3
5.5 (7.4)	B7	1264.0	754.5	2.481	154.8	2.640			9,340	10,181	27.0
	B8	1263.0	758.0	2.500	156.0	2.564			8,540	9,309	25.0
	B9	1272.0	759.5	2.482	154.8	2.604	16.1	4.5	8,720	9,505	26.5
				2.488	155.2	2.603				9,665	26.2
6.0 (8.1)	B10	1265.0	744.5	2.430	151.6	2.551			9,150	9,516	24.0
	B11	1273.5	761.5	2.489	155.4	2.609			6,500	7,085	21.0
	B12	1260.0	756.5	2.502	156.0	2.599	17.0	4.4	6,720	7,325	22.0
				2.474	154.3	2.586				7,975	22.3
6.5 (8.7)	B13	1273.0	762.0	2.491	155.4	2.608			5,550	5,772	19.0
	B14	1258.0	740.0	2.429	151.6	2.514			6,680	6,947	21.5
	B15	1281.5	749.5	2.409	149.8	2.546	18.5	4.5	6,320	6,320	21.5
				2.443	152.3	2.556				6,346	20.7

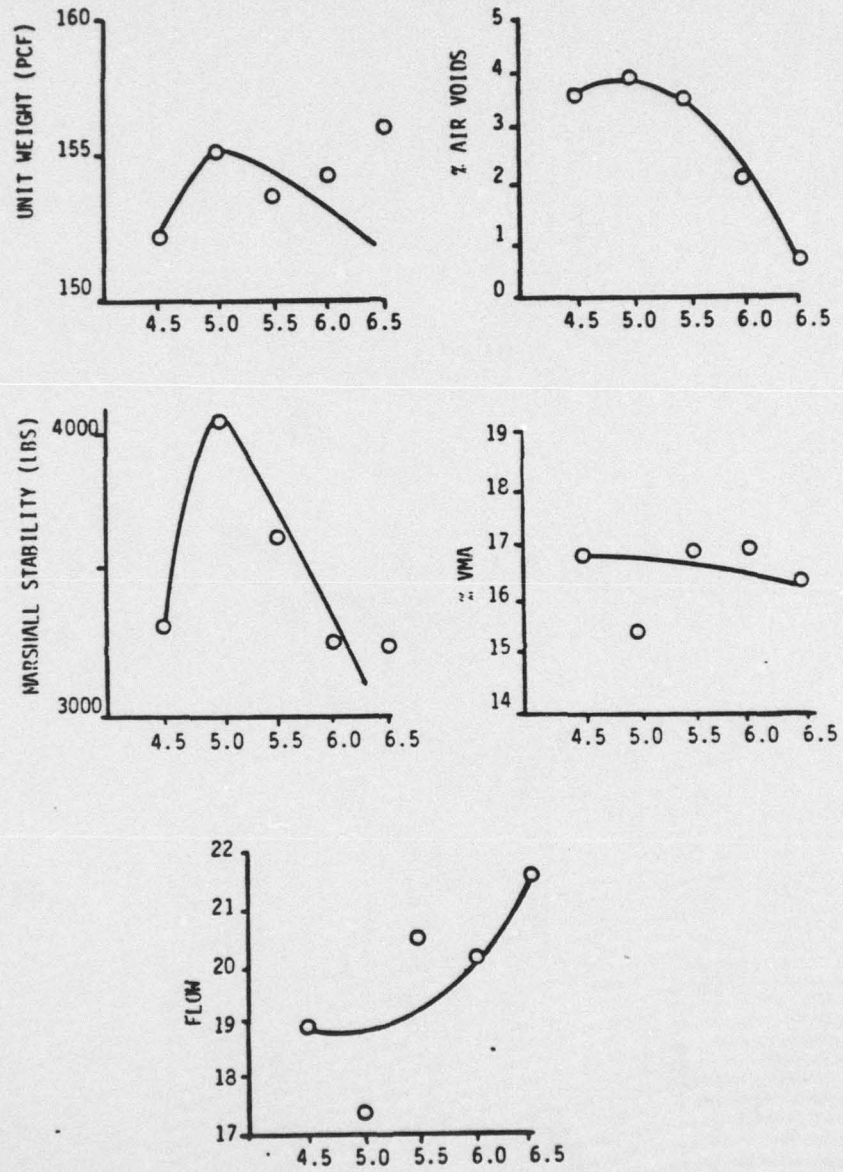


Figure 3.6. MARSHALL MIX DESIGN DATA CURVES
100/0 ASPHALT/SULPHUR RATIO

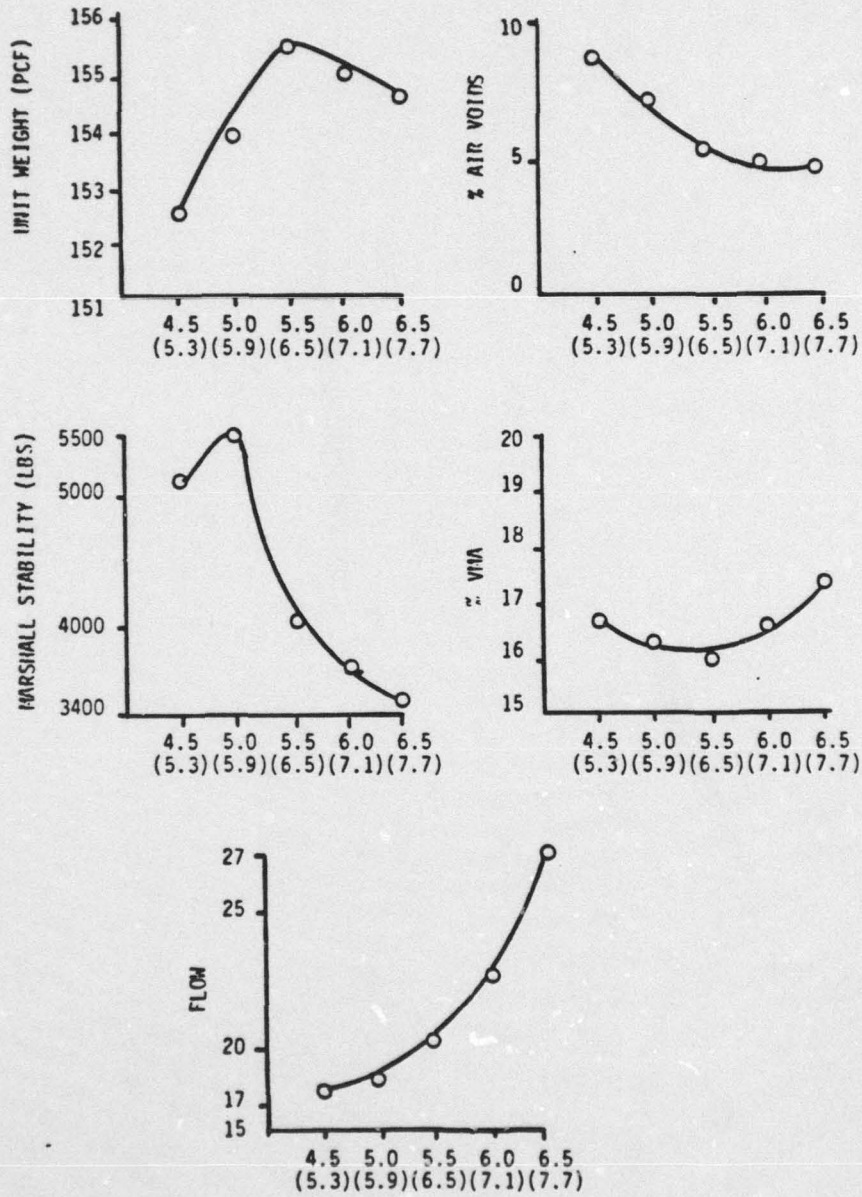


Figure 3.7. MARSHALL MIX DESIGN DATA CURVES
70/30 ASPHALT/SULPHUR RATIO

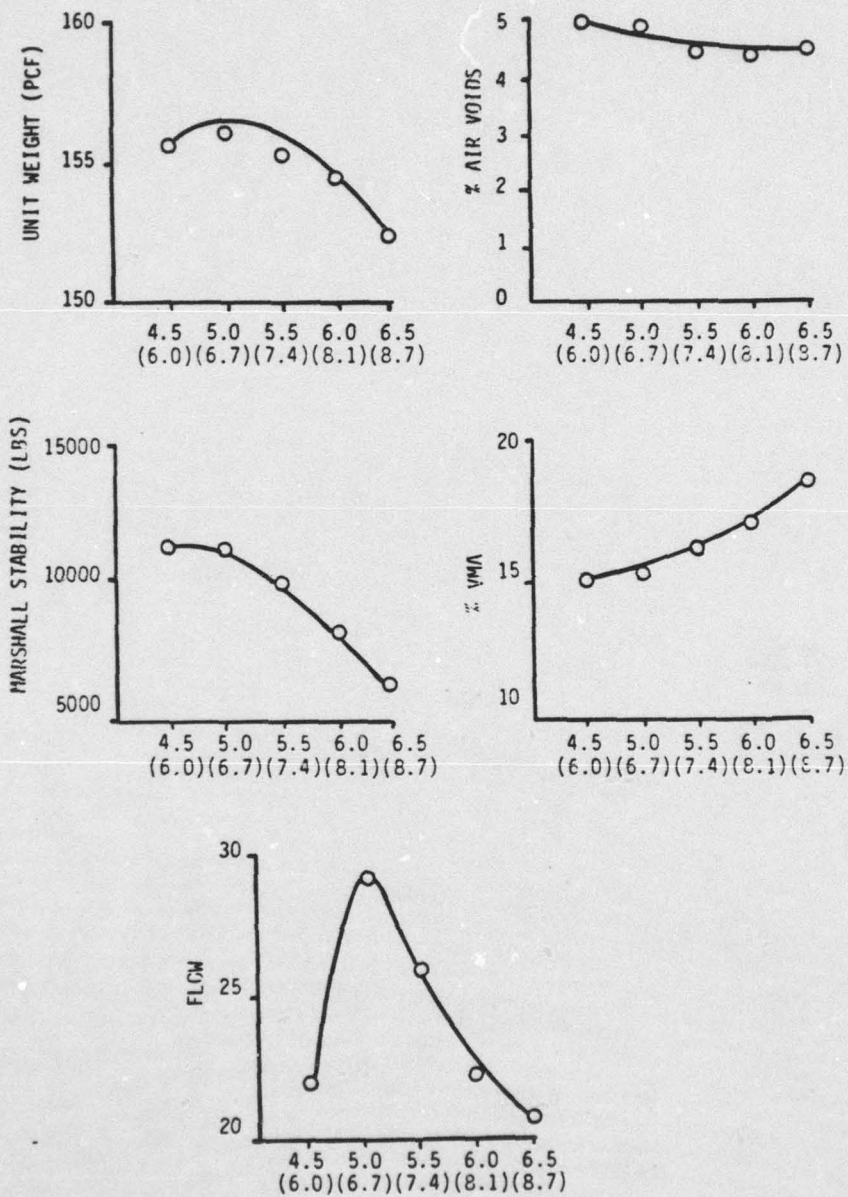


Figure 3.8. MARSHALL MIX DESIGN DATA CURVES
50/50 ASPHALT/SULPHUR RATIO

Determined Optimum Binder Contents100/0 S/A Ratio

<u>Data Type</u>	<u>Value</u>	<u>Binder Content</u>
Stability	4061 lb.	5.0
Unit weight	155.4 pcf	5.0
Air voids	4.0%	<u>5.0</u>
Average (optimum) binder content:		5.0

50/50 S/A Ratio

<u>Data Type</u>	<u>Value</u>	<u>Binder Content</u>
Stability	11,243 lb.	4.5 (6.1)
Unit weight	156.0 pcf	5.0 (6.7)
Air voids	4.4%*	<u>6.0 (8.1)</u>
Average (optimum) binder content:		5.2 (7.0)

30/70 S/A Ratio

<u>Data Type</u>	<u>Value</u>	<u>Binder Content</u>
Stability	5410 lb.	5.0 (5.9)
Unit weight	155.4 pcf	5.5 (6.5)
Air voids	4.7%*	<u>6.5 (7.7)</u>
Average (optimum) binder content:		5.7 (6.7)

*The median value of 4.0% air voids was never reached for the 30/70 and 50/50 mixes; 4.4% and 4.7% are the lowest values attained.

AD-A083 725

ARMY MILITARY PERSONNEL CENTER ALEXANDRIA VA
INITIAL ANALYSIS OF THE SULFUR-EXTENDED TEST TRACK CONSTRUCTED --ETC(U)
MAR 80 R L GARMAN

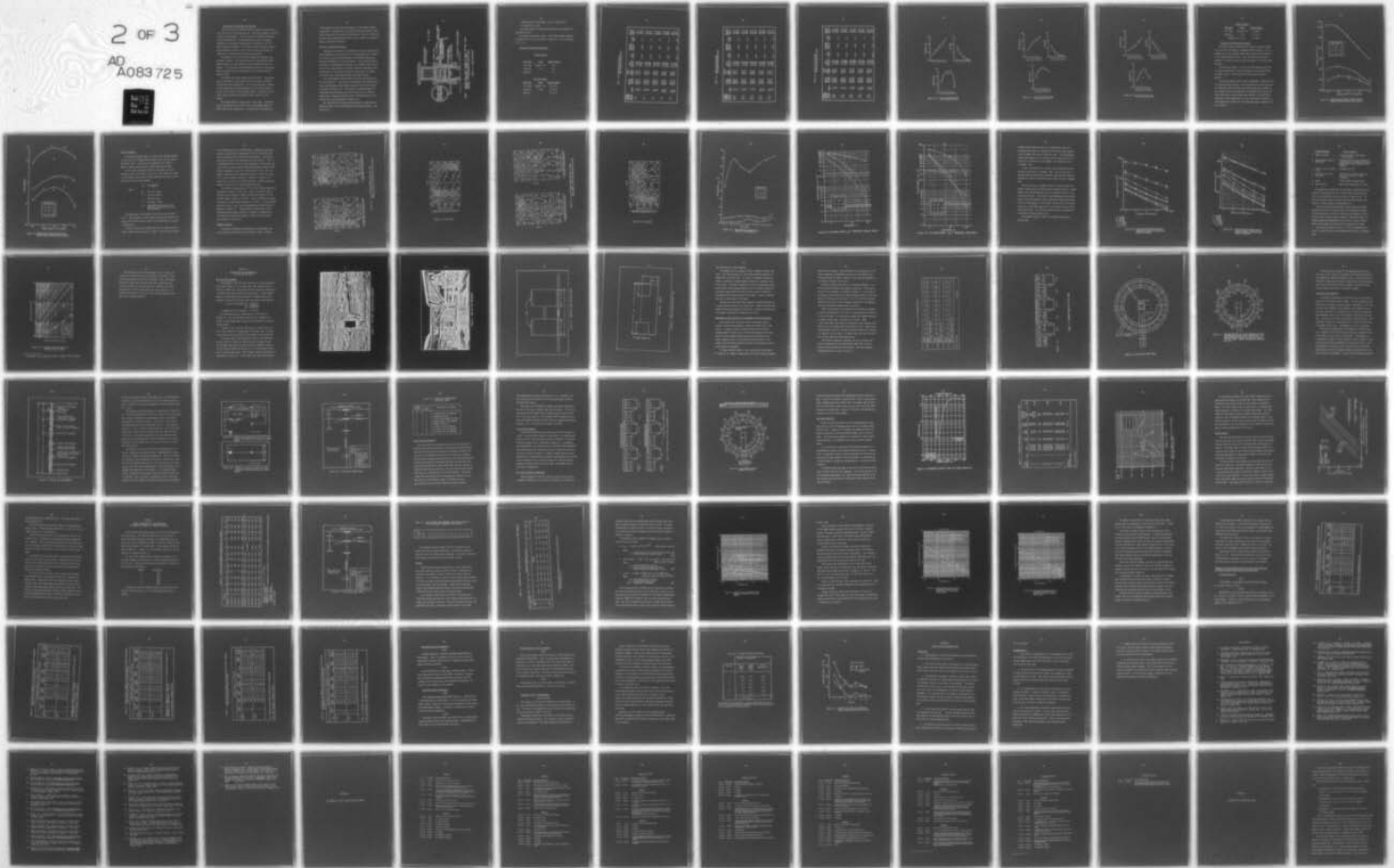
F/G 11/4
--ETC(U)

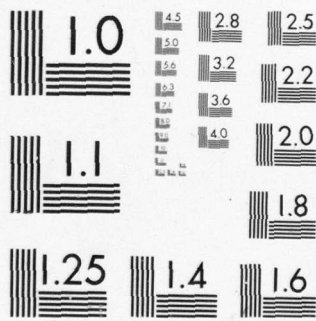
UNCLASSIFIED

NL

2 OF 3

AD
A083 725





MICROCOPY RESOLUTION TEST CHART
NATIONAL BUREAU OF STANDARDS-1963-A

Discussion of the Marshall Mix Designs

The data curves for stability and unit weight were quite conclusive, but the air void curves were not. There was a problem of high air voids in the SEA samples. High air voids are frequently associated with high permeability. High permeability may lead to premature hardening of the binder by permitting the circulation of air and water through the pavement. This could possibly have been corrected by the addition of mineral filler to more closely approximate the gradation of a maximum density grading curve [26,35].

Furthermore, it was felt that the compaction temperature may have been a problem. The molds were kept hot (approximately 200°F) between samples, but were exposed to room temperature during compaction. It is possible that the hardening of the sulfur during compaction affected the void content and also the structure and the stability [26].

The maximum unit weight results are very similar. The maximum value is reached at 5.0%, 5.0% and 5.5% for the 0/100, 50/50 and 70/30 binder ratios respectively. This is not surprising, although a wider range might have been expected due to the higher specific gravity of the sulfur in the SEA samples [26]. It appears that the higher specific gravity may have been offset by the air voids present.

The maximum stability values cover a large range. The maximum value is reached at 5.0%, 4.5% and 5.0% for the 0/100, 50/50 and 30/70 binder ratios respectively. The stability of the 100/0 and

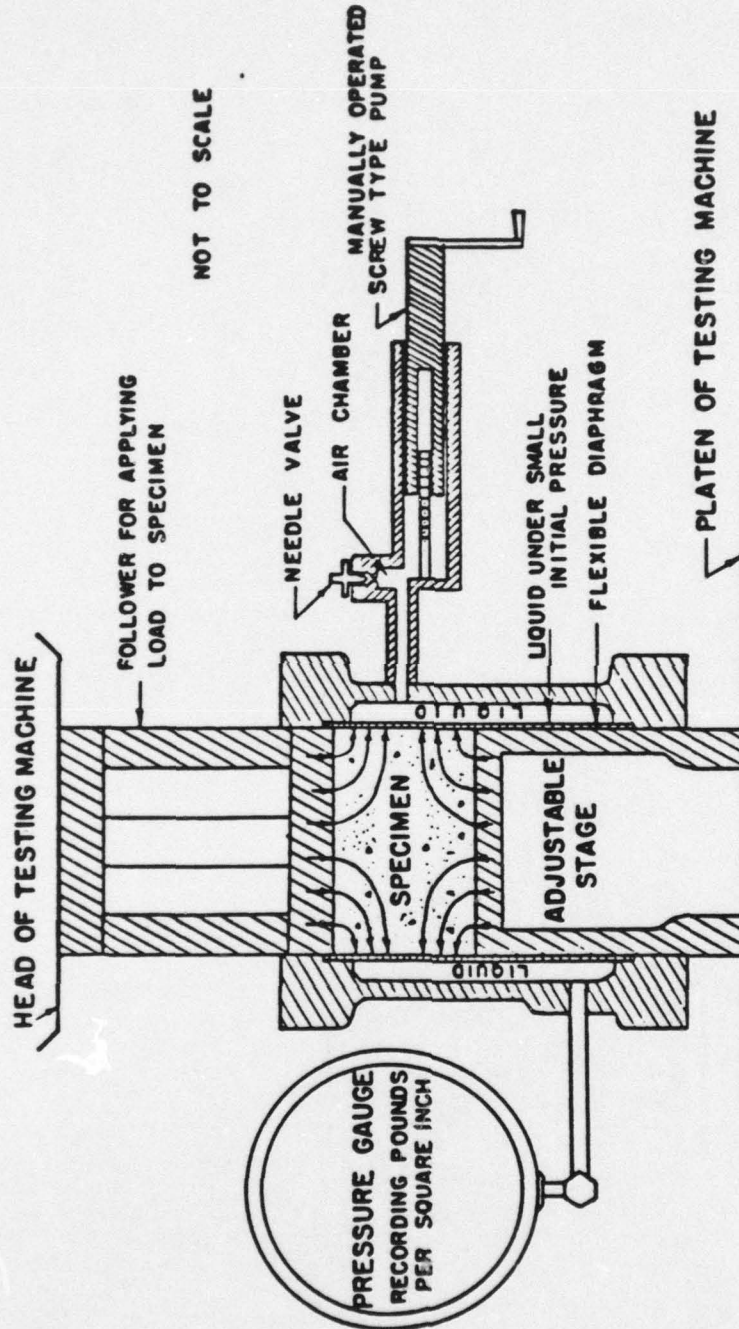
70/30 samples are quite similar through all of the binder contents tested [26]. The stability of the 50/50 mix was much higher, approximately twice that of the 0/100 or 30/70 mixes. This is in line with previous testing conducted by Gulf Oil, Pronk and the U.S. Bureau of Mines as discussed in Chapter I.

Results of the Hveem Mix Design

Based upon the results of the Marshall mix design investigation, it was decided by the principals of this investigation that it would be of value to test the Hveem samples at 4.0% binder content and drop the investigation of the 6.5% samples. This change was made in an attempt to investigate the stability, unit weight and per cent air voids of the mixtures below 4.5%, which graphically were quite flat, particularly for the 50/50 S/A mixture in the Marshall mix design (see Figure 3.8), below approximately 5.0% binder content.

This design method is based upon the friction and cohesion of the paving material. The friction is evaluated by the Hveem stabilometer, which measures the horizontal pressure as vertical pressure is applied (see Figure 3.9). The cohesion is tested by means of a cohesiometer, which measures the force required to pull the test sample apart. Because the cohesive test is destructive, it was not performed, but the stabilometer evaluation was.

The determination of optimum binder content is accomplished by comparing results of the Hveem testing with standard criteria. The criteria are:



NOTE: SPECIMEN GIVEN LATERAL SUPPORT BY FLEXIBLE SIDE WALL WHICH TRANSMITS HORIZONTAL PRESSURE TO LIQUID MAGNITUDE OF PRESSURE MAY BE READ ON GAUGE

Figure 3.9. HVEEM STABILOMETER

- maximum value of stabilometer value in excess of 35
- a minimum 4% air voids

The binder content is determined graphically, then compared to the above criteria.

The tabular and graphic results of the Hveem testing conducted on sample sets D, E and F are shown in Tables 3.8 - 3.10 and Figures 3.10 - 3.12.

Determined Optimum Binder Content

0.100 S/A Ratio

<u>Data Type</u>	<u>Value</u>	<u>Binder Content</u>
Air voids	Approx. 4.0	4.6
Stability	47.1	4.5
Optimum		4.6

30/70 S/A Ratio

<u>Data Type</u>	<u>Value</u>	<u>Binder Content</u>
Air voids	Approx. 4.0	4.4 (5.2)
Stability	50.4	4.5 (5.3)
Optimum		4.4 (5.2)

Table 3.8. HVEEM MIX DESIGN DATA
100/0 ASPHALT/SULPHUR RATIO

BINDER CONTENT (%) BY WEIGHT	SAMPLE	WEIGHT IN AIR (GRAMS)	WEIGHT IN WATER (GRAMS)	BULK SPECIFIC GRAVITY	UNIT WEIGHT	MAXIMUM SPECIFIC GRAVITY	% AIR VOIDS	STABLO- METER VALUE
4.0	D1	1217.0	724.0	2.468				42.3
	D2	1231.0	735.0	2.482				42.1
	D3	1236.0	732.0	2.452	153.9	2.665	8.1	40.4
				<u>2.467</u>				<u>41.6</u>
4.5	D4	1238.0	742.0	2.496				52.4
	D5	1236.0	742.0	2.502				46.0
	D6	1223.0	738.0	2.522	156.4	2.619	4.2	43.1
				<u>2.507</u>				<u>47.1</u>
5.0	D7	1232.0	748.0	2.545				52.7
	D8	1234.0	746.0	2.529				46.8
	D9	1233.0	750.0	2.553	1.587	2.591	1.6	40.0
				<u>2.542</u>				<u>46.5</u>
5.5	D10	1239.0	760.0	2.587				47.0
	D11	1232.5	757.0	2.592				47.0
	D12	1235.0	748.0	2.536	160.6	2.587	0.5	49.4
				<u>2.572</u>				<u>47.8</u>
6.0	D13	1236.0	760.0	2.597				40.0
	D14	1211.0	748.0	2.616				40.0
	D15	1257.0	777.0	2.619	163.1	2.614	0.04	34.5
				<u>2.611</u>				<u>38.2</u>

Table 3.9. HVEEM MIX DESIGN DATA
70/30 ASPHALT/SULPHUR RATIO

BINDER CONTENT (%) BY WEIGHT	SAMPLE	WEIGHT IN AIR (GRAMS)	WEIGHT IN WATER (GRAMS)	BULK SPECIFIC GRAVITY	UNIT WEIGHT	MAXIMUM SPECIFIC GRAVITY	% AIR VOIDS	STABILO- METER VALUE
4.0 (4.7)	F1	1233.0	732.0	2.461				47.0
	F2	1236.0	731.0	2.448				52.4
	F3	1238.0	737.0	2.471	153.5	2.639	6.4	40.4
				2.460				46.6
4.5 (5.3)	F4	1249.0	755.0	2.528				51.1
	F5	1237.0	742.0	2.499				47.5
	F6	1246.0	753.0	2.527	157.2	2.597	3.0	52.6
				2.518				50.4
5.0 (5.9)	F7	1243.0	757.0	2.558				50.9
	F8	1252.0	759.0	2.540				55.6
	F9	1248.0	759.0	2.552	159.1	2.592	1.6	51.7
				2.550				52.7
5.5 (6.5)	F10	1262.0	771.0	2.570				49.9
	F11	1236.0	756.0	2.575				53.6
	F12	1254.5	763.0	2.552	160.2	2.587	0.8	53.2
				2.566				52.2
6.0 (7.1)	F13	1249.0	772.0	2.618				48.3
	F14	1254.0	773.0	2.607				52.6
	F15	1252.0	763.0	2.560	162.1	2.599	0.08	51.1
				2.595				50.7

Table 3.10. HVEEM MIX DESIGN DATA
50/50 ASPHALT/SULPHUR RATIO

BINDER CONTENT (%) BY WEIGHT	SAMPLE	WEIGHT IN AIR (GRAMS)	WEIGHT IN WATER (GRAMS)	BULK SPECIFIC GRAVITY	UNIT WEIGHT	MAXIMUM SPECIFIC GRAVITY	% AIR VOIDS	STABLO- METER VALUE
4.0 (5.4)	E1	1241.0	736.0	2.458				58.6
	E2	1248.0	740.0	2.457				63.0
	E3	1243.0	736.0	2.452	153.3	2.651	7.6	55.4
				2.456				59.2
4.5 (6.1)	E4	1261.0	752.0	2.477				62.4
	E5	1257.0	755.0	2.504				64.8
	E6	1248.0	746.0	2.486	155.4	2.630	5.3	65.0
				2.489				64.1
5.0 (6.7)	E7	1254.0	753.0	2.503				62.1
	E8	1243.0	741.0	2.476				59.7
	E9	1244.0	743.0	2.483	155.1	2.610	5.0	61.6
				2.487				61.1
5.5 (7.4)	E10	1263.0	770.0	2.562				65.2
	E11	1266.0	766.0	2.532				69.7
	E12	1258.0	764.0	2.547	158.9	2.575	1.1	65.3
				2.547				66.7
6.0 (8.1)	E13	1242.0	760.0	2.577				65.0
	E14	1265.0	774.0	2.576				66.1
	E15	1243.0	754.0	2.542	160.2	2.571	0.2	52.7
				2.565				61.4

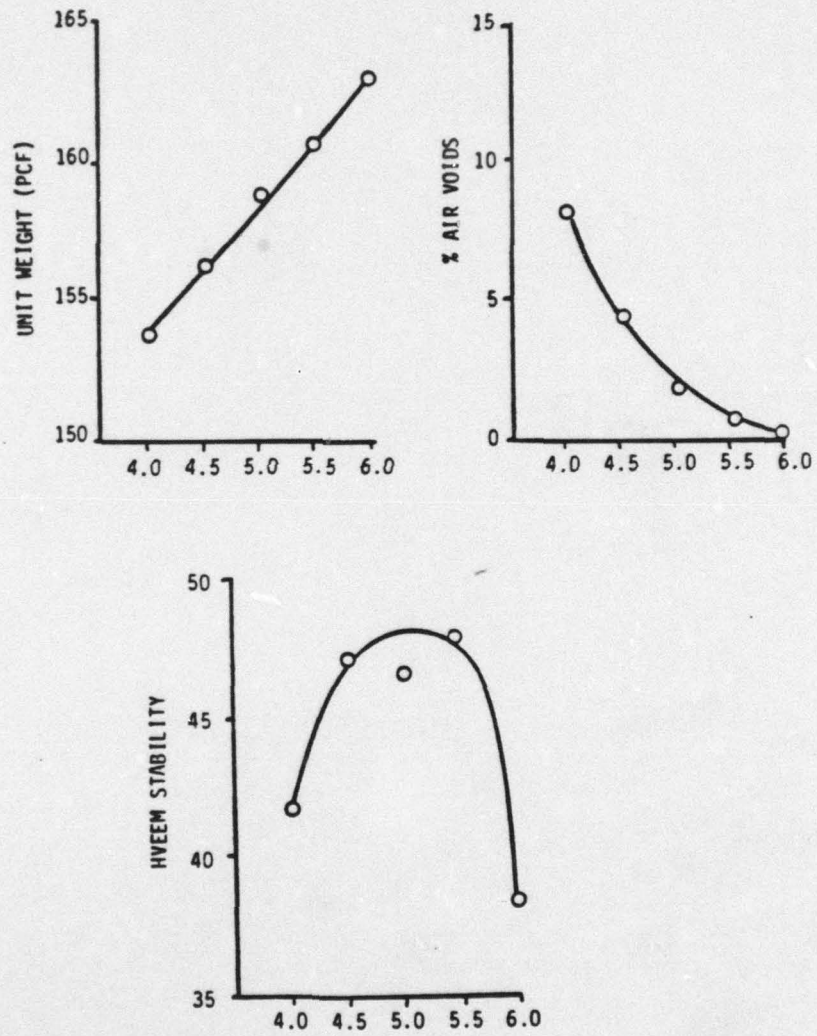


Figure 3.10. HVEEM MIX DESIGN DATA CURVES
100/0 ASPHALT/SULPHUR RATIO

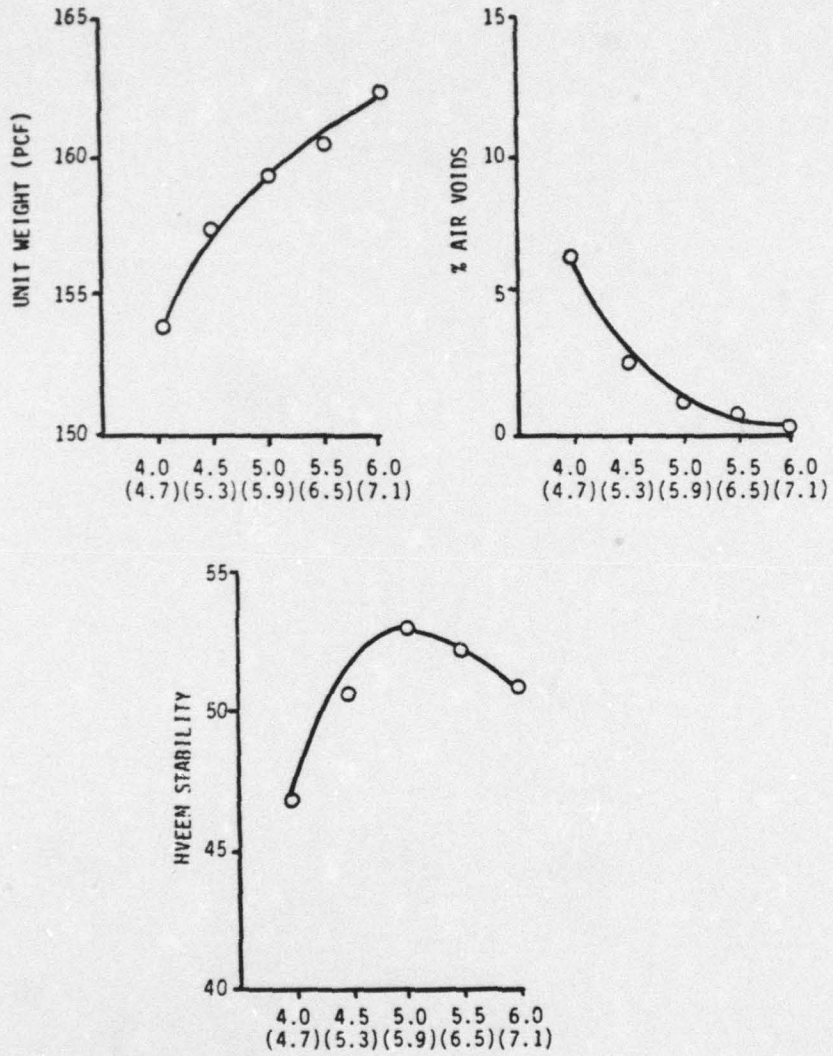


Figure 3.11. HVEEM MIX DESIGN DATA CURVES
70/30 ASPHALT/SULPHUR RATIO

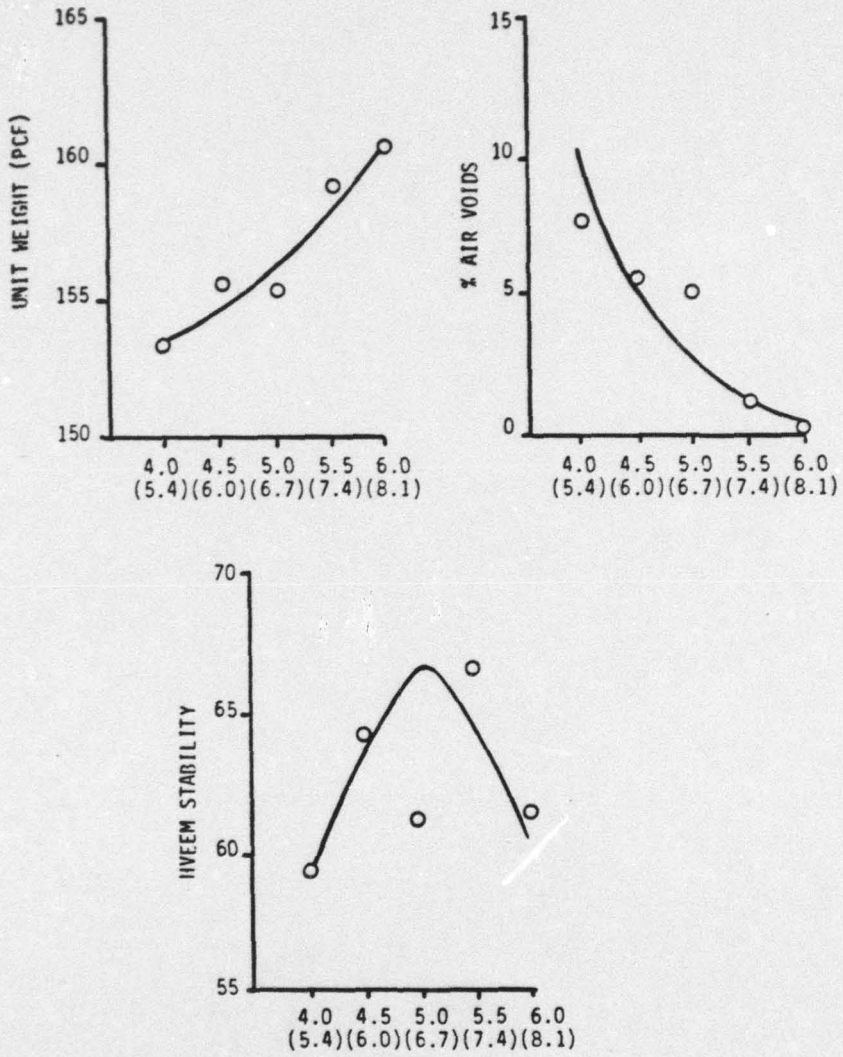


Figure 3.12. HVEEM MIX DESIGN DATA CURVES
50/50 ASPHALT/SULPHUR RATIO

<u>50/50 S/A Ratio</u>		
<u>Data Type</u>	<u>Value</u>	<u>Binder Content</u>
Air voids	Approx. 4.0	5.1 (6.9)
Stability	61.1	5.0 (6.7)
	Optimum (5.1 - 0.3)	5.1 (6.9)

Discussion of the Hveem Mix Designs

The Hveem indicated optimum binder contents are approximately 0.5% lower than the Marshall recommended binder contents. This is probably due to the automated compaction method and the heated mold in the Hveem compaction device. With the heated mold, no sulfur bridging is allowed to build up where the sample is in contact with the mold.

Examination of Figures 3.13 and 3.14 shows marked correlation in shape and magnitude of the Hveem stability for 0/100 and 30/70 S/A binder ratios. This concurs with other research noted in Chapter I.

The optimum asphalt binder content recommended to WSDOT was 5.5% of equivalent binder content. This was based upon close scrutiny of all laboratory work (including a mix design work done by SUDIC for this project) and the knowledge that the optimum binder content for field conditions are often higher than obtained in the laboratory. Subsequent to the recommendation, it was learned that historically, the optimum binder content for this aggregate blend is between 5.5% and 6.0% [26].

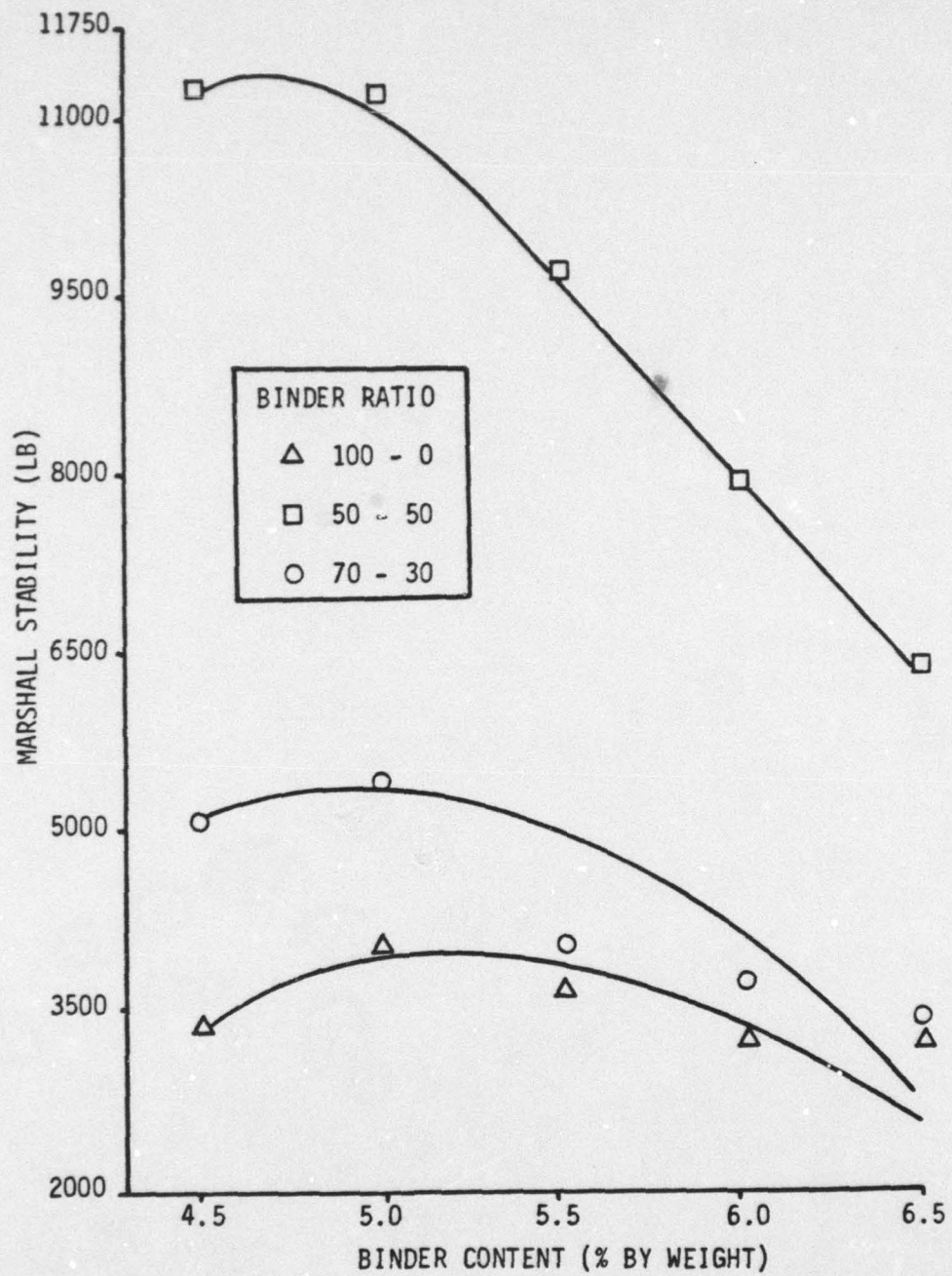


Figure 3.13 COMPARISON OF MARSHALL STABILITIES OF VARIOUS ASPHALT/SULPHUR RATIO SAMPLES

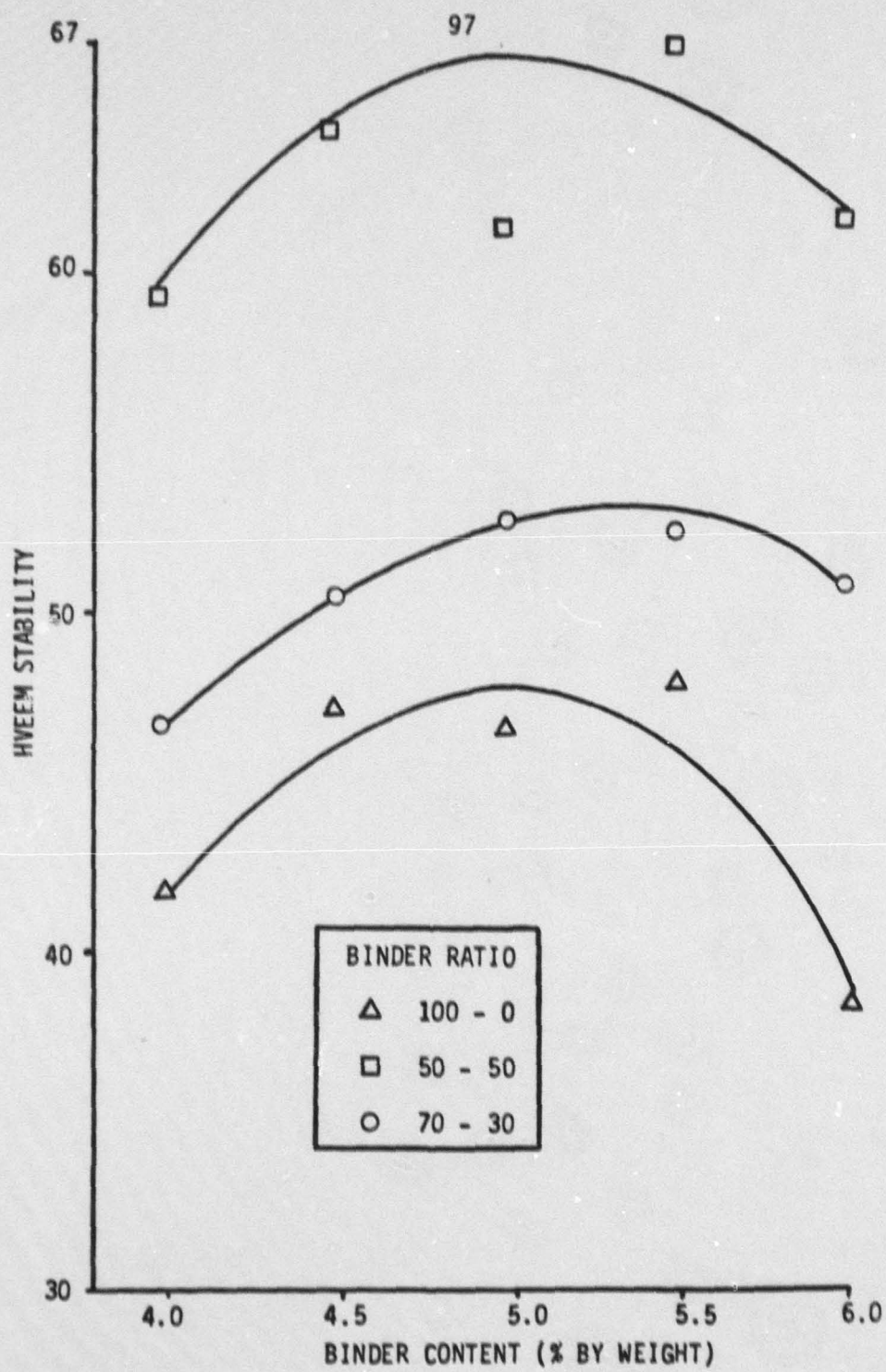


Figure 3.14 COMPARISON OF HVEEM STABILITIES OF VARIOUS ASPHALT/SULPHUR RATIO SAMPLES

Resilient Modulus

The resilient modulus (M_R) is a dynamic test response defined as the ratio of the repeated axial deviator stress to the recoverable axial strain. The test may be conducted on all types of material ranging from cohesive to stabilized materials [36].

In this study, the M_R was tested on each sample for seven consecutive days (see Figures 3.4 and 3.5). Each sample was loaded on two diametral axes and the average deformation was used to calculate M_R with the following formula:

$$M_R = \frac{P(\mu + 0.2734)}{t\Delta h}$$

where

M_R = resilient modulus

P = vertical pressure

μ = Poisson's ratio

t = thickness, inches

Δh = deformation calculated from the amplitude of graph from a strip chart recorder

The temperature of the samples during this testing was 25°C (77°F). Upon completion of the seven days testing, the samples were tested at 5°C (41°F) and 40°C (104°F) to determine M_R as a function of temperature.

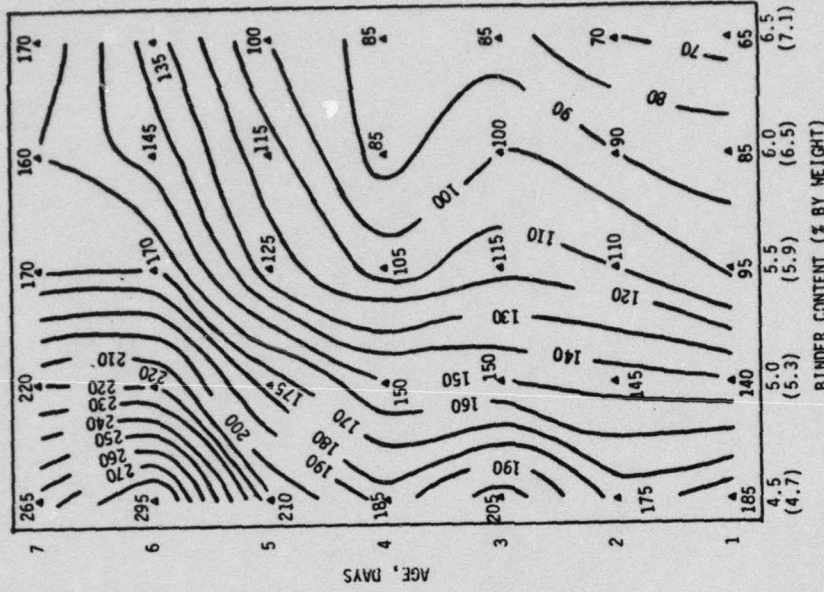
Poisson's ratio was also determined for each sample (Poisson's ratio = lateral strain to vertical strain). Due to large variations

in the determined values, the method used in determining them were suspect, particularly the measurement of vertical deflection that had to be measured with a non-recording dial gauge. The Poisson's ratio that was used in the determination of M_R 's was 0.3. This is a comparable Poisson's ratio to that determined in the Boulder City Field Trials [3] and by Schmidt [37] and by Galloway and Saylak [38]. Schmidt recommends a value of 0.35 for Poisson's ratio. This was based on experiments which showed that Poisson's ratio varies from 0.2 to 0.5 for asphaltic materials. Therefore, a value of 0.35 would result in an error of not more than 25%. Galloway and Saylak suggest a value of 0.3 for sulfur-asphalt materials.

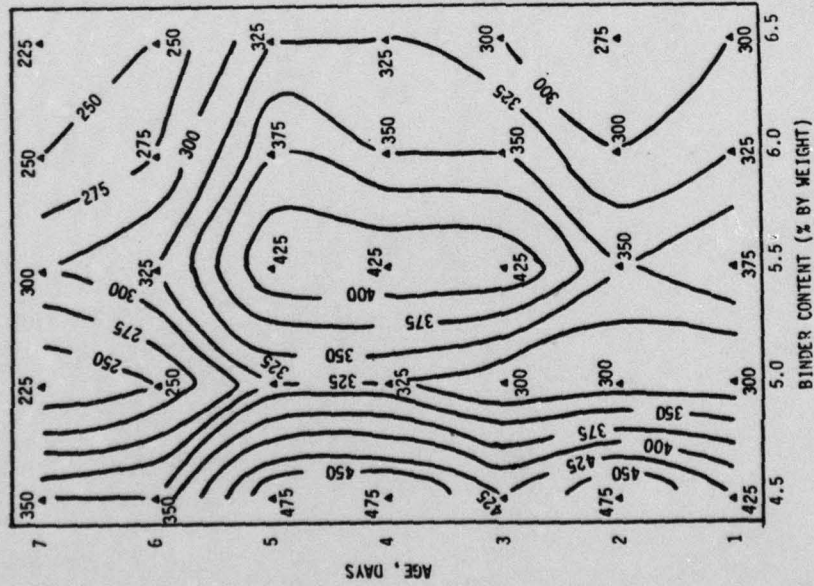
The results of the M_R values at 25°C (77°F) have been graphically contoured in Figures 3.15 and 3.16. Figure 3.15 depicts lines of constant M_R with respect to sample age and binder content for the Marshall samples (samples A, B and C). Figure 3.16 depicts the same information for Hveem samples (samples D, E and F). A cross-sectional depiction of M_R vs. age at the recommended design binder content is depicted in Figure 3.17. The M_R response of the samples at the recommended design binder content as a function of temperature is illustrated for the Marshall samples in Figure 3.18 and for the Hveem samples in Figure 3.19.

Pavement Thickness

To design the appropriate thicknesses for the different test track sections, one key factor had to be kept in mind. Previous

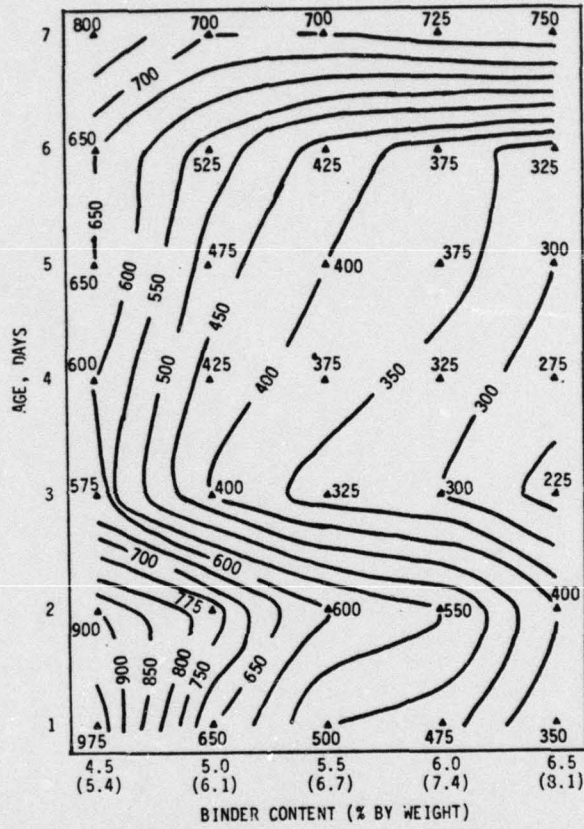


M_R VS BINDER CONTENT AND DAYS OF CURE AT 25°C (77°F)
MARSHALL SAMPLES, 70/30 ASPHALT/SULPHUR RATIO



M_R VS BINDER CONTENT AND DAYS OF CURE AT 25°C (77°F)
MARSHALL SAMPLES, 100/0 ASPHALT/SULPHUR RATIO

Figure 3.15. M_R VS BINDER CONTENT AND DAYS OF CURE,
MARSHALL SAMPLES, VARYING ASPHALT/SULFUR RATIOS



N. VS BINDER CONTENT AND DAYS OF CURE AT 25°C (77°F)
 F. MARSHALL SAMPLES, 50/50 ASPHALT/SULPHUR RATIO

Figure 3.15 (continued)

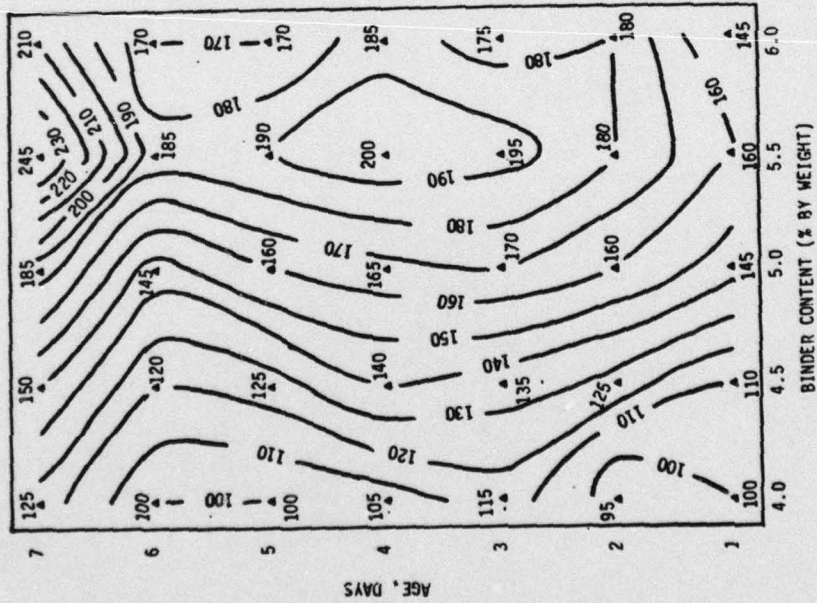
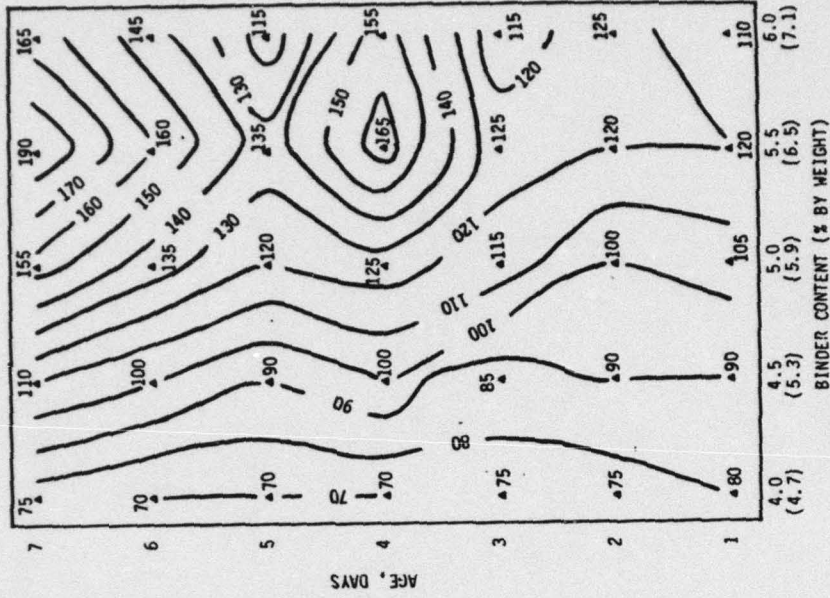


Figure 3.16. M_R VS BINDER CONTENT AND DAYS OF CURE, HVEEM SAMPLES, VARYING ASPHALT/SULFUR RATIOS

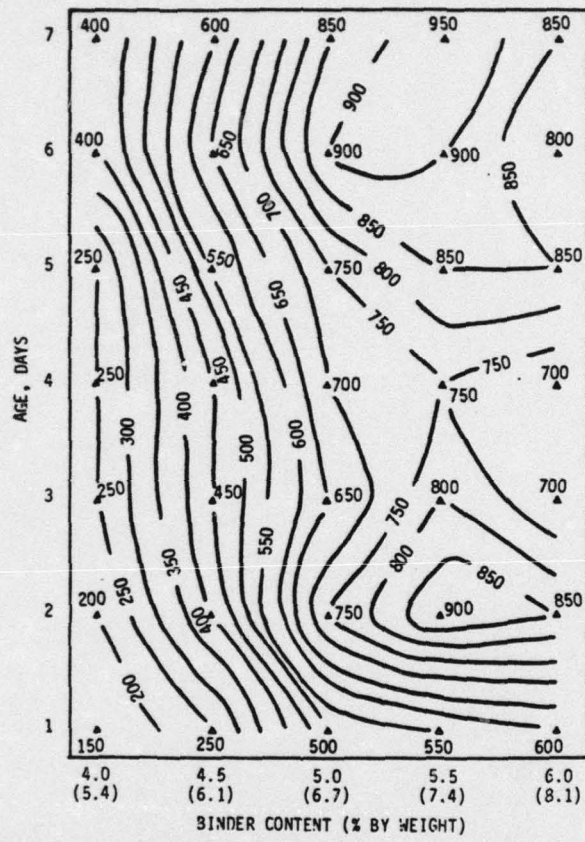


Figure 3.16 (continued)

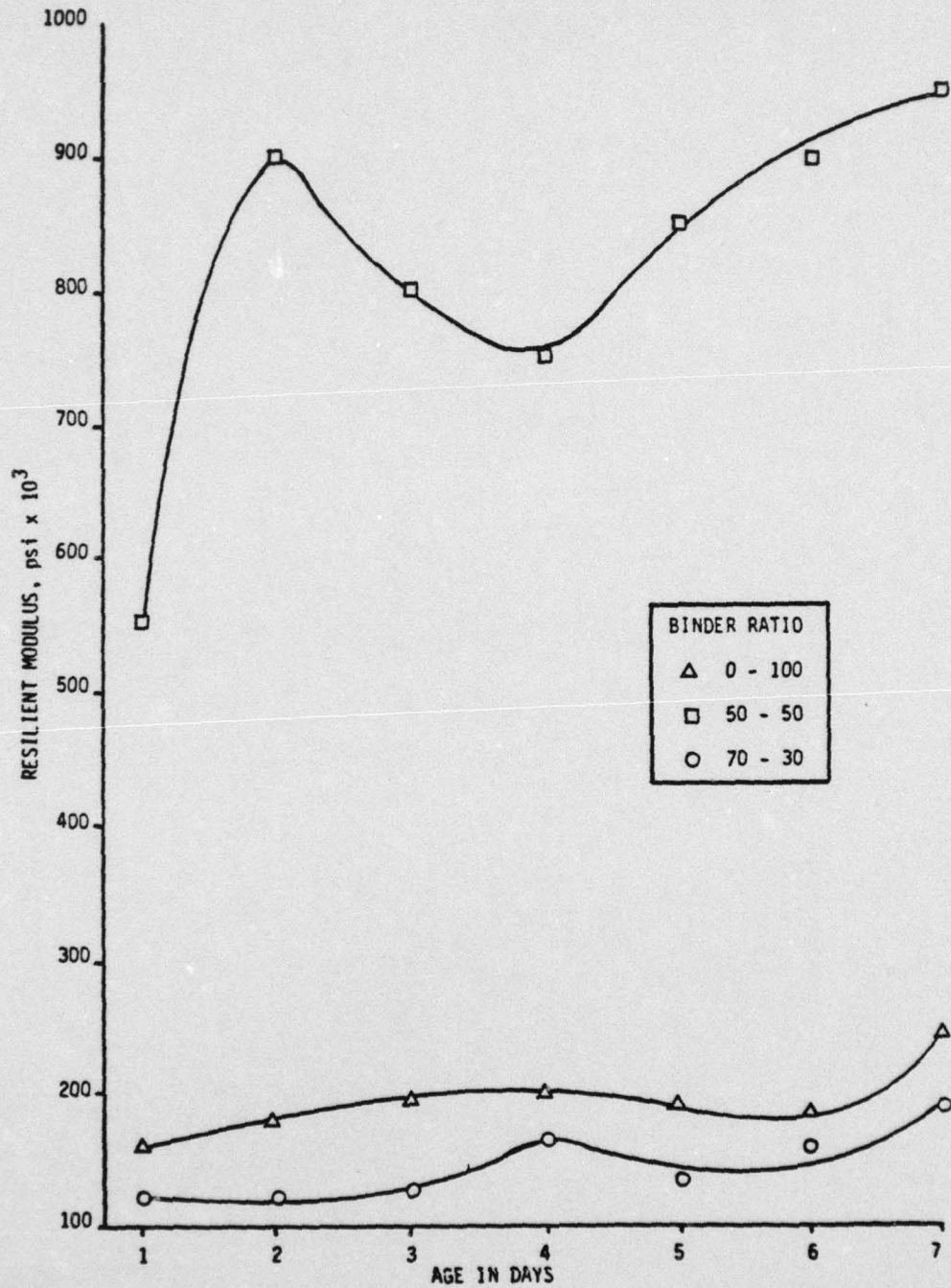


Figure 3.17. CROSS SECTION OF M_R VALUES OF HVEEM SAMPLES AT 5.5% BINDER CONTENT

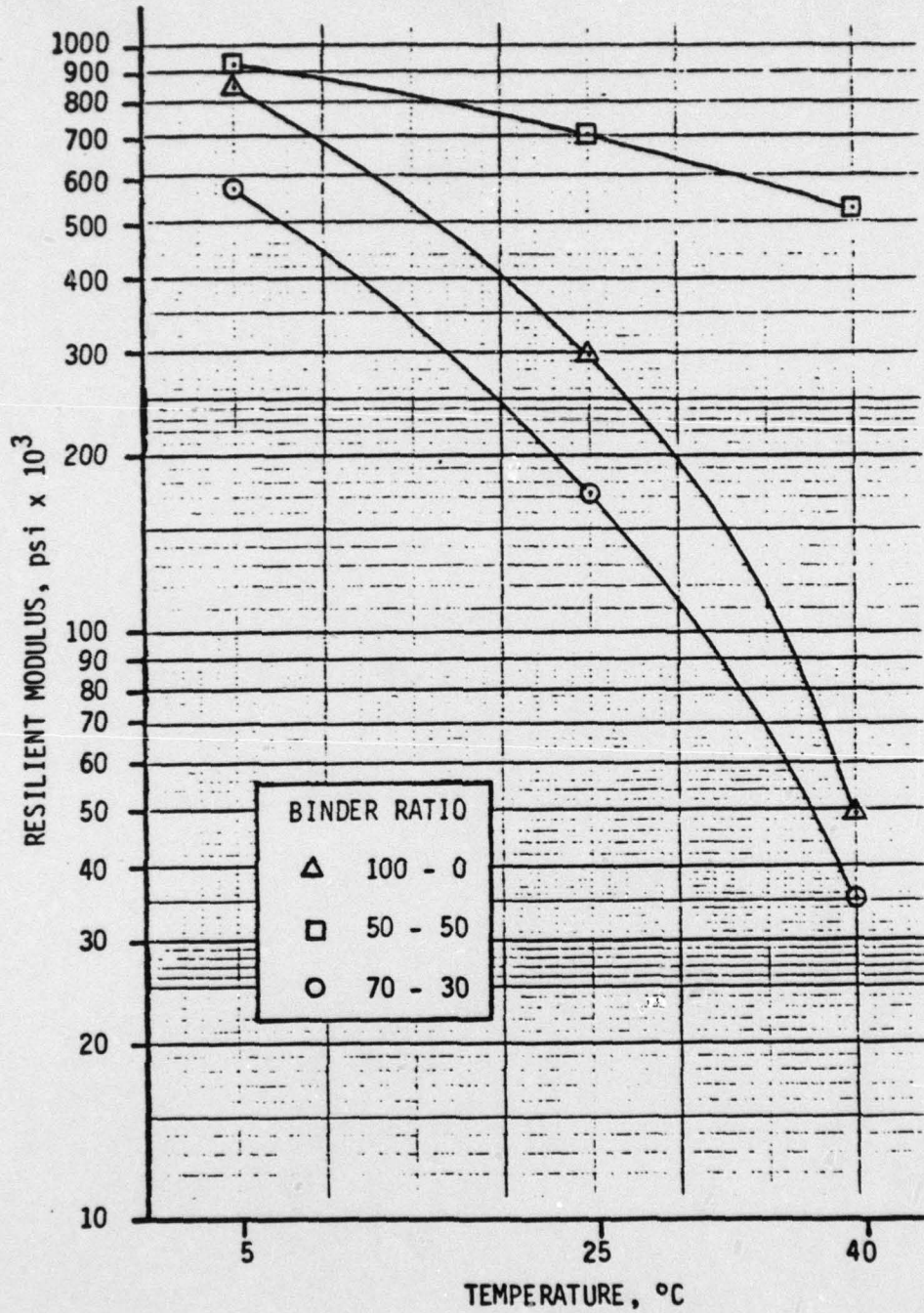


Figure 3.18 5.5% BINDER CONTENT, M_R VS TEMPERATURE: MARSHALL SAMPLES

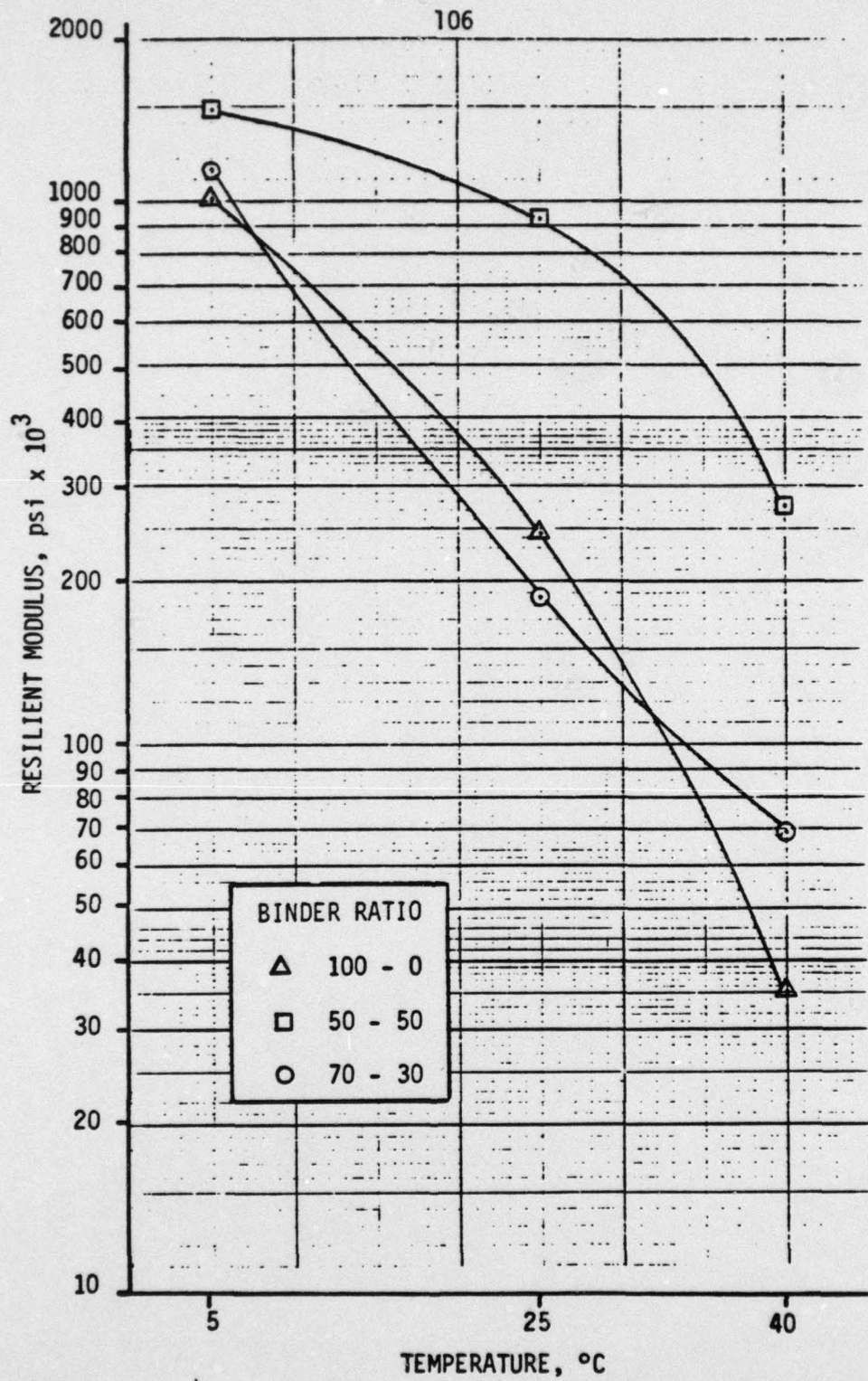


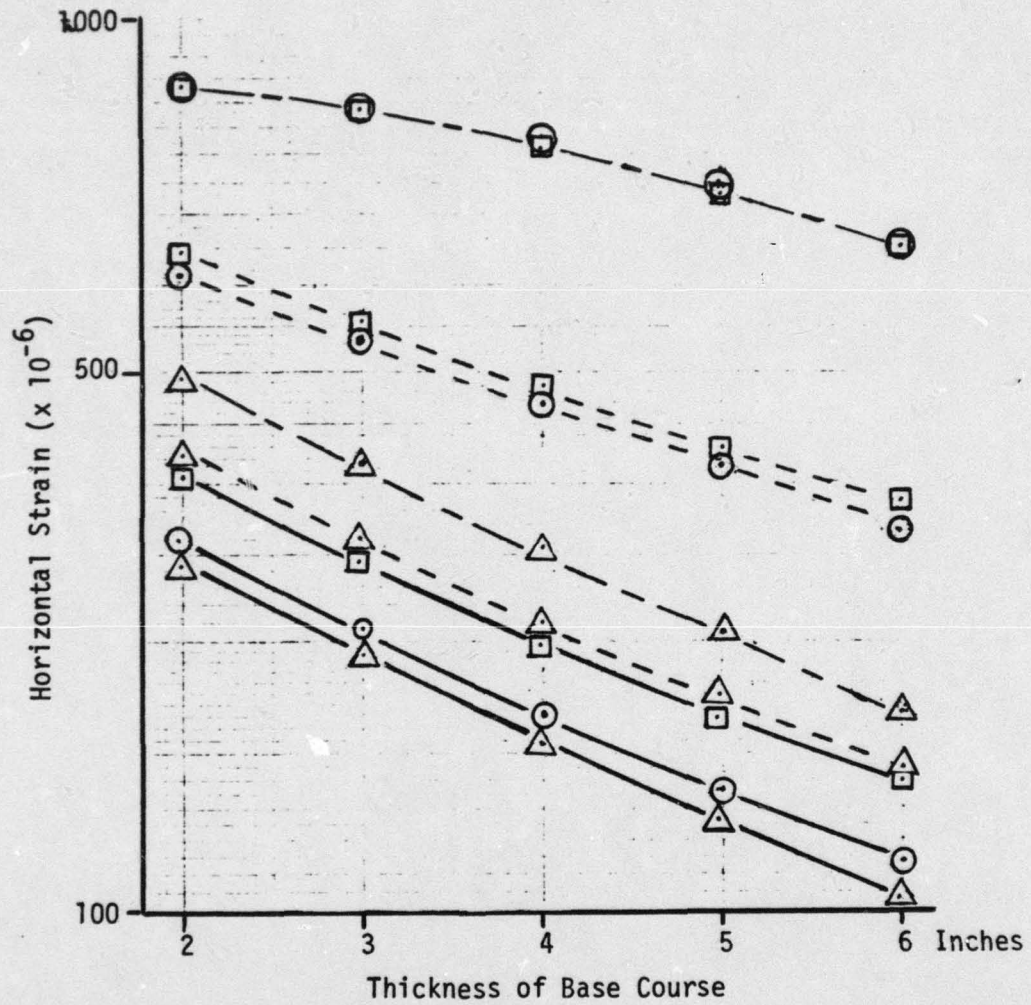
Figure 3.19. 5.5% BINDER CONTENT, M_R VS TEMPERATURE: HVEEM SAMPLES

pavement studies that had been run at the WSU test track had indicated that there was a tendency for the spring thaw to dramatically promote the failure of the test track. It was, therefore, thought advantageous by all concerned to have failure in all sections prior to freezing of the subgrade. This date was set as 1 December 1979.

It was calculated that 1.5 million load repetitions could be applied to the track by 1 December 1979. This was based on an average expected loading rate of 500,000 repetitions per month and expected full months of operation from 1 August through 1 December 1979.

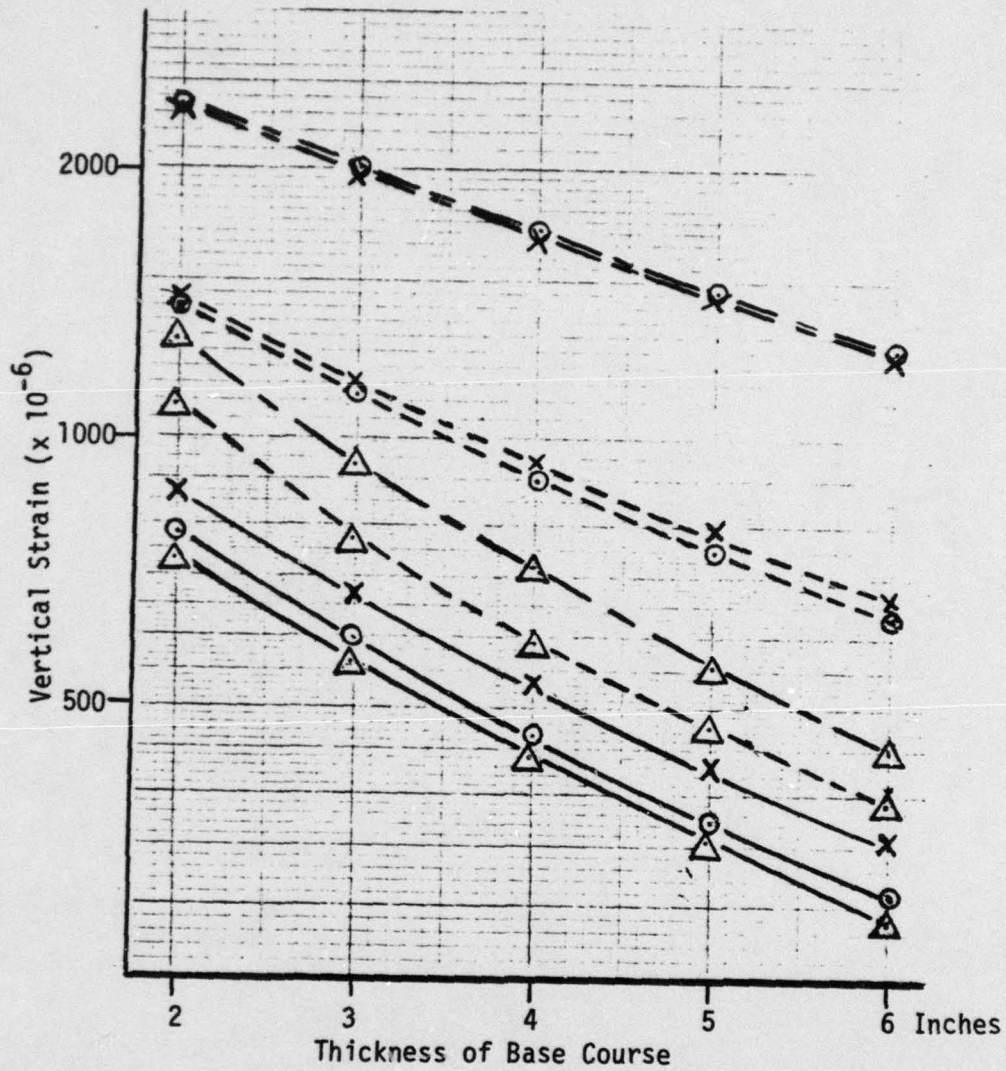
With this in mind, a computer analysis utilizing Shell Oil's computer program [42], entitled Bitumen Structures Analysis in Roads (BISAR), was developed whereby various thicknesses of each of the mixes were analyzed. The essential items developed from the BISAR analysis were the predicted initial maximum horizontal and vertical strains in the pavement for thicknesses varying from a 2-inch base course to a 6-inch base course at 5°, 25° and 40°C for each thickness and S/A ratio. The results of this analysis are graphically illustrated in Figures 3.20 and 3.21.

The essential items of input for the BISAR program are as follows [42]:



- 0-100%
- 30-70%
- △ 50-50%
- 40°C
- .-. 25°C
- 5°C

Figure 3.20 BISAR PREDICTED MAXIMUM INITIAL HORIZONTAL STRAIN VS VARIOUS BASE COURSE THICKNESSES



o 0-100%
 x 30-70%
 Δ 50-50%
 --- 40°C
 - - - 25°C
 ——— 5°C

Figure 3.21. BISAR PREDICTED MAXIMUM INITIAL VERTICAL STRAIN VS VARIOUS BASE COURSE THICKNESSES

<u>Element Required</u>	<u>Used in Analysis</u>
1. Number of layers	3 (surface course, base course and subgrade)
2. Young's Modulus (M_R) of each layer	Appropriate M_R for each temperature as developed in laboratory for Hveem samples and a M_R of 18,000 for the subgrade
3. Poisson's ratio of each layer	Assumed to be 0.30
4. Thickness of all but base layer	1.8 inches for surface course and from 2 to 6 inches in 1-inch increments
5. Loads	2 each 5,300-lb. normal loads
6. Load Position	Above loads separated by 13 inches

A subgrade M_R of 18,000 psi was based upon an expected moisture content of approximately 16-17%. During actual construction and during track operations this was found to be much too low. The M_R of the subgrade should have been closer to 4,000, which corresponds to a water content of approximately 21%.

Utilizing the maximum horizontal strains developed by BISAR and Kingham and Kallas's equation [44] for estimating the number of load repetitions to failure, Figure 3.22 was developed. Utilizing this figure, given a specific number of load applications, an expected operating temperature and a S/A ratio of 0/100, 30/70 or 50/50, the thickness of the base course required can be found.

Upon entering Figure 3.22 with 1.5×10^6 load repetitions at 25°C, a 5½-inch SA 30/70 or 0/100 pavement would fail by 1 December, 1979.

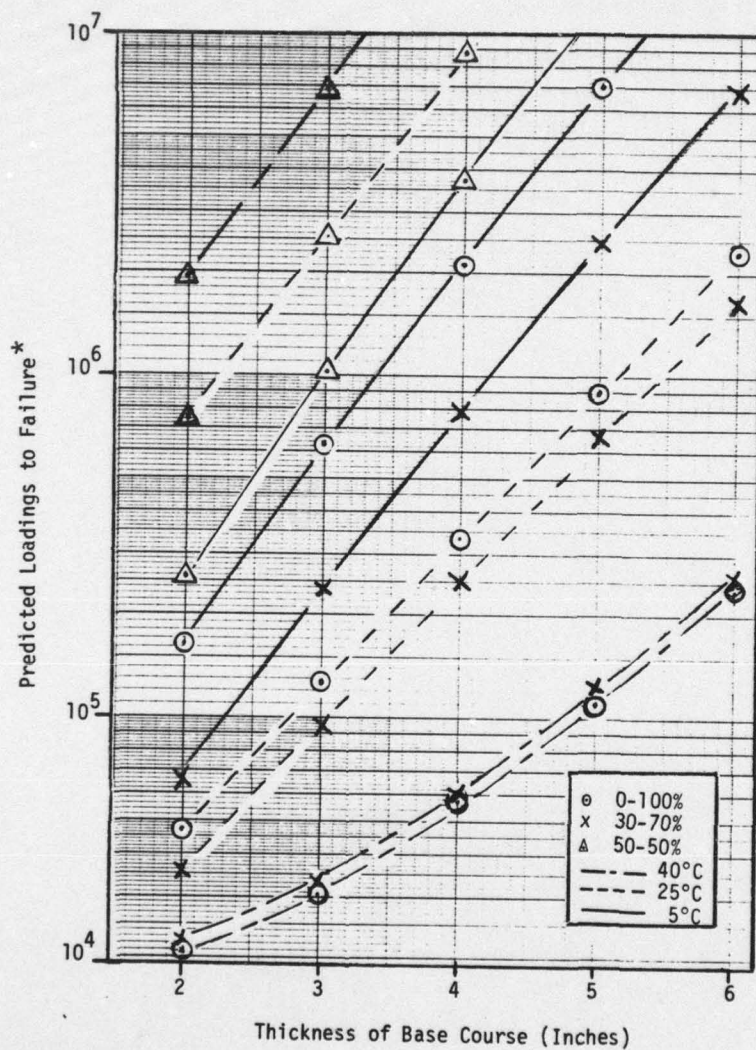


Figure 3.22. PREDICTED LOADS TO FAILURE VS THICKNESS OF BASE COURSE

*See Chapter V for Kingham and Kallas' fatigue criteria equation.

The thicknesses finally selected were 5 and 2.5 inches, respectively, for the thick and thin sections' base courses. This decision was based on two lines of reasoning. First, it had been decided for simplicity's sake that the thick sections would be twice the thickness of the thin sections. Secondly, it was felt that perhaps 1.5 million repetitions was overly optimistic. By reducing the thickness an extra 1/2 inch, failure could be insured before the 1 December deadline.

CHAPTER IV
CONSTRUCTION AND INSTRUMENTATION
OF THE WSU TEST TRACK

WSU Test Track Equipment

The equipment at the test track consists of a 15-ton structural steel frame (Figures 4.1 - 4.3) and a water tank revolving over an 85.54-ft. diameter ring. This applies what was previously thought to be a 10,600 lb. load to each of three sets of dual wheels. Actual weights taken by the Washington State Department of Transportation with a lodometer indicated the following loads are actually being applied:

Arm and Tire Assembly #1: 11,400 lbs.
#2: 11,650 lbs.
#3: 10,350 lbs.

Average Arm and Tire Assembly: 11,133 lbs.

All instrumentation was constructed to be activated by Assembly #1. This was done because Wheel and Arm Assembly #1 is closest to the average weight (actually, approximately 2% above the average weight).

A feature of the test track that was not utilized during this test is the capability of adding water to the water tank. By doing so the load on each set of duals can be brought to over 20,000 lbs.

To keep the wheels from continuously moving in the same wheel path, the center of rotation of the structure is designed so that various wheel path widths can be applied to the pavement structure. In this study the wheel path was set at 4 ft. from outside of wheel path to inside of wheel path. This yielded a loading distribution as illustrated in Figure 4.4. A 4-ft. wheel path closely approximates

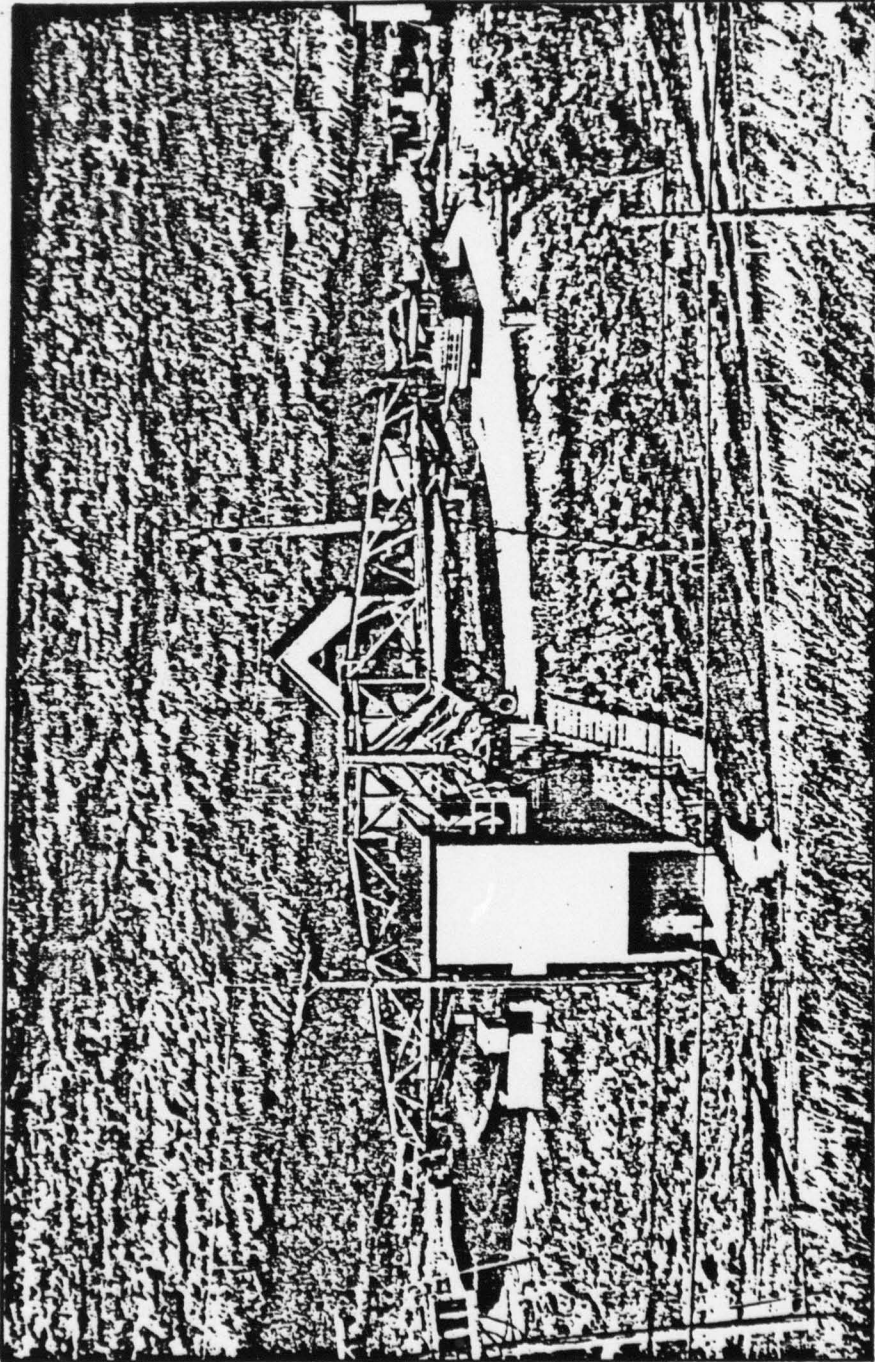


Figure 4.1 TEST TRACK - WASHINGTON STATE UNIVERSITY

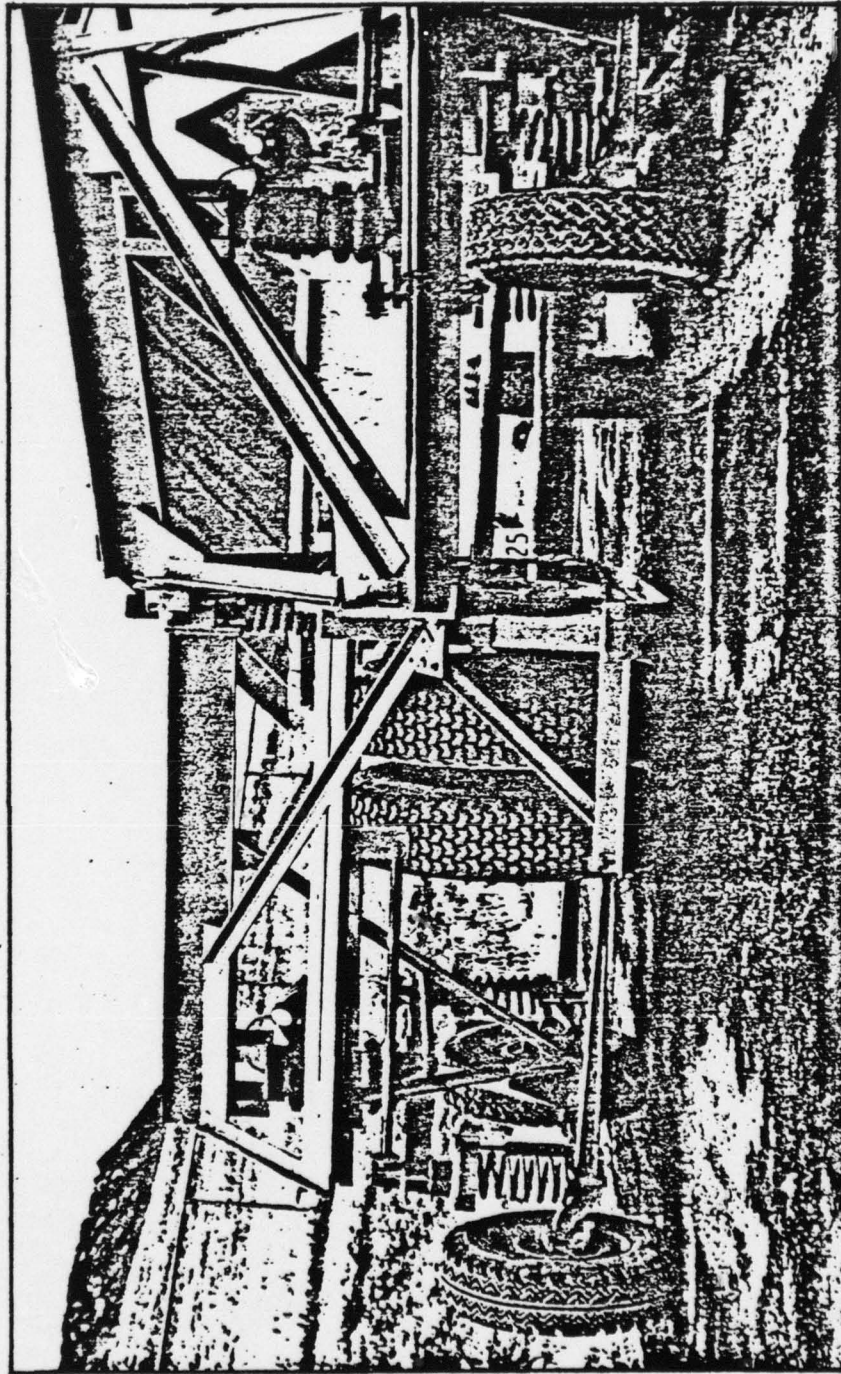


Figure 4.2 WHEEL AND TIRE ARRANGEMENT

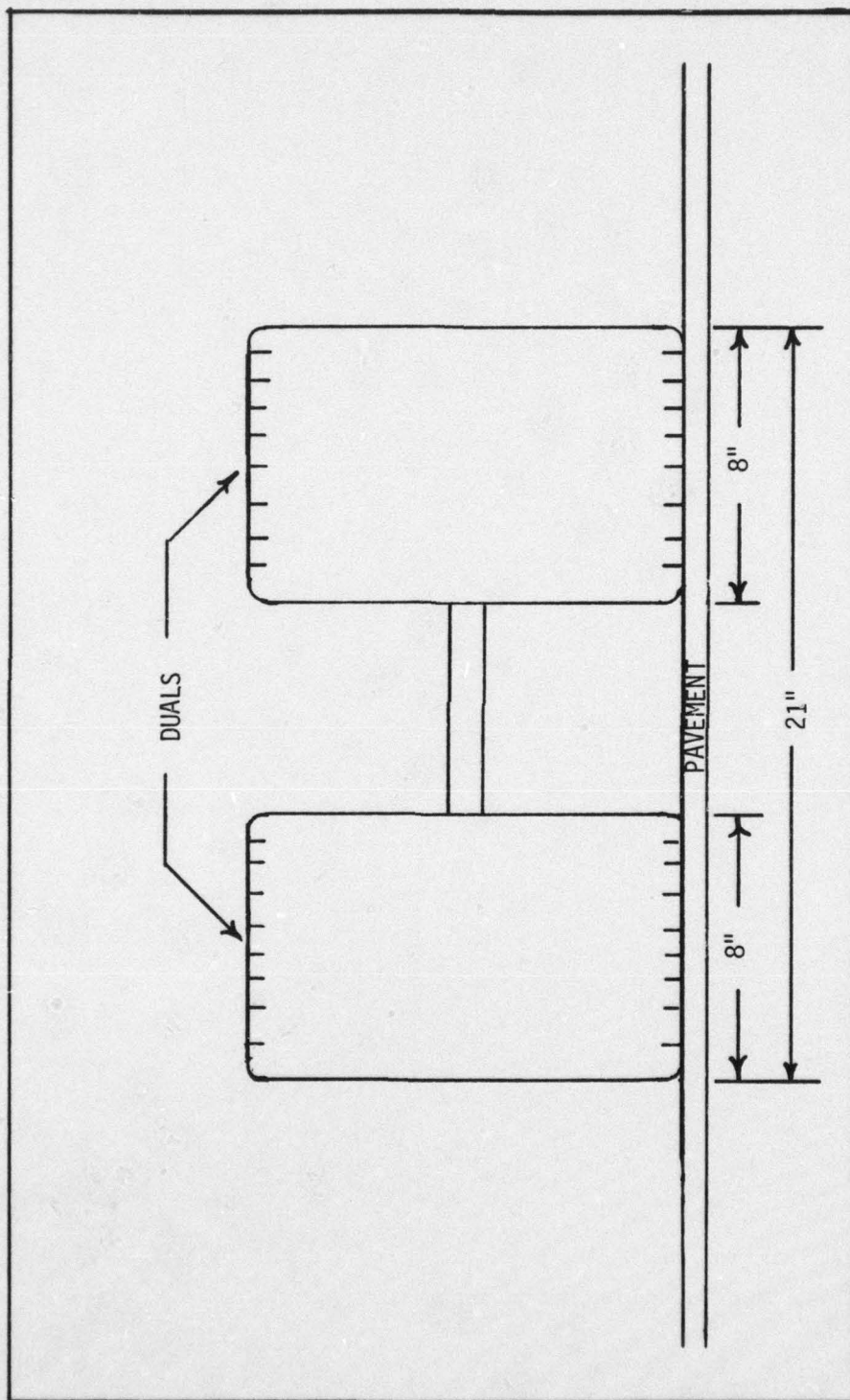


Figure 4.3. SCHEMATIC OF DUAL SIZE AND SPACING

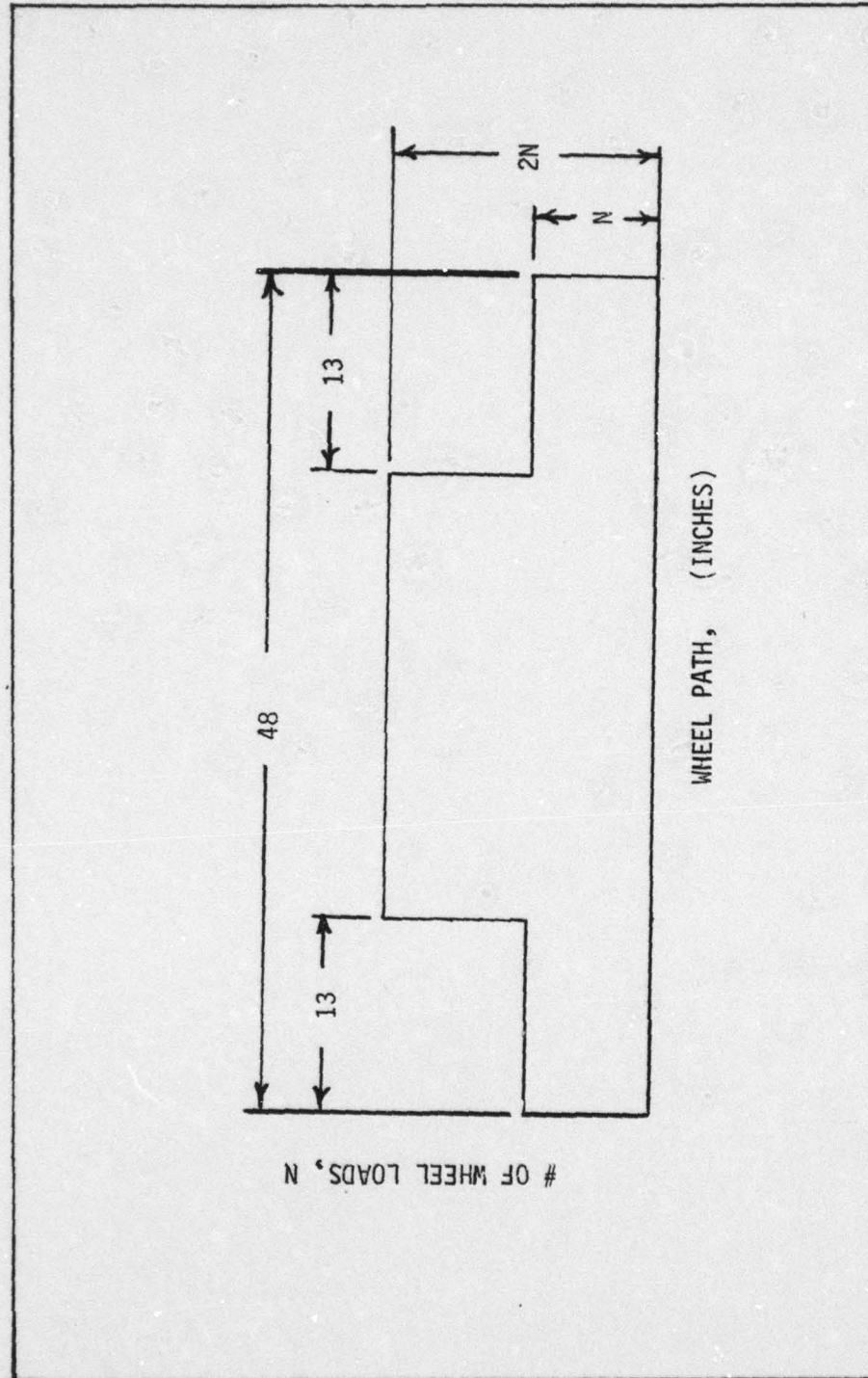


Figure 4.4. LOAD DISTRIBUTION IN WHEEL PATH

that experienced on actual highways.

The loading frame is guided by a 6½-in. diameter vertical steel shaft. This shaft rotates in a self-aligning bearing mounted in a power-driven revolving frame. The frame is designed to operate in either a clockwise or counterclockwise direction at speeds of from 15 to 45 mph. The frame is powered by a 440-volt three-phase alternating current 200-horsepower General Electric Kinamatic Speed Variator which supplies 220-volt direct current to each of three 60-horsepower motors geared directly to the wheels. Power is supplied only to the inside wheel of each dual.

During this testing the frame rotated in a clockwise direction at a normal operating speed of less than 30 mph. Speed was reduced even further when the track began to deteriorate in order to reduce excessive dynamic loading due to bouncing of the tires.

Preparation of the Track Prior to Placement of the Test Sections

The previous test track had utilized reinforced concrete sections placed on approximately 6 inches of crushed basalt base course. In order to insure a uniform platform for the sulfur-extended asphalt sections and to simplify the analysis of the test section failures without taking into account the effects of an overly supportive base, it was decided by the principals of the project to build the test sections directly on the naturally occurring Palouse Silt subgrade.

To insure complete removal of the crushed basalt base course, all material to a depth of approximately 12 inches below the previous

test track was removed. Once all material was removed down to the Palouse subgrade, uncontaminated Palouse Silt was placed in two lifts and brought to grade to support 12 test sections designed as illustrated in Figures 4.5 and 4.6.

Moisture contents were taken of the imported subgrade. The initial moisture contents were sampled as emplaced. The moisture content of the subgrade is presented in Figure 4.7. An average of all samples taken indicates an average moisture content for the subgrade as initially placed of 20.2%. It was felt that this moisture content was too high to afford adequate compaction of the subgrade and that the moisture content should be reduced.

After scarification of the subgrade and allowing the subgrade to dry for approximately a full day, an average moisture content of 17.5% was attained. At this moisture content the subgrade appeared to compact readily than it had when it was wetter. When it was wetter, there was excessive deformation of the subgrade after every pass of the smooth wheel 10-ton Gallion roller. Samples indicated, however, that this lowering of moisture content was effective to a depth of 6 to 12 inches. At depths lower than that, the moisture content remained at approximately 21%.

Once the new subgrade was emplaced and cut to conform with Figure 4.5, densities of the subgrade were taken with a Troxler Nuclear Relative Compaction Testing Device. The final achieved subgrade densities are given in Table 4.1.

Table 4.1. TEST TRACK SUBGRADE DENSITIES

	SECTION	1	2	3	4	5	6	7	8	9	10	11	12
8/15/79	DRY DENSITY *	102.5	100.4	100.4	105.3	105.3	106.4	106.4	103.4	103.0	102.3	102.3	102.5
	DESCRIPTION:	ORIGINAL SUBGRADE											
8/16/79	DRY DENSITY *	96.7	96.7	98.5	N/A	110.2	105.4	N/A	100.1	98.7	98.3	98.3	N/A
	DESCRIPTION:	FIRST LIFT (6")											
8/17/79	DRY DENSITY *	105.1	N/A	101.1	101.1	N/A	96.2	96.2	100.2	98.4	97.7	97.7	99.8
	DESCRIPTION:	SECOND (FINAL) 6" LIFT											
N/A = not available													
*lbs/ft ³													

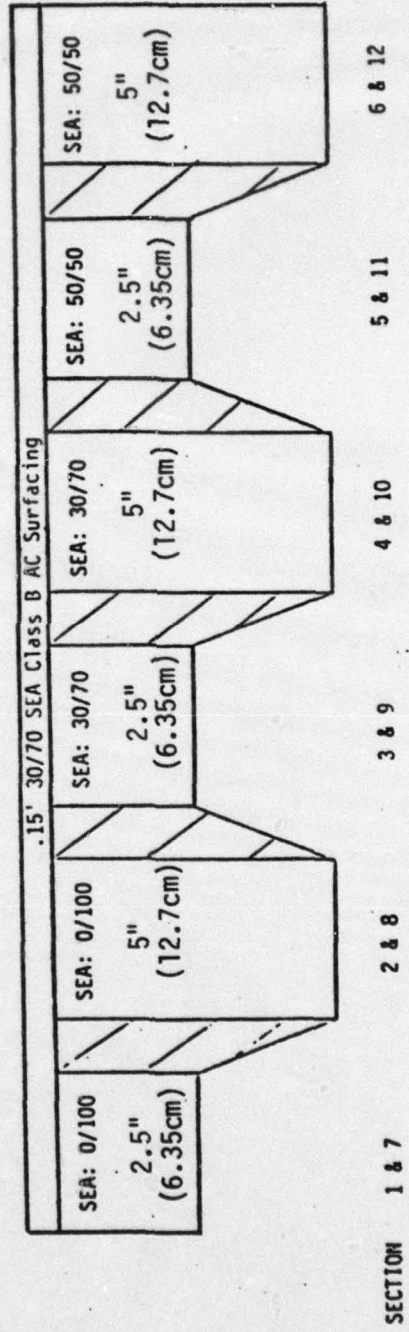


Figure 4.5 SCHEMATIC PROFILE OF TEST TRACK

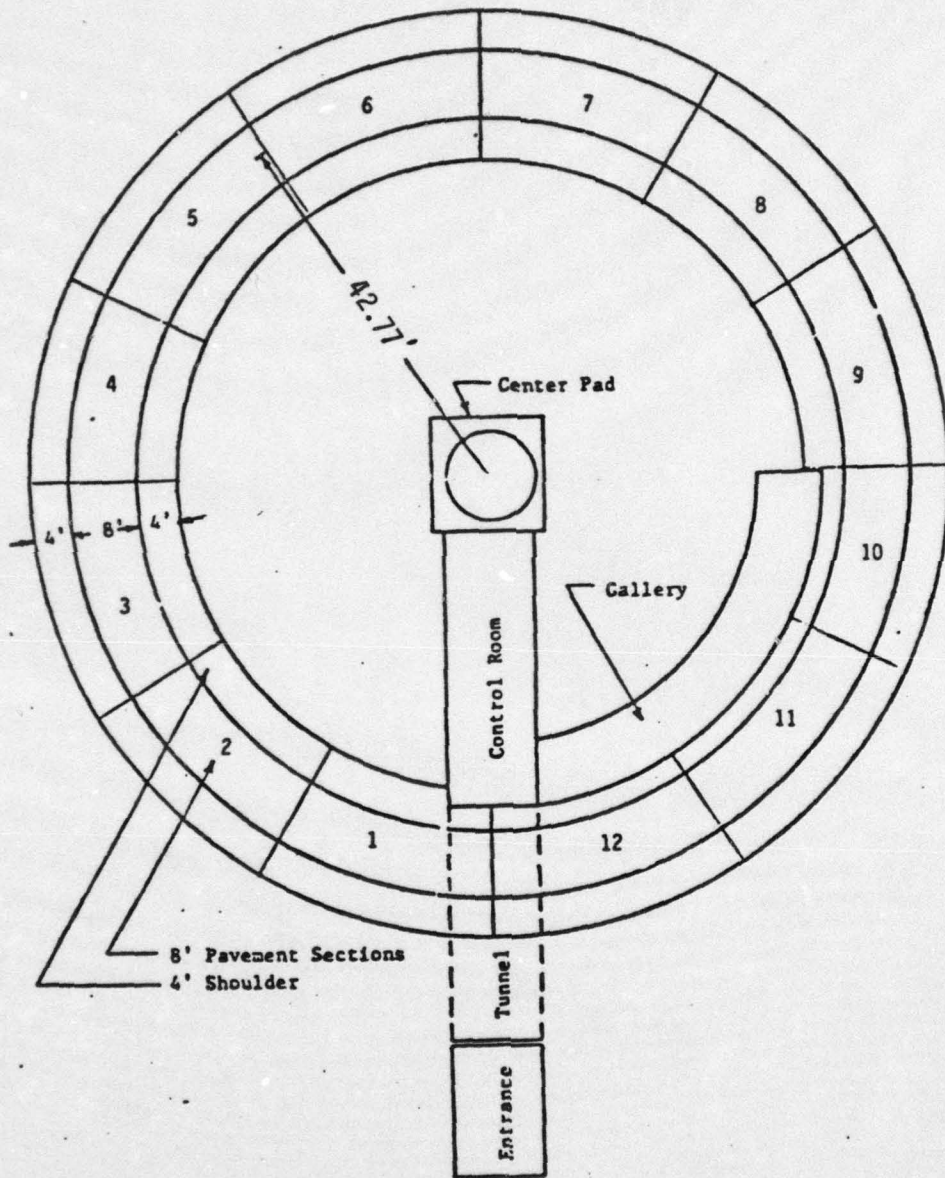


Figure 4.6 PLAN VIEW OF TEST TRACK

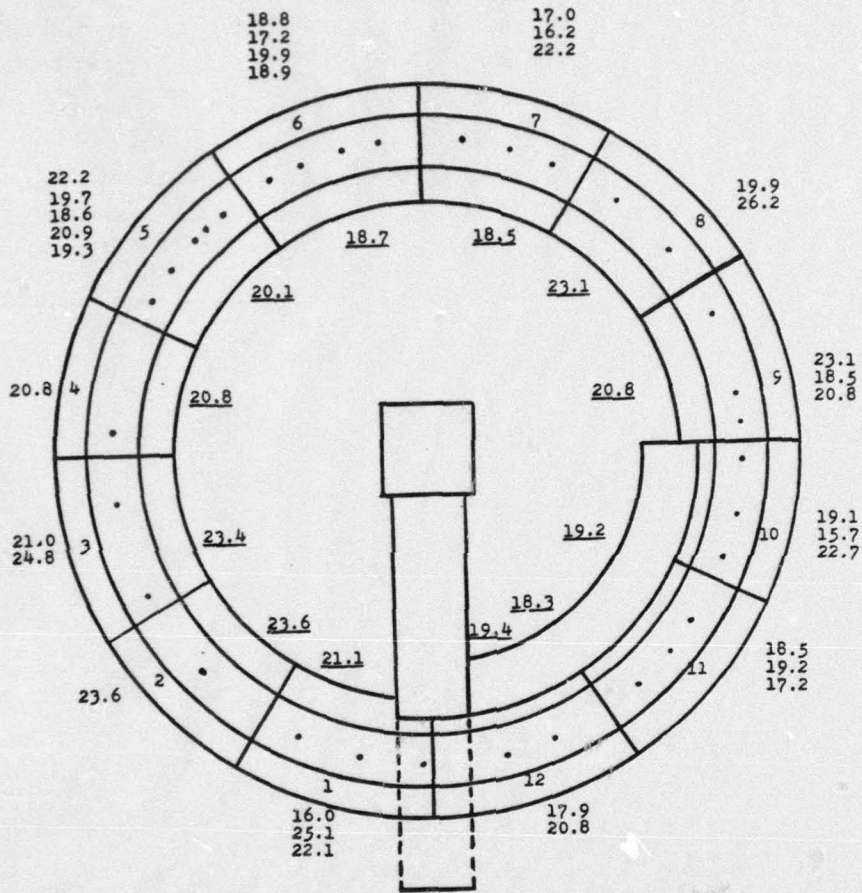


Figure 4.7. MOISTURE CONTENT (%) OF THE SUBGRADE AS PLACED AND AVERAGE MOISTURE CONTENT PER SECTION. THE AVERAGE MOISTURE CONTENT IS INDICATED INSIDE THE TEST TRACK. SAMPLE LOCATIONS ARE INDICATED BY (.)'S.

Various moisture contents of the subgrade taken after the track was in full operation indicated that the moisture content in the subgrade had stabilized between 20 - 21%. This was due to the migration of water from the wetter subgrade below that imported and due to water infiltration from the pavement, particularly after some cracking had occurred in the asphalt pavement.

Test Track Instrumentation

The primary instrumentation installed at the test track were Bison Soil Strain Gauges (Model 4101A). The strain gauges use the principle of inductance coupling between a combination of two "free floating" coils embedded in the pavement and/or underlying soils. One strain gauge coil is connected to an oscillator to produce the electromagnetic field in the soil/pavement surrounding the buried coil. An electrical current is developed in the mating coil. This electrical current has a magnitude that is a function of the spacing between the two coils. See Appendix B for coil calibration.

Following the preparation of the subgrade at the test track, 4-in. diameter holes were drilled to a depth not to exceed 16 feet at the center of each of the 12 subsections. Extensometers, as illustrated in Figure 4.8, were installed in each of these 12 holes. The base plate of each extensometer was grouted into place. The extensometers were placed so that the thick sections would have approximately 8 inches of subgrade between the uppermost coil and upper surface of the subgrade. The thin sections had approximately

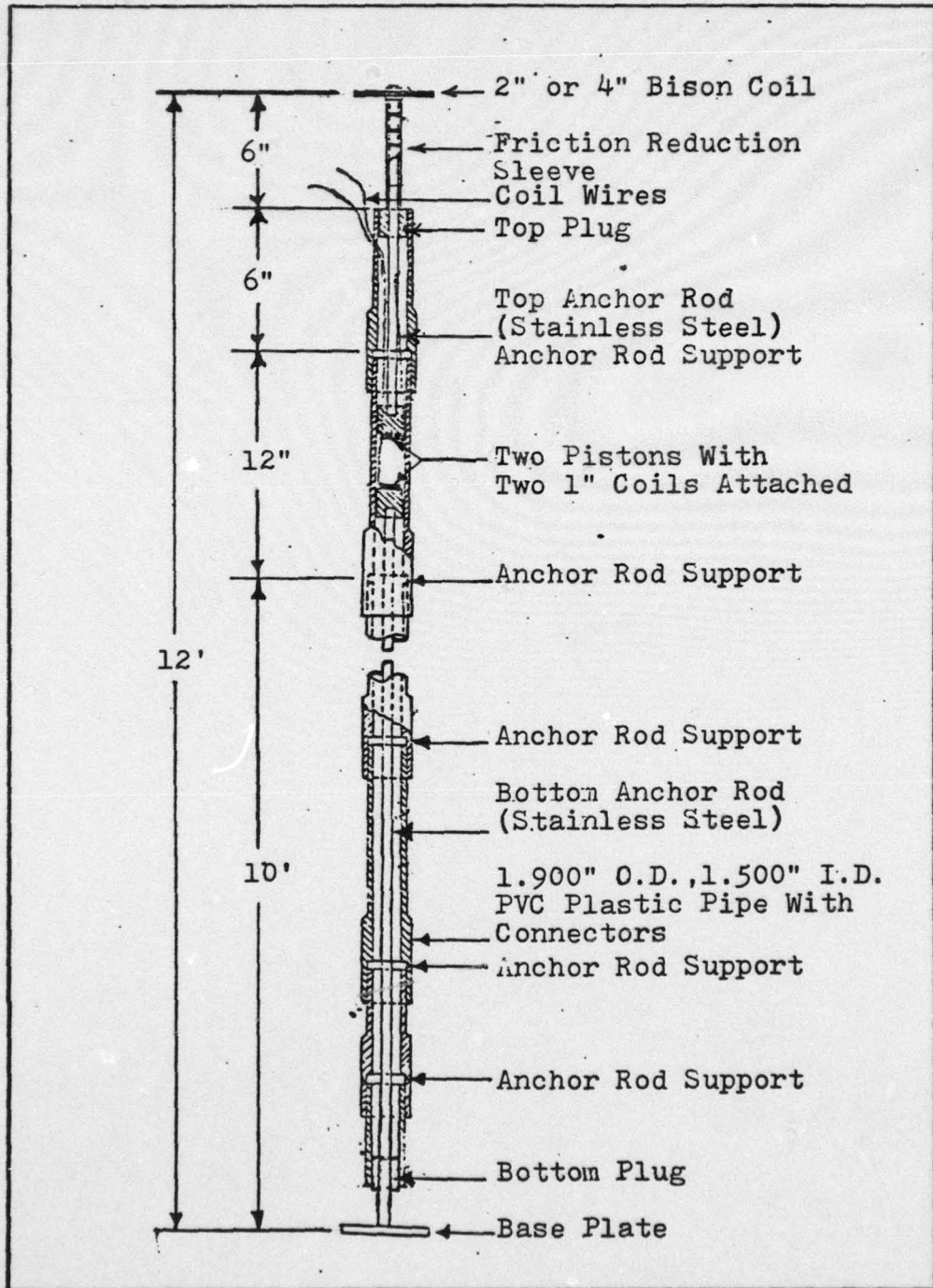


Figure 4.8 VERTICAL SOIL EXTENSOMETER

4 inches of subgrade placed over the topmost coil on the extensometer. The upper coil on the extensometer for the thick sections were 4-in. coils. The upper coil on the extensometer in the thin sections were 2-in. coils.

The remaining coils were emplaced as illustrated in Figures 4.9-4.11. With this configuration of coils, vertical strain in the pavement and upper subgrade could be measured, as well as horizontal, longitudinal and transverse strains. The two 1-in. coils in the extensometer measured total displacement of coil C. The purpose of having 2-in. coils in the thin sections and 4-in. coils in the thick sections was to have the coils operating at their peak efficiency. If the 4-in. coils had been emplaced in the thin sections, there would have been erroneous strain readings because the coils would have been too close together and vice versa for the 2-in. coils in the thick sections.

In addition to the strain and deflection measurements, continuous temperature readings were taken. Measurements were taken of the air, pavement and subgrade temperatures. Table 4.2 indicates the locations of the thermocouples installed at the WSU test track. This will be extremely important for later data analysis for several reasons, the first being the dependence of resilient modulus of the pavement upon temperature, and secondly, if the subgrade became frozen, it would have much greater supportive capability than prior to freezing. Third, it would be interesting to note if there was any failure of the pavement associated with thawing of the subgrade.

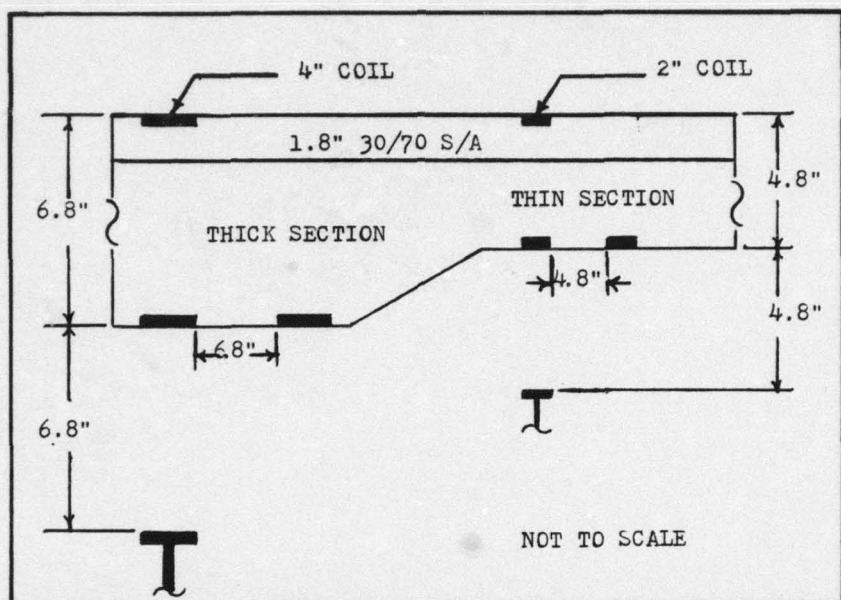


Figure 4.9. PARTIAL CROSS-SECTION OF TWO WSU TEST TRACK SECTIONS ILLUSTRATING POSITIONING OF STRAIN GAUGES

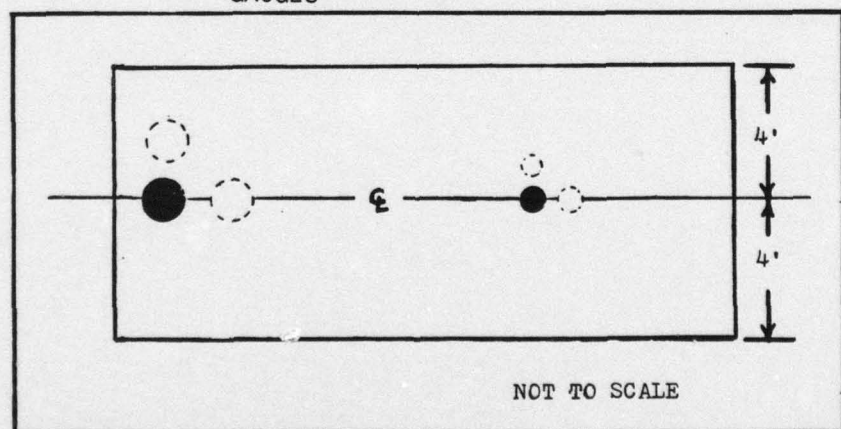


Figure 4.10. PARTIAL PLAN VIEW OF TWO WSU TEST TRACK SECTIONS ILLUSTRATING POSITION OF STRAIN GAUGES

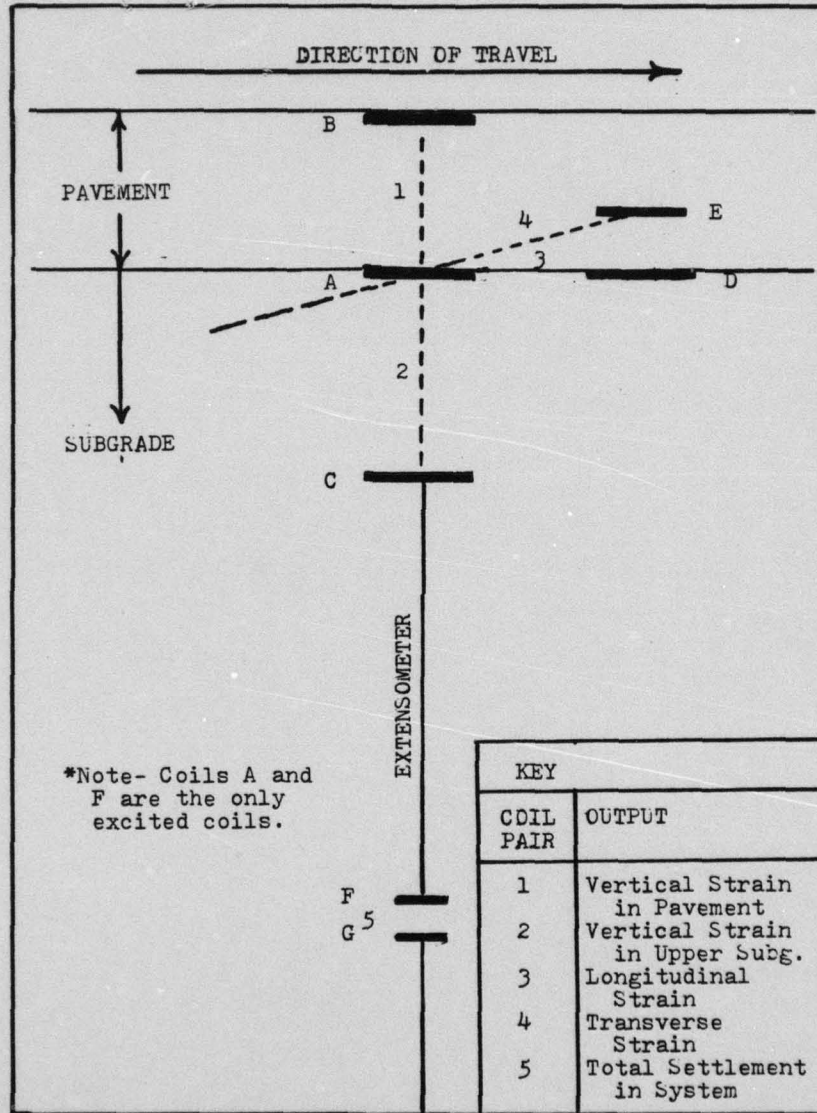


Figure 4.11. BISON STRAIN GAUGE LAYOUT

Table 4.2. LOCATION OF THERMOCOUPLES
AT WSU TEST TRACK

Thermo- couple #	Test Section	Description of Location
1	5	15 inches into the subgrade
2	6	exposed to the air
3	6	½ inch below pavement surface
4	6	between asphalt and subgrade
5	9	exposed to the air
6	9	2 inches into the subgrade
7	9	15 inches into the subgrade
8	10	4½ inches into the subgrade

Test Sections, Background

The test sections as planned would have had four sections of SEA:0/100 (two thick and two thin), four sections of SEA:30/70 (two thick and two thin) and four sections of SEA:50/50 (two thick and two thin) as illustrated in Figure 4.12. But due to an unforeseen quality control problem during construction, the actual construction produced four sections of SEA:0/100 (two thick and two thin) four sections of SEA:30/70 (two thick and two thin) and four sections of SEA:40/60 (two thick and two thin). The test sections with the SEA:40/60 were also laid down with a lean binder content. The binder content that was put down was 6.6% (adjusted for specific gravity) which was the correct binder content if the SEA ratio had been 30/70, but with the actual attained SEA ratio of 40/60

the optimum binder content should have been 7.1%. Therefore, the test sections with the 40/60 SEA mix were approximately $\frac{1}{2}$ % below optimum binder content.

The reason for the production problems were quite complicated and will be discussed in detail under quality control. Once it was discovered that SEA: 40/60 (lean) had been placed on the SR 270 as well as the test sections, it was decided that for comparative purposes the planned SEA:50/50 sections should be replaced by SEA:30/70 sections. This is illustrated in Figure 4.12 as well.

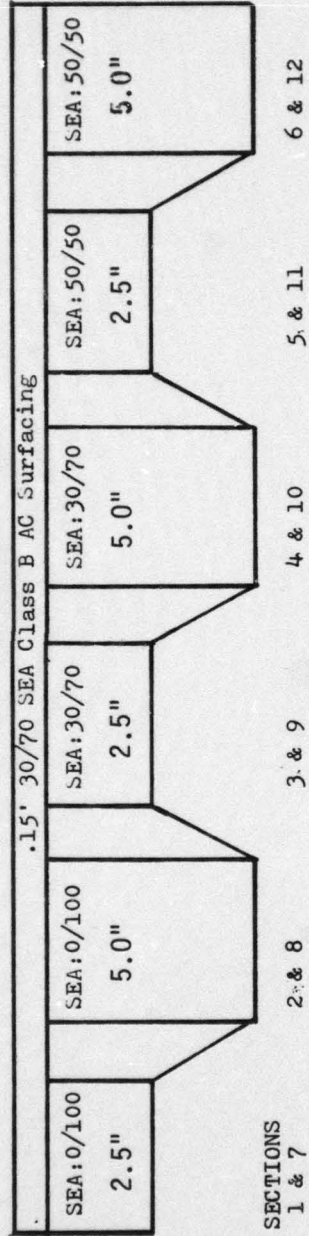
Test Track Thicknesses

The test track sections were designed to have thin sections $2\frac{1}{2}$ inches thick and thick sections 5 inches thick. All sections were to have a 1.8-in. leveling course overlay of SEA:30/70. The actual achieved thicknesses are illustrated in Figure 4.13. According to core measurements, most sections tend to be thinner than anticipated. The leveling course was intentionally varied to make the surface of the track as level as possible. In order to compute the base course thickness for a given section, the reader should subtract the leveling course thickness given at the top of Figure 4.13 from the average pavement thicknesses given around the inner circumference of the test track in Figure 4.13.

Test Track Placement Temperatures

During placement of the test sections, special care was taken to measure temperatures of the mixes as delivered, as laid down and

TEST TRACK SECTIONS AS PLANNED



TEST TRACK SECTIONS AS BUILT

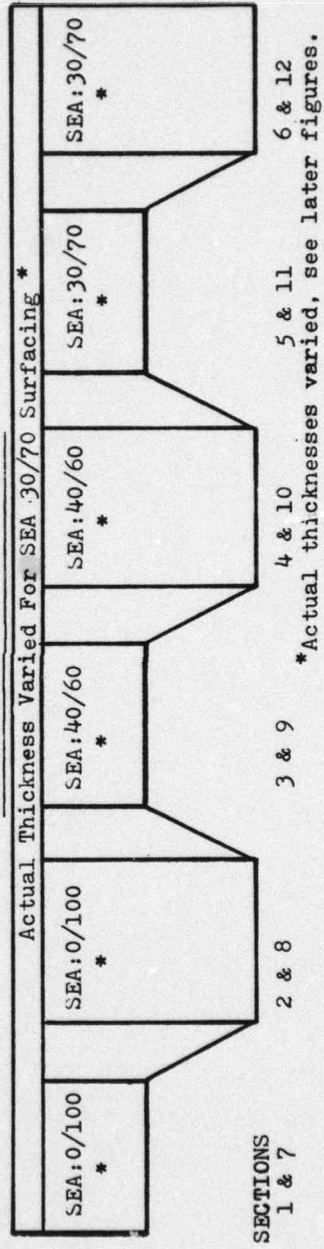


Figure 4.12. SCHEMATIC PROFILE OF TEST TRACK AS PLANNED COMPARED TO AS BUILT

THICKNESS OF LEVELING COURSE IN INCHES

THICKNESS SECTION	1.1	1.4	1.4	1.2	1.1	1.9	1.6	1.6	1.1	1.7	1.5	1.5
	1	2	3	4	5	6	7	8	9	10	11	12

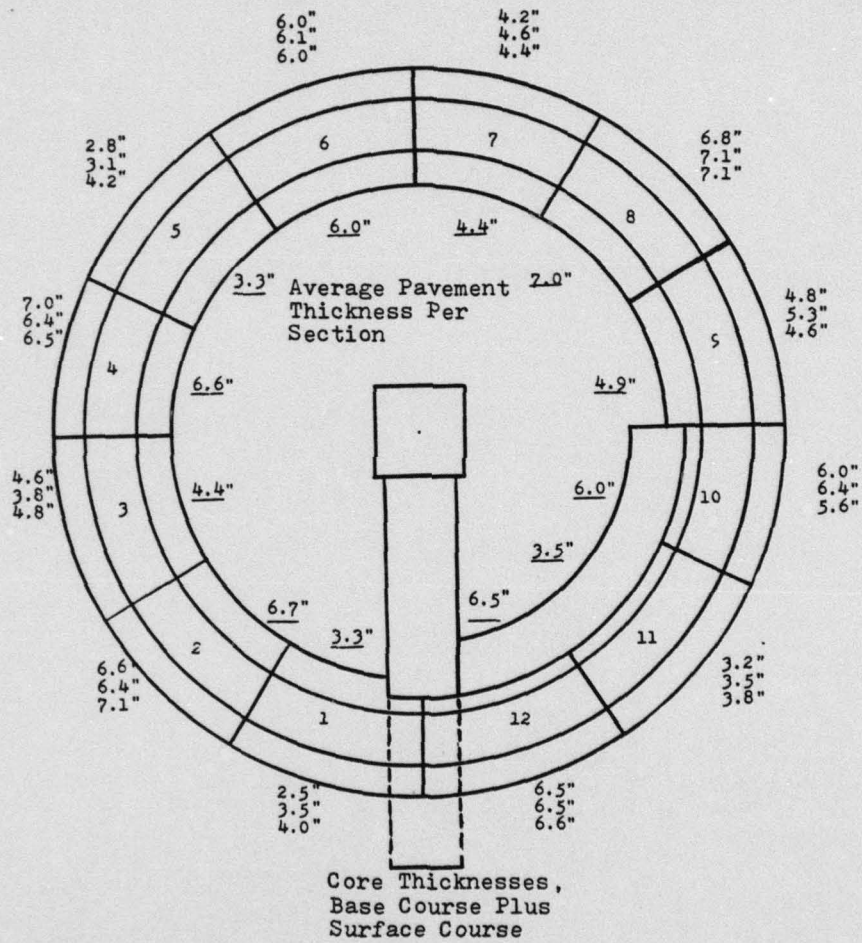


Figure 4.13. ACTUAL PAVEMENT THICKNESSES ACHIEVED AT TEST TRACK

rolled at temperatures below that recommended by other researchers [45]. Figure 4.14 indicates a workable lower limit of approximately 250°F, although generally accepted limits are between 225° to 300°F (124° to 149°C).[45]. Further analysis of the test track data should recognize this possibility. Table 4.3 illustrates the temperatures as taken at the test track by WSDOT.

Test Track Densities

As the test track was being laid and compacted, densities were being taken of each lift between passes of the 10-ton smooth wheel Gallion roller. Figure 4.15 illustrates the compaction versus the density achieved for the three different binders laid at the test track. This density was compared to Rice Density of 160 PCF developed by Sharkey in his laboratory work using this same aggregate binder.

It is interesting to note that 30/70 SEA density peaks out at approximately 4 passes and the 40/60 SEA peaks out at 6 or 7 passes. This is an apparent savings of time and equipment for the mixes containing sulfur when compared to the conventional mix which required 10 passes before it reached its maximum density. This bears further research.

It should be noted also that in the case of the 0/100 and 30/70 mixes, the test track was over-compacted. As with the possibility of cool placement temperatures, this lower-than-optimum density of the test sections should be kept in mind during further analysis of the test track data.

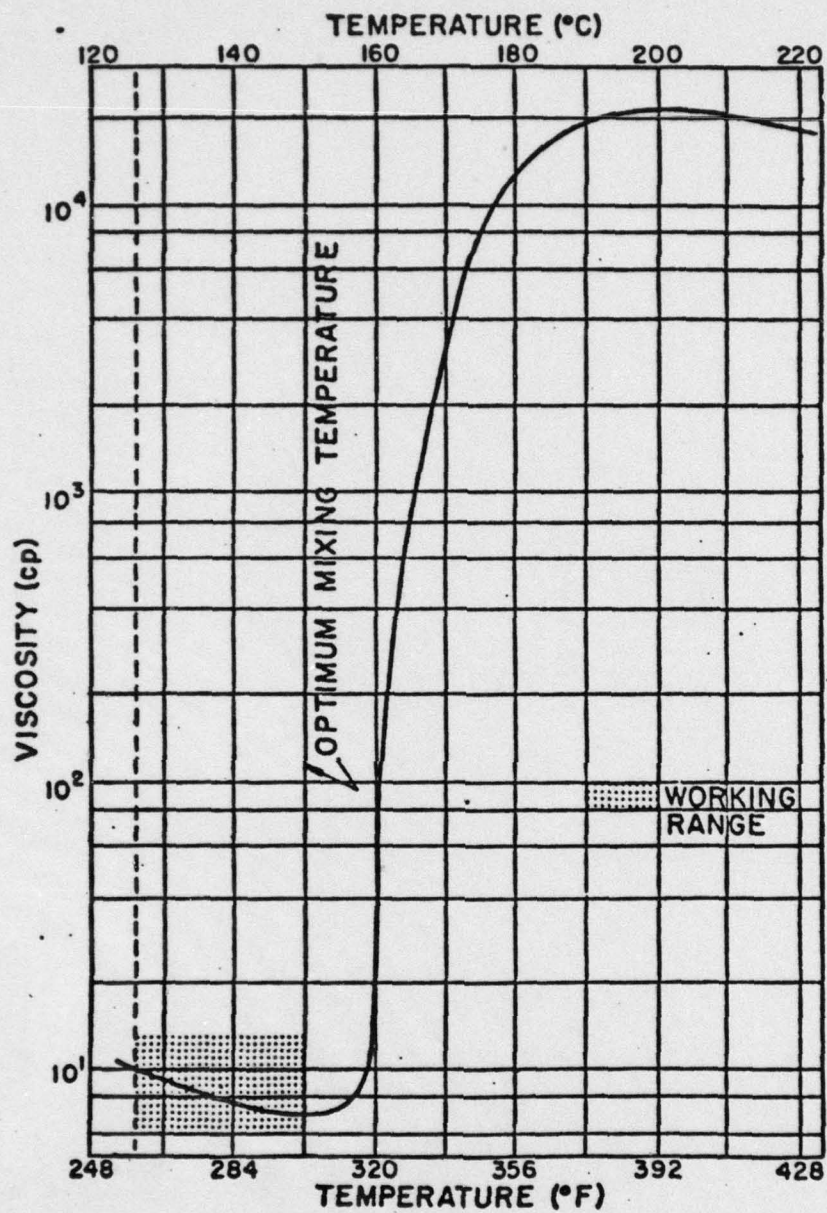


Figure 4.14 TEMPERATURE-VISCOSITY CURVE FOR LIQUID SULPHUR [45]

Table 4.3. PLACEMENT TEMPERATURES OF S/A MIXES AT THE WSU TEST TRACK

Test Section	Lift	Date	Air Temp.	Truck Temp.	Lay Down Temp.	Finished Rolling Temp.	S/A
2	1	8/21/79	70		235	180	
8	1	8/21/79	70	250	225	160	
1	1	8/21/79	70	250	230	185-200	
2	2	8/21/79	60	250	230	185-200	0/100
8	2	8/22/79	80	NA	250	200	
7	1	8/22/79	80	NA	250	200	
10	1	8/24/79	NA	NA	240	NA	
4	1	8/24/79	NA	NA	240	NA	
9	1	8/24/79	NA	NA	235	NA	
10	2	8/24/79	NA	NA	235	NA	40/60
3	1	8/24/79	NA	NA	235	NA	
4	2	8/24/79	NA	NA	235	NA	
12	1	8/27/79	75	280	260	160	
6	1	8/27/79	75	280	250	NA	
12	2	8/27/79	75	285	265	NA	
11	1	8/27/79	75	285	265	NA	30/70
6	2	8/27/79	75	285	260	NA	
5	1	8/27/79	75	285	260	NA	
Overlay/ Leveling Course		8/28/79	70	270	210-250	170	

NA = not available

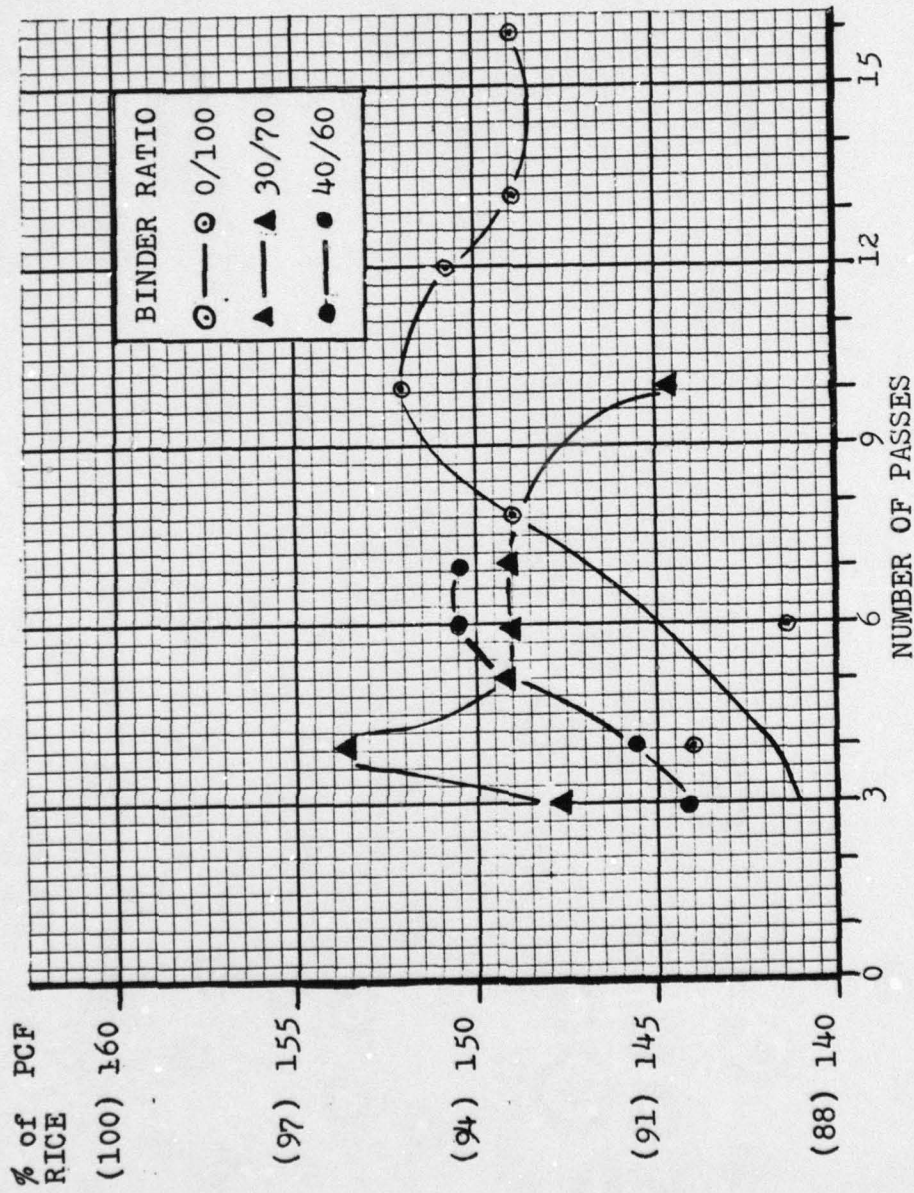


Figure 4.15. DENSITY VS NUMBER OF PASSES WITH A 10-TON SMOOTH STEEL WHEEL GALLION ROLLER

As discussed by Sharkey [26], when the SEA samples were over-compacted when allowed to cool below 200°F there appeared to be a fracturing of the sulfur bridges as they formed in the Marshall sample. On a much larger scale this may be what is happening when excess compaction is applied to an actual SEA pavement. The future commercial application of sulfur-extended asphalts may realize a savings of time and equipment because of the reduced amount of compaction necessary, but will have a quality control problem to insure that compaction is not carried beyond a certain number of passes nor below a certain temperature of the laid mix.

Quality Control

The most important aspects of quality control at the test track were insuring that a mix with the optimum binder content be produced and placed and that the mix be of the specified sulfur-asphalt proportion. The primary means of controlling the binder content of a given mix was by means of quick extractions performed by the Washington State Department of Transportation (WSDOT) at the batch plant. There were no problems in this area.

The most critical area was that of controlling the per cent of sulfur in a given mix. The primary method of control was by calibration of the Pronk sulfur pump. The Pronk sulfur pump is an in-line pump which, when properly calibrated, produces a given flow of sulfur for a given pump RPM. To back up the pump, a graphic comparison of SEA binder composition versus specific gravity of the binder was available. The graph used was similar to Figure 4.16, but had

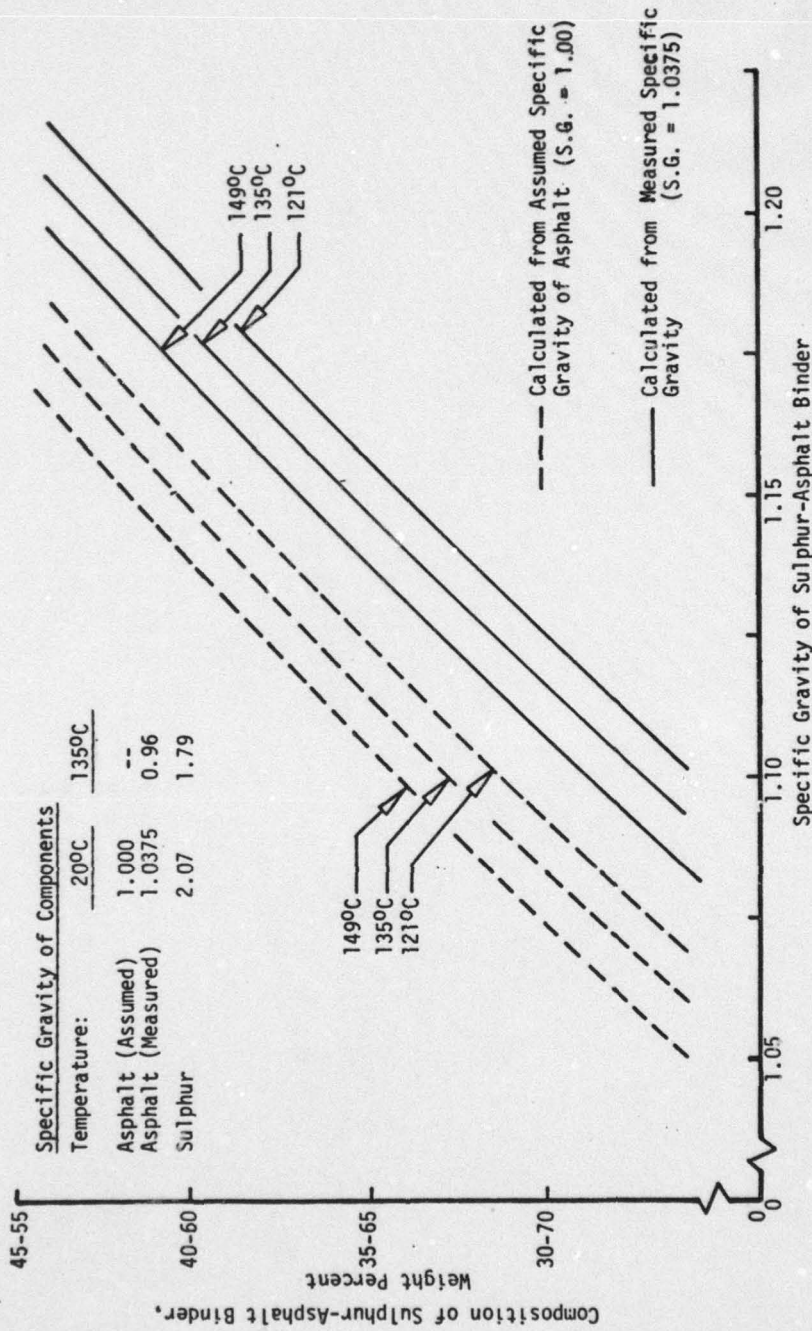


Figure 4.16. SULFUR-ASPALT BINDER -- COMPOSITION VS SPECIFIC GRAVITY

been developed at room temperature only. The samples were taken at approximately 260°F.

The sulfur pump was calibrated by SUDIC at the United Paving asphalt plant. It unfortunately pumped sulfur in excess of its calibrated output once it was hooked up.

The initial SEA mix that was to be produced was that for the 30/70 sections. The pump was producing approximately a 40/60 S/A ratio, however. When the pump was checked against the graphic backup, both the pump miscalibration and the graph had erred in the same direction and both indicated that a 30/70 S/A ratio was being produced.

The problem was not detected until it was discovered that more sulfur was being used than anticipated. Reworking of the specific gravity versus binder composition curve to reflect the actual temperature of the samples solved the problem and the remaining SEA mixes were produced accurately.

The result of this error was, as had already been discussed, that no 50/50 S/A mix was produced and that it was replaced by a 40/60 S/A mix. Because the S/A mix was thought to have a sulfur content of 30%, the optimum binder content was 6.6% (5.7% for conventional binder adjusted by specific gravity for 30/70 S/A). The actual S/A content of 40/60 S/A required a binder content of 7.1% to be at the optimum binder content. Therefore, the actual mix laid down on SR 270 and the test track was 0.5% too lean.

CHAPTER V
FATIGUE CHARACTERISTICS AND COMPARISON
OF MEASURED TO THEORETICAL PAVEMENT RESPONSES

Initial strains were computed manually from the instrumentation at the test track. This data was taken by use of a strip chart which recorded the increase or decrease in voltage between any two given sets of coils dependent upon whether the coils in that set were moved closer together, or further apart. These computed strains are shown in Table 5.1. Figure 4.11 is reproduced as Figure 5.1 for convenience in interpreting Table 5.1.

The strip chart readings were not taken with the duals of arm and wheel Assembly #1 positioned so as to produce maximum deflection over the coils. They were positioned with the center of rotation at the following eccentricities:

STRAIN	ECCENTRICITY
1	313°
2	310°
3	307°
4	300°
5	300°

The distances from the innermost edge of the wheel path to the vertical axis of coils A, B, C, F and G were measured to be as follows:

Table 5.1. INITIAL STRAINS MANUALLY COMPUTED AND COIL SPACING

Section:	1	2	3	4	5	6	7	8	9	10	11	12
Strain* 1	17,314	7,158	3,773	1,354	2,632	128	2,913	N/A	0	346	291	794
Strain* 2	575	377	792	256	799	302	1,271	N/A	1,244	289	2,172	497
Strain* 3	-350	-100	-266	0	-384	-82	-980	N/A	-224	428	-1575	222
Strain* 4	-359	-211	-336	-34	-241	-148	-198	N/A	-515	489	-1269	301
Strain* 5	1,107	437	1,011	398	781	344	505	298	865	286	841	688
Spacing** 1	5.815	7.794	5.454	7.366	4.531	6.855	4.799		4.885	6.103	3.272	5.952
Spacing** 2	4.090	7.003	5.087	8.315	3.302	6.522	1.995	13.488***	2.535	7.385	3.023	8.221
Spacing** 3	4.918	7.088	3.310	7.476	2.926	6.622	3.702	4.345	2.535	7.385	3.023	8.221
Spacing** 4	4.103	7.824	3.381	7.133	3.267	7.208	3.434	4.345	3.104	6.166	3.386	7.038
Spacing** 5	1.435	1.428	1.304	1.545	1.322	1.369	1.540	1.5153	1.298	1.404	1.047	1.400

*Strain in microstrains, i.e., $\times 10^{-6}$ in/in.

**Spacing in inches.

***Section 8 had coil C inoperable; by activating coil B the distance between A and B could be calculated.

- Indicates tension

+ Indicates compression

N/A=Not available.

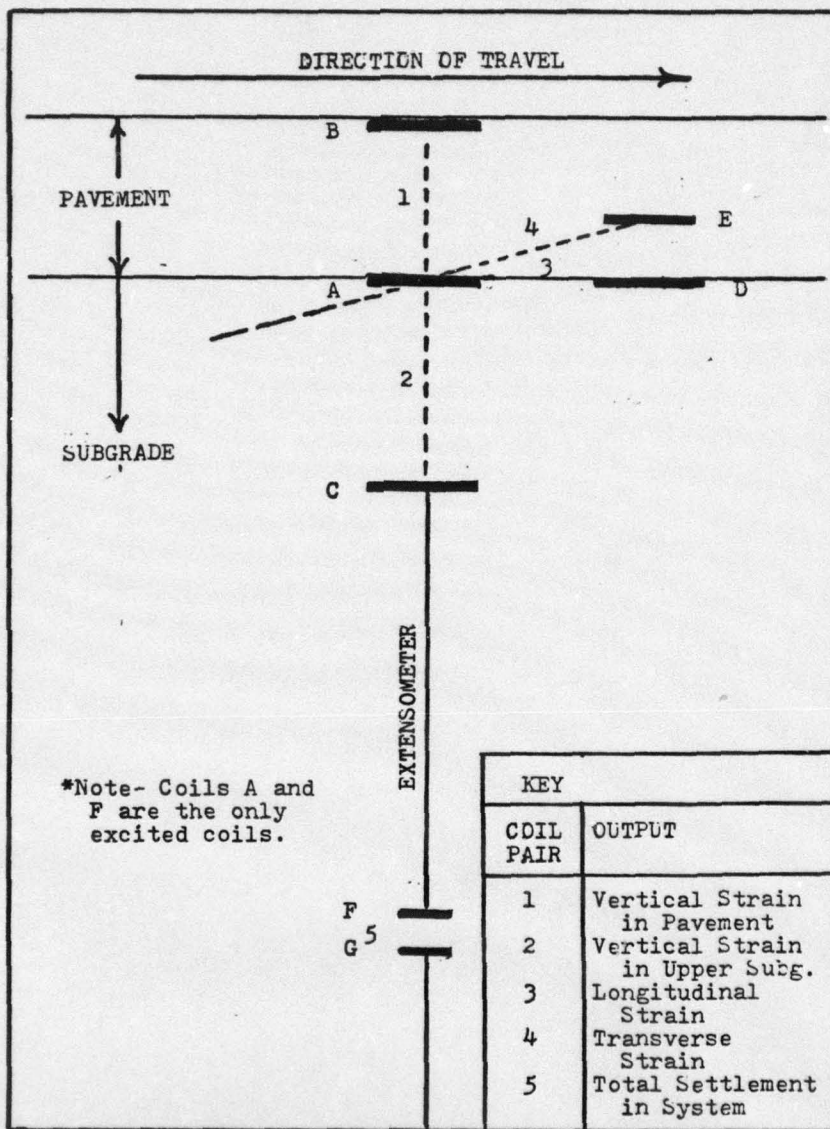


Figure 5.1. BISON STRAIN GAUGE LAYOUT

Table 5.2. COIL DISTANCE FROM INNERMOST EDGE OF WHEEL PATH TO COILS AND ANGULAR LOCATION OF EACH COIL SET

Section	1	2	3	4	5	6	7	8	9	10	11	12
Distance (inches)	21.5	24.5	23.0	29.0	14.0	15.5	34.0	28.0	28.5	22.0	28.5	27.0
Angular location	16.1	46.0	75.3	105.7	133.6	163.4	196.4	223.9	254.4	286.6	316.1	346.3

The computed distances between the coil's central axis and central point of the wheel loads were as illustrated in Table 5.3 when the strip chart readings were completed. The loads in Section 4 were further from the coils than in any other section.

Fatigue

Extensive work has been accomplished in various laboratories which have resulted in tensile stress or strain relationships as a function of the number of loads to failure for asphalt concrete materials. It is difficult to obtain a true consensus among engineers as to how well these laboratory-derived relationships duplicate actual in-service asphalt concrete pavements. Many research engineers believe that laboratory-derived fatigue relationships underestimate fatigue life by more than an order of magnitude [48].

In an attempt to avoid some of the pitfalls associated with laboratory fatigue relationships, three fatigue relationships were obtained from available literature. These were developed directly from AASHO Road Test data or laboratory results based on field sawed

Table 5.3. LOCATION OF DUALS IN RELATION TO BISON COILS FOR INITIAL STRAIN READINGS

		Spacing to Center of Load											
		1	2	3	4	5	6	7	8	9	10	11	12
Coil Set		(inches)											
1	13.8	-1.2	-11.4	-26.3	-14.0	-12.0	-20.3	-3.0	8.4	23.6	19.4	17.3	
2	12.7	-2.4	-12.5	-26.8	-14.0	-11.3	-19.1	-1.8	9.5	24.1	19.3	16.6	
3	11.5	-3.7	-13.6	-27.4	-13.9	-10.6	-17.9	-0.5	10.4	24.6	19.2	15.8	
4 & 5	8.8	-6.6	-15.8	-28.3	-13.3	-8.6	-15.1	2.3	12.6	25.4	18.6	13.9	

(-) indicates that the loading center was located inside the coils within the wheel path

specimens obtained from the Washington State University test track during studies reported by Kingham and Kallas in 1972. All three relationships are shown in Figure 5.2, while the same relationship for the 30/70 and 0/100 S/A samples at the test track are shown in Figures 5.3 and 5.4.

The equations used to compute the fatigue criteria curves in Figure 5.2 are as follows:

$$1. w_{18} = 9.7255 \times 10^{-5} (1/\epsilon)^{5.1627} \quad (\text{ARE fatigue criteria})$$

where

$$\begin{aligned} w &= \text{load repetitions to failure with an 18 kip load} \\ \epsilon &= \text{initial horizontal tensile strain} \end{aligned} \quad [49]$$

$$2. \log N_f (<10\%) = 15.947 - 3.291 \log (\epsilon/10^{-6}) - .854 \log (E/10^3) \quad (\text{PDMAP fatigue criteria})$$

where

$$\begin{aligned} N_f &= \text{load repetitions to failure} \\ \epsilon &= \text{initial horizontal tensile strain} \\ E &= \text{Complex Modulus (Assumed equal to } M_R) \end{aligned} \quad [50]$$

$$3. \log N_f = -17.2278 + 5.87687 \log (1/\epsilon) + 0.033594 (\text{temp.}) \quad (\text{WSU Test Track Lab fatigue criteria})$$

where

$$\begin{aligned} N_f &= \text{load repetitions to failure} \\ \epsilon &= \text{initial horizontal strain} \\ \text{temp.} &= \text{temperature in degrees F} \end{aligned} \quad [44]$$

The relationship which provides the most conservative estimate for limiting horizontal tensile strains contained in Figure 5.2 was developed by Austin Research Engineers for the Federal Highway Administration (FHWA) and is normally used in overlay design purposes [49]. Data from 27 AASHO road tests which included traffic repetitions and predicted tensile strains were utilized in the development

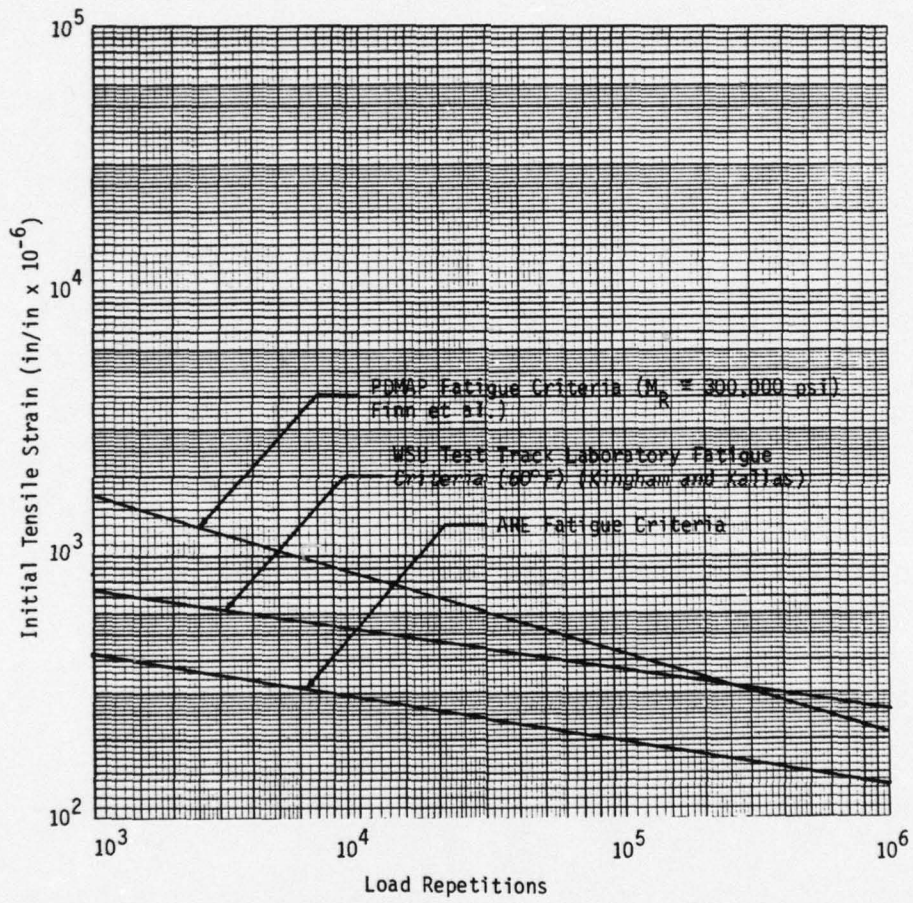


Figure 5.2 FATIGUE CRITERIA FOR HORIZONTAL TENSILE STRAIN AT THE BOTTOM OF THE TEST TRACK PAVEMENT

of this curve.

A less conservative relationship was developed by Finn et al. for the PDMAP computer program, which can be utilized in the prediction of fatigue cracking and deformation [50]. Based on AASHO road test data, a shift factor relationship was developed which predicts repetitions to failure for input values of predicted initial tensile strain and modulus.

Finally, the laboratory fatigue relationship developed by Kingham and Kallas of the Asphalt Institute tends to fall between the two previously described fatigue relationships. This relationship was obtained from testing flexural beams sawed from one of the experimental test rings constructed at WSU in 1971 [44].

The fatigue curves developed for each of the three sulfur-asphalt ratios utilized at the WSU test track during this study were developed from the data points shown in Figures 5.3 and 5.4. Figure 5.3 is for a sulfur/asphalt ratio of 0/100, and Figure 5.4 is for a sulfur/asphalt ratio of 30/70.

Figure 5.3 does not show a Bison data point for section 8. There is no data point for section 8 because of the non-operative coil as previously discussed.

Figure 5.4 does not show a Bison data point for section 12 because the initial strain taken from the Bison gauges indicated that under that particular load configuration, the horizontal strains were in compression, not tension.

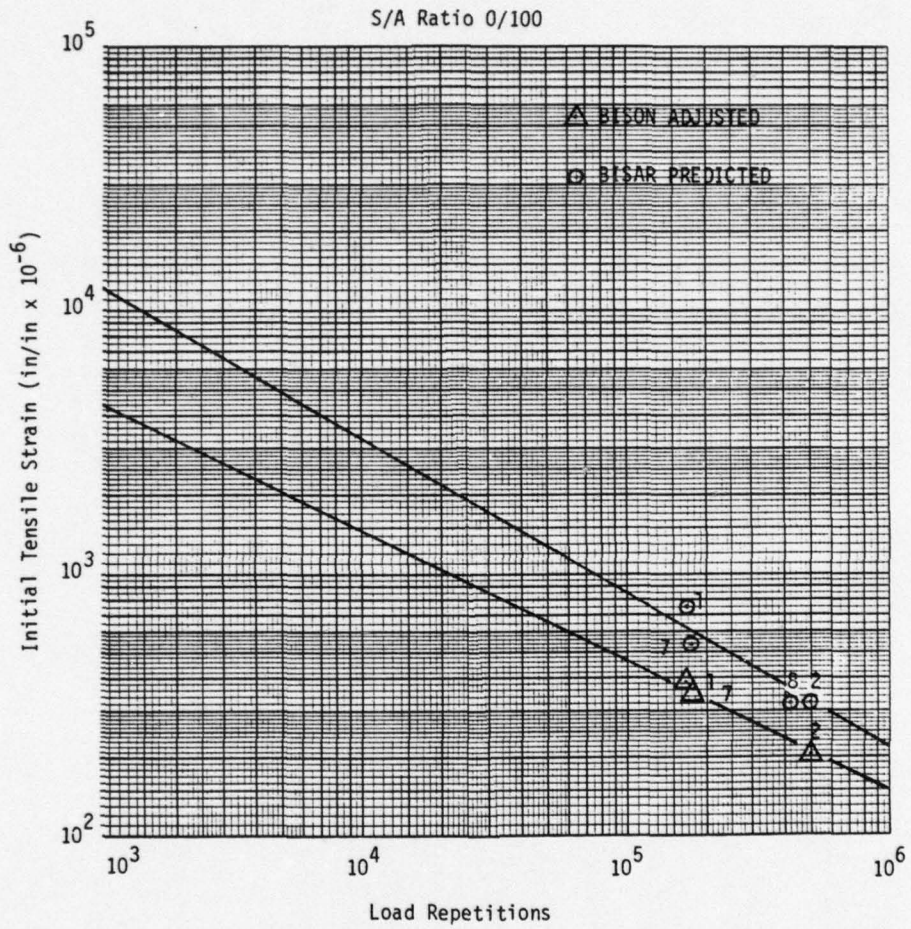


Figure 5.3 INITIAL HORIZONTAL TENSILE STRAIN VS THE NUMBER OF LOAD REPETITIONS TO FAILURE FOR THE 0/100 S/A SECTIONS (BISAR & BISON)

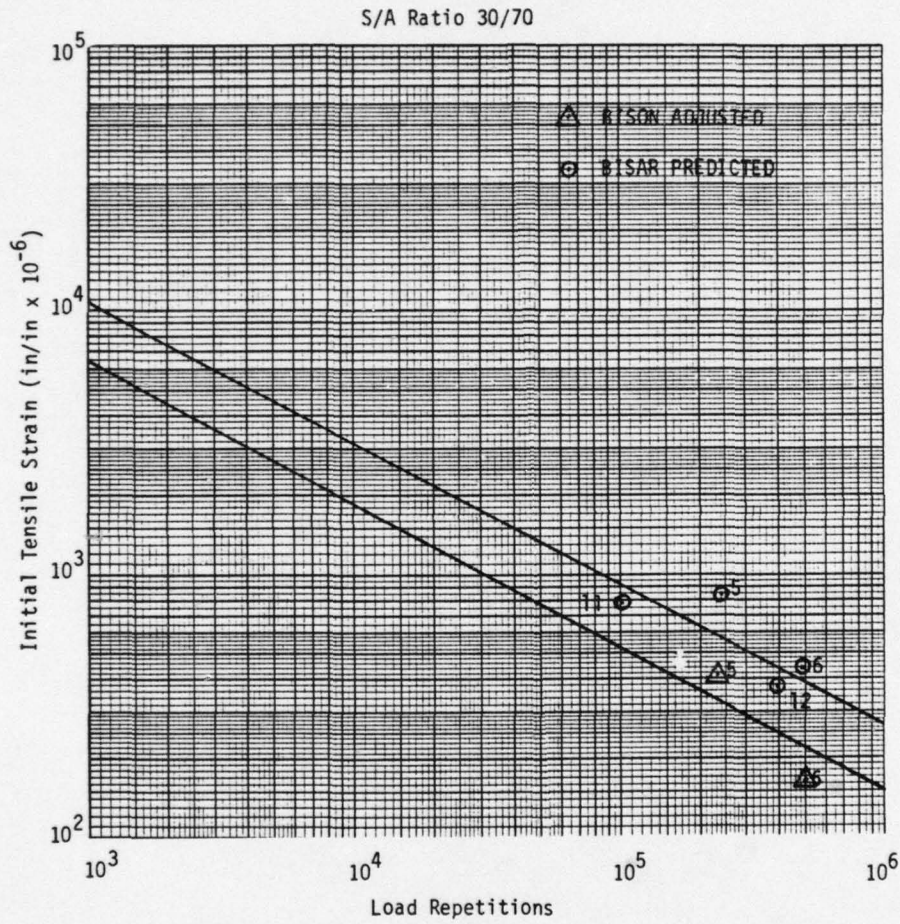


Figure 5.4 INITIAL HORIZONTAL TENSILE STRAIN VS THE NUMBER OF LOAD REPETITIONS TO FAILURE FOR THE 30/70 S/A SECTIONS (BISON & BISON)

The number of repetitions to failure was taken from a daily journal kept by the operators at the test facility at WSU. A summation of this journal is presented in Appendix A.

Also shown in Figure 5.3 and 5.4 are the predicted initial strains for the 0/100 and 30/70 sections. The 40/60 sections were not characterized using the BISAR elastic layer flexible pavement computer program, because it was felt that not enough was known about the resilient modulus or other material characteristics of this lean mix to provide adequate input for the computer modeling. The M_R 's used in this modeling were based upon those derived in laboratory work done by Sharkey [26] for the pavement temperature at the time the strip charts were developed.

During this computer modeling, two sets of predicted data were derived -- one for the 11,400-lb. load of arm and wheel assembly #1 centrally located over the various coils, and the other with the same load located as shown in Table 5.3.

In preparation of Figures 5.3 and 5.4, the actual Bison readings were multiplied by the strain ratio shown in Table 5.6, column 3. This was done in order to give a more realistic value for the initial horizontal tensile strain indicated by the Bison gauges, since the loads were not positioned over the coils to give maximum strains.

Figures 5.3 and 5.4 have two graphical representations of the fatigue criteria as developed by the adjusted actual Bison readings and by the theoretical BISAR predictions.

In both figures the BISAR predicted curve is higher than the adjusted Bison readings. From the limited number of data points, it is felt that there is fairly good agreement in slope between the curves drawn from BISAR predicted data points and those drawn from adjusted Bison data points.

The comparison of Figures 5.3 and 5.4 to Figure 5.2, however, shows that the curves developed from this study are much steeper than those predicted by ARE, Kingham and Kallas, or by Finn. The cause of this disagreement bears further research and study.

Key elements of this computer characterization are shown in Tables 5.4 - 5.8. Predicted surface deflection, horizontal strain (longitudinal and transverse), vertical strain in the subgrade and deflections at the top of the extensometer were computed.

Comparison of Bison Indicated Initial Strains and Deflections to BISAR Predicted Initial Strains and Deflections

Surface Deflections

30/70

BISAR OFFSET is consistently greater than BISON outputs by a factor of from 4.3 to 15.

0/100

BISAR OFFSET is less than the Bison outputs for sections 1 and 2 by a factor of 1.4 and 1.2, but for section 7 the BISAR OFFSET is 2.9 times greater. Section 8, surface deflection was not computable because of an inactive coil "C".

Table 5.4. BISAR PREDICTED COMPARED TO BISON INDICATED SURFACE DEFLECTIONS
FOR S/A 30/70 AND S/A 0/100 SECTIONS

SURFACE DEFLECTION ($\times 10^{-3}$ INCHES)										
S/A	SECTION NO.	BISAR OFFSET	DEFL. RATIO	BISAR CENTERED	DEFL. RATIO	BISON	DEFL. RATIO	BISON	DEFL. RATIO	BISAR OFFSET
30/70	5	66.6	1.4 <	90.1 >	5.8 >	15.5	4.3 <	66.6		
	6	51.8	1.1 <	56.5 >>	17.0 >>	3.3	15.6 <	51.8		
	11	51.5	1.7 <	86.4 >>	10.3 >>	8.4	6.1 <	51.5		
	12	43.5	1.2 <	52.7 >	5.4 >	9.8	4.4 <	43.5		
0/100	1	72.6	1.2 <	88.0	1.2 <	104.6 >	1.4 >	72.6		
	2	49.6	1.0 =	49.5	1.2 <	59.0 >	1.2 >	49.6		
	7	49.9	1.4 <	70.9 >	4.1 >	17.3	2.9 <	49.9		
	8	47.7	1.0 =	47.7	N/A	N/A	N/A	47.7		

N/A = NOT AVAILABLE, INSTRUMENTATION FAILURE

Table 5.5. BISAR PREDICTED COMPARED TO BISON INDICATED LONGITUDINAL HORIZONTAL STRAINS FOR S/A 30/70 AND S/A 0/100 SECTIONS

LONGITUDINAL HORIZONTAL STRAIN ($\times 10^{-6}$ IN/IN)													
S/A	SECTION NO.	BISAR OFFSET	STRAIN RATIO	BISAR CENTERED	STRAIN RATIO	BISON	STRAIN RATIO	BISON	STRAIN RATIO	BISAR OFFSET	S/A	SECTION NO.	BISAR OFFSET
30/70	5	- 65	- 3.2*	<	206	<	1.9	305	>	- 5.9*			- 65
	6	174	1.2	<	211	>	2.6	82	<	2.1			174
	11	-163	1.3*	<	218	<	7.2	1575	>	- 9.7*			-163
	12	19	10.6	<<	201	<	1.1	-221	>>	-11.7*			19
0/100	1	131	1.5	<	200	<	1.8	350	>	2.7			131
	2	212	>	1.2	178	>	1.8	100	<	2.1			212
	7	67	3.2	<	217	<	4.5	980	>>	14.6			67
	8	172	=	1.0	172	=	N/A	N/A	N/A	N/A			172

*INDICATES ONE ELEMENT OF THE STRAIN RATIO IS IN TENSION AND THE OTHER IS IN COMPRESSION (- COMPRESSION, + TENSION).

N/A = NOT AVAILABLE, INSTRUMENT FAILURE.

Table 5.6. BISAR PREDICTED COMPARED TO BISON INDICATED TRANSVERSE HORIZONTAL STRAINS FOR S/A 30/70 AND S/A 0/100 SECTIONS

TRANSVERSE HORIZONTAL STRAIN ($\times 10^{-6}$ IN/IN)											
S/A	SECTION NO.	BISAR OFFSET	STRAIN RATIO	BISAR CENTERED	STRAIN RATIO	BISON	STRAIN RATIO	BISAR OFFSET	STRAIN RATIO	BISON	BISAR OFFSET
30/70	5	497	1.7 <	845 >	3.5	241	2.1 <	497			
	6	381	1.1 <	424 >	2.8	148	2.6 <	381			
	11	262	3.0 <	796 >	1.6	1269 >	4.8	262			
	12	249	1.5 <	381 >	- 1.3*	-301 >	- 1.2*	249			
0/100	1	673	1.1 <	759 >	2.1	359	1.9 <	673			
	2	310	1.0 <	323 >	1.5	211	1.5 <	310			
	7	297	1.9 <	554 >	2.8	198	1.5 <	297			
	8	305	= 1.0	305 =	N/A	N/A	N/A	305			

*INDICATES ONE ELEMENT OF THE STRAIN RATIO IS IN TENSION AND THE OTHER IS IN COMPRESSION (- COMPRESSION, + TENSION)
 N/A = NOT AVAILABLE, INSTRUMENT FAILURE

Table 5.7. BISAR PREDICTED COMPARED TO BISON INDICATED VERTICAL STRAINS
FOR S/A 30/70 AND S/A 0/100 SECTIONS

VERTICAL STRAIN ($\times 10^{-6}$ IN/IN)										
S/A	SECTION NO.	BISAR OFFSET	STRAIN RATIO	BISAR CENTERED	STRAIN RATIO	BISON	STRAIN RATIO	BISON	STRAIN RATIO	BISAR OFFSET
30/70	5	1500	2.0 <	3040	1.2 <	3605	1.2 <	3605	>	1500
	6	1120	1.3 <	1430	1.7 <	2441	1.7 <	2441	>	1120
	11	703	4.1 <	2850	2.6 <	7446	2.6 <	7446	>>	703
	12	666	1.9 <	1280	3.9 <	5049	3.9 <	5049	>	666
0/100	1	1730	1.6 <	2830	1.4 <	3943	1.4 <	3943	>	1730
	2	1140	1.0 >	1120	2.9 <	3264	2.9 <	3264	>	1140
	7	687	3.0 <	2040	1.6 <	3313	1.6 <	3313	>	687
	8	1060	1.0	1060	N/A	N/A	N/A	N/A	N/A	1060

ALL PREDICTED AND MEASURED STRAINS WERE IN COMPRESSION

N/A = NOT AVAILABLE, INSTRUMENT FAILURE

Table 5.8. BISAR PREDICTED COMPARED TO BISON INDICATED DEFLECTION AT TOP OF EXTENSOMETER FOR S/A 30/70 AND S/A 0/100 SECTIONS

DEFLECTION AT TOP OF EXTENSOMETER ($\times 10^{-3}$ INCHES)										
S/A	SECTION NO.	BISAR OFFSET	DEFL. RATIO	BISAR CENTERED	DEFL. RATIO	BISON	DEFL. RATIO	DEFL. RATIO	BISAR OFFSET	
30/70	5	62.9	1.3 <	80.2	77.9 >>	1.033	61.1 <<	62.9		
	6	45.6	1.1 <	47.9	101.7 >>	0.471	96.8 <<	45.6		
	11	50.5	1.5 <	78.0	88.6 >>	0.880	57.4 <<	50.5		
	12	38.9	1.1 <	43.4	45.1 >>	0.963	40.4 <<	38.9		
0/100	1	64.0	1.1 <	70.0	44.0 >>	1.589	40.3 <<	64.0		
	2	41.3	1.0 <	42.3	67.8 >>	0.624	66.2 <<	41.3		
	7	52.6	1.3 <	66.9	86.0 >>	0.778	67.6 <<	52.6		
	8	42.5 =	1.0 =	42.6	N/A	N/A	N/A	42.5		

NOTE: ALL READINGS AND PREDICTIONS INDICATE DOWNWARD DEFLECTION

N/A = NOT AVAILABLE, INSTRUMENTATION FAILURE

Horizontal Strain (Longitudinal)

30/70

No pattern apparent in deviations between BISAR OFFSET and Bison output. There is a problem in that for all but section 6, BISAR OFFSET indicates either tension or compression and the Bison gauges indicate the opposite.

0/100

Both BISAR OFFSET and Bison output indicate tension. No tendency indicated for Bison or BISAR OFFSET to dominate. Section 7 has a high disparity between BISAR OFFSET and Bison, and Bison readings are 14.7 times larger than BISAR OFFSET predicted. The reason for this disparity is not apparent.

Horizontal Strain (Transverse)

30/70

Good agreement between BISAR OFFSET and Bison. Sections 5 and 6 indicated values of BISAR OFFSET 2.1 - 2.6 times greater than Bison output yielded. Section 11 indicates Bison reading 4.8 times greater than BISAR OFFSET yielded. In section 12, BISAR predicts tension and Bison predicts compression.

0/100

The same is true for 0/100 as for 30/70; that is, BISAR predicts uniformly higher results than yielded by Bison. (BISAR OFFSET predicts values 1.5 - 1.9 times greater than Bison.)

Vertical Strain at Top of Subgrade

30/70

Bison yields higher vertical strain for all 30/70 sections than predicted by BISAR OFFSET. Bison is greater than BISAR OFFSET by a factor of 2.2 to 10.6. Sections 5 and 6 are close to each other in that Bison is 2.2 - 2.4 times greater than predicted by BISAR. Sections 11 and 12 are close to each other in the same manner as were 5 and 6 close to each other. Sections 11 and 12 vary from predicted by considerably more -- 10.6 and 7.6 times, respectively.

0/100

Good agreement for all three sections. Bison output is greater than predicted by BISAR OFFSET by a factor of 2.3 to 4.8.

Deflection at Top of Extensometer

30/70 and 0/100

This appears to be the worst agreement of all examinations. In all cases BISAR OFFSET predicted is much greater than the Bison output. The reason is not apparent but could be that the estimated M_R for the Palouse Silt (4,000) is too low.

BISAR OFFSET predictions are from 40.4 to 96.8 times greater than Bison obtained readings. This indicates a major problem with either the extensometer or the BISAR computer characterizations.

General comparison of BISAR OFFSET predicted versus Bison indicated readings show the overall best agreement was attained for transverse horizontal strains at the lower surface of the pavement. With the exception of the readings for deflections at the top of the extensometer, there is fairly good agreement between BISAR OFFSET predicted and Bison indicated as measured strains and deflections.

In an effort to examine the obvious problem at the extensometer, an examination was made of what would have happened to the surface deflection of the pavement if the BISAR OFFSET predicted deflection at the top of the extensometer were substituted for the Bison deflection at the extensometer. The results of this substitution are given in Table 5.8 and Figure 5.5.

This examination shows two trends of interest. First, the Bison gauge measurements indicate the lowest surface deflections by of all eight examined sections except in sections 1 and 2. Second, the surface deflection from the hybrid combination of Bison vertical strains and BISAR OFFSET predicted extensometer deflection yields favorable comparison to those predicted than does the Bison data alone.

Indications are that there was either something wrong with the extensometer's design or with the BISAR modeling. Benkelman beam data is available which should be examined to shed further light on this question.

Table 5.9. CALCULATED SURFACE DEFLECTION

Section	METHOD OF CALCULATION		
	Bison Gages Only	BISAR OFFSET Only	Bison/BISAR Hybrid*
1	104.6	72.6	167.0
2	59.0	42.6	99.7
5	15.5	66.5	77.4
7	17.3	49.9	48.4
11	8.4	51.5	58.0
12	9.8	43.5	47.7
	x 10 ⁻³ inches		

*Bison/BISAR Hybrid computed by summing BISAR OFFSET deflection of coil "C" and deflections indicated by Bison measured vertical strains between coil sets AB and AC.

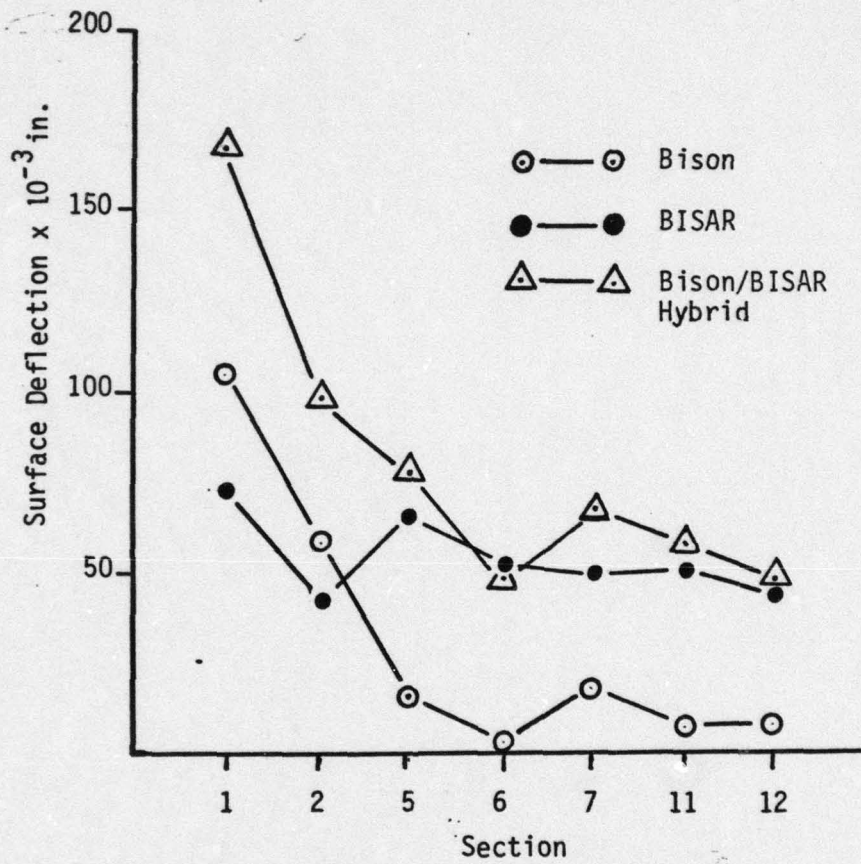


Figure 5.5. SURFACE DEFLECTIONS AS COMPUTED BY BISON, BISAR AND BISON/BISAR HYBRID

CHAPTER VI
CONCLUSIONS AND RECOMMENDATIONS

Conclusions

1. There appears to be similar performance from the 30/70 SEA and the 0/100 conventional test sections.
2. The initial strains versus load repetitions to failure graphs show a marked similarity between the 30/70 SEA and the 0/100 conventional asphalt sections, both in load repetitions and initial strains.
3. The prediction of pavement response by elastic layer theory as applied by the Shell Oil BISAR computer program appears to be valid for horizontal strains at the bottom of the pavement. The surface deflections, vertical strain in the pavement and vertical displacement at the top of the extensometer do not show the same degree of agreement. It is possible that as the material characteristics of the different sections are more accurately determined the BISAR predicted vertical strains and deflections will come into better agreement.
4. In any future utilization of SEA two factors must be taken into account at the job site. Improper placement temperature and the potential for overcompaction appear to be real concerns for the future user of sulfur-extended asphalt.
5. Indications are that there will be saving of time and equipment associated with the ease of placement and compaction characteris-

tic of SEA mixes.

Recommendations

1. M_R 's should be determined for all coring samples at not only the traditional 5, 20, and 40°C temperatures, but also at 13°C which was the temperature at which the strip chart records, indicating initial strain, were taken.

2. Further testing of the subgrade material should be conducted to check the M_R of the Palouse Silt against the assumed M_R of 4,000 psi used during this study. The 4,000 psi M_R was based upon previous studies conducted at the Washington State University Test Track Facility.

3. The characteristics of the 40/60 S/A sections are, as yet, completely unknown. A regime of laboratory tests, to include M_R , specific gravity, specific density and extractions to determine the actual sulfur and asphalt composition of the mixture placed on test track sections 3,4,9 and 10, should be undertaken.

4. The actual temperature environment experienced by the test track must be taken into account. The test track operations were normally carried out at temperatures significantly below the 13°C at which the initial strains were measured. Initial strains may have been lower if they had been measured at the average operating temperature.

5. Though fatigue failure was the failure experienced at the test track, sufficient data should have been gathered to examine rutting as a possible mode of failure. Any further testing at the test track should include rut measurements.

6. As long as the WSU test track remains exposed to the elements, instrumentation should be placed in the subgrade that would give continuous moisture content readings. This is particularly critical since the strength of the Palouse Silt fails so rapidly with increased moisture content. This would be invaluable information for later evaluation and modeling of pavement performance.

BIBLIOGRAPHY

1. The Asphalt Institute, "Introduction to Asphalt," Manual Series No. 5, Fourth Edition, pp. 1, 3, November 1962.
2. The Asphalt Institute, "Specification for Paving and Industrial Asphalts," Specification Series No. 2 (SS-2), 1977-1978 Edition, 1977.
3. Al-Otaishan, A.T.A., "Structural Evaluation of Sulfur-Asphalt Pavements," Ph.D. Dissertation, University of Washington, 1979.
4. Shell International Research Maatschaapij, Gen. Offen. 2, 149, 646. Brit. Pat. No. 1,076,866, Canadian Pat. No. 755,999. Deme, I., "The Use of Sulfur in Asphalt Paving Mixes," ACS-CIC Vancouver, 1973; "Basic Properties of Sand-Asphalt-Sulfur Mixes," AAPT, Williamsburg, Virginia, 1973; "The Development of the Use of Sulfur Paving Mixes," ACS, Los Angeles, 1974.
5. Deme, I., "Processing of Sand-Sulfur Mixes," Shell Canada Ltd., 1974.
6. Societe Nationale des Petroles d'Acquitaine, "Properties of Sulphur-Bitumen Binders," VII. International Road Federation World Meeting, Munich, 1973; "Sulfur Asphalt Concrete," 67th ACS Meeting, Los Angeles, 1974.
7. Kennepohl, G.J.A., A Logan and D.C. Beam, "Conventional Paving Mixes with Sulfur-Asphalt Binders," Gulf Oil Canada Ltd., presented at the Annual Meeting of the AAPT, Phoenix, Arizona, February 1975.
8. "Beneficial Use of Sulfur in Sulfur-Asphalt Pavement," Vol. 1, Texas A&M Research Foundation, College Station, Texas, prepared for the U.S. Department of the Interior Bureau of Mines and Sulfur Institute, 1974.
9. Waddill, P.M., D.W. Cagle, J.A. Price and D.M. Little, "Silicones Combat Foaming in Residium Storage Tanks," Oil and Gas Journal, February 1976.
10. "Effect of Silicones on Hot Mix Asphalt Pavements," Information Series 16, National Asphalt Paving Association, December 1966.
11. Rennie, W.J., "Sulfur Asphalts," New Uses for Sulfur Technology Series No. 2, SUDIC, p. 5, 1979.

12. Pickett, D.E., D. Saylak, R.L. Lytton, W.E. Conger, D. Newcomb and R.A. Schapery, "Extension and Replacement of Asphalt Cement with Sulfur," Federal Highway Administration Report FHWA-RD-78-95, March 1978.
13. Gallaway, B.M., "Fatigue of Compacted Bituminous Aggregate Mixtures," ASTM Special Publication 508, 1972.
14. Handbook of Fatigue Testing, ASTM Special Technical Publication 566, October 1974.
15. Kennedy, T.W., R. Haas, P. Smith, G.A. Kennepohl and E.T. Hignell, "An Engineering Evaluation of Sulphur-Asphalt Mixtures," a paper prepared for presentation at the 56th Annual Meeting of the Transportation Research Board, Austin Research Engineers, Inc., December 1976.
16. Lee, D., "Modification of Asphalt and Asphalt Paving Mixtures by Sulphur Additives," Engineering Research Institute, Iowa University, March 1971.
17. McBee, W.C and T.A. Sullivan, "Sulfur Utilization in Asphalt Paving Materials," New Uses of Sulfur-II, Advances in Chemistry Series, No. 165, American Chemistry Society, 1978.
18. Saylak, D., B.M. Gallaway and H. Ahmad, "Beneficial Use of Sulfur in Sulfur-Asphalt Pavements," New Uses of Sulfur, Advances in Chemistry Series, No. 140, American Chemistry Society, 1975.
19. Newcomb, D., "Analysis of Sulfur-Asphalt Field Trials in Texas," a thesis for Texas A&M University, August 1979.
20. Gallaway, B.M. and D. Saylak, "Sulphur/Asphalt Mixture Design and Construction Details - Lufkin Field Trials," Federal Highway Administration Report No. FHWA-TS-78-203, January 1976.
21. Izatt, J.O., B.M. Gallaway and D. Saylak, "Sand-Asphalt-Sulphur Pavement Field Trial, Highway U.S. 77, Kenedy County, Texas," a Construction Report, Federal Highway Administration Report FHWA-TS-78-204, April 1977.
22. Izatt, J.O., "Sulphur-Extended Asphalt Paving Project, Hwy U.S. 93-95, Boulder City, Nevada," Construction Report, The Sulphur Institute, Washington, D.C., January 1977.

23. Mahoney, J.P. and R.L. Terrel, "Sulphur-Extended Asphalt Binder Evaluation," a proposal submitted by the University of Washington to the Washington State Department of Transportation, May 1979.
24. ASTM Designation: C127-77, 1979 Annual Book of ASTM Standards, Part 14, American Society for Testing and Materials.
25. ASTM Designation: D 70, 1979 Annual Book of ASTM Standards, Part 14, American Society for Testing and Materials.
26. Sharkey, Paul D., "Mix Design and Resilient Modulus Evaluation of Sulphur-Extended Asphalt Pavements," Master's Thesis, University of Washington, October 1979.
27. Evans, Michael L., "Preparation and Evaluation of Lignin-Extended Asphalt Binders and Mixtures," Master's Thesis, University of Washington, 1978.
28. Rimsritong, Sveng, "Wood Lignins used as Extenders for Asphalt in Bituminous Pavements," Ph.D. Dissertation, University of Washington, 1978.
29. ASTM Designation: D 1559, 1979 Annual Book of ASTM Standards, Part 15, American Society for Testing and Materials.
30. Rennie, W.J., "Sulphur Asphalts: The Pronk S/A Emulsion Binder System," Second Edition, No. 3, Sulphur Development Institute of Canada, 1978.
31. WSDOT Test Method 704, Laboratory Manual, Washington State Highway Commission, Department of Highways, 1 July 1979.
32. WSDOT Test Method 705, Laboratory Manual, Washington State Highway Commission, Department of Highways, 1 July 1979.
33. WSDOT Test Method 703, Laboratory Manual, Washington State Highway Commission, Department of Highways, 1 July 1979.
34. ASTM Designation: C 496, 1979 Annual Book of ASTM Standards, Part 14, American Society for Testing and Materials.
35. "Mix Design Methods for Asphalt Concrete and Other Hot-Mix Types," Asphalt Institute Manual Series, No. 2, The Asphalt Institute, July 1978.
36. Yoder, E.J. and M.W. Witzak, Principles of Pavement Design, Second Edition, John Wiley and Sons, Inc., New York, 1975.

37. Schmidt, R.J., "A Practical Method for Measuring the Resilient Modulus of Asphalt-Treated Mixes," Highway Research Record, No. 404, Highway Research Board, 1972.
38. Gallaway, B.M. and D. Saylak, "Evaluation of Sand-Asphalt-Sulphur Mixtures Under Repetitive Loading Conditions," Final Report on Texas A&M Research Foundation Project RF 983-1B, August 1974.
39. Pronk, F.E., A.F. Soderberg and R.T. Frizzell, "Sulphur Modified Asphaltic Concrete," Annual Conference of the Canadian Technical Asphalt Association, Toronto 1975.
40. McBee, W.C. and T.A. Sullivan, "Direct Substitution of Sulphur for Asphalt in Paving Materials," TRB Annual Meeting, Washington, D.C., 1978.
41. Schmidt, R.J., "A Practical Method for Measuring the Resilient Modulus of Asphalt-Treated Mixes," Highway Research Record No. 404, Highway Research Board, pp. 22-32, 1972.
42. Users Manual (Abbreviated Version), Bitumen Structures Analysis in Roads, Shell-Laboratorium, Amsterdam, Netherlands, July 1972.
43. Elkins, H.B., "The Chemistry of Industrial Toxicology," John Wiley and Sons, Inc., New York, pp. 95, 232, 1950.
44. Kingham, R.I. and B.F. Kallas, "Laboratory Fatigue and Its Relationship to Pavement Performance," Research Report 72-3, The Asphalt Institute, April 1972.
45. Izatt, J.O., "Sulphur Extended Asphalt Field Trials - MH 153, Brazos County, Texas," a draft construction report, Texas Transportation Institute, Texas A&M University, September 1978.
46. Fatigue and Dynamic Testing of Bituminous Mixtures, ASTM Special Publication 561, 1974.
47. The AASHO Road Test, Report 5, Pavement Research, Special Report 61E, 1962.
48. Mahoney, J.P., J.Y. Tsuneta and R.L. Terrel, "Pavement Testing and Analysis of Heavy Hauls for SR 12," Research Report prepared for Washington State Department of Transportation by the Civil Engineering Department, University of Washington, October 1979.

49. Austin Research Engineers, "Asphalt Concrete Overlays of Flexible Pavements - Vol. I, Development of New Design Criteria," Report No. FHWA-RD-75-75, Federal Highway Administration, U.S. Department of Transportation, Washington, D.C., June 1975.
50. Finn, F. et al., "The Use of Distress Prediction Subsystems for the Design of Pavement Structures," Proceedings, Fourth International Conference on the Structural Design of Asphalt Pavements, 1977, pp. 3-38.
51. Izatt, J. O. "Sulphur-Extended Asphalt Field Trials, MH 153 Brazos County, Texas. A Detailed Construction Report, Texas Transportation Institute, Texas A & M University, December 1978.

APPENDIX A

WSU SUMMARY OF DAILY TRACK OPERATORS JOURNAL

Section 1

<u>Date</u>	<u>Revolutions</u>	<u>Description of Events</u>
10-25-79	5,875	Round the clock track operation begun
11-02-79	28,152	Pavement okay, no visible cracking
11-06-79	43,225	Half of section developing alligator cracks; longitudinal crack (3 ft) along outside edge of wheel path
11-09-79	50,639	3 ft long, ½" longitudinal shear failure on outside edge of wheel path; continued development of alligator cracking within wheel path of beginning half of the section
11-11-79	57,698	Continued expansion of longitudinal crack; noticeable shear separation outside edge of wheel path; permanent deformation beginning
11-12-79	62,052	Cold patched deepest deflections
11-14-79	72,140	Pavement outside wheel path heaving, 2½" vertical separation
11-17-79	81,475	Water ponding in deflected areas; subgrade pumping; entire length of section failed
11-18-79	83,068	Section dug out; hot asphalt placed

Section 2

10-25-79	5,875	Round the clock track operation begun
11-02-79	28,152	No visible cracking
11-06-79	43,225	No visible cracking
11-29-79	108,090	No apparent cracking
12-02-79	120,567	No apparent cracking
12-14-79	129,323	Transition 2-3 forming transverse cracks (18" length)
12-18-79	133,698	No change
01-02-80	138,659	No evidence of cracking
01-23-80	152,000	No evidence of cracking

Section 3

<u>Date</u>	<u>Revolutions</u>	<u>Description of Events</u>
10-25-79	5,875	Round the clock track operation begun
11-02-79	28,152	8 transverse cracks within wheel path; 2 ft lengths
11-06-79	43,225	10 transverse cracks across complete wheel path; permanent deformation noticeable
11-09-79	50,639	No noticeable change
11-11-79	57,698	Noticeable deflection; longitudinal crack development at middle of section and on outside edge of wheel path; alligator cracking beginning to develop
11-14-79	68,517	Transverse crack the width of the wheel path covering entire first half of section
11-15-79	77,713	Water ponding in permanent deformation; mud visible in cracks; considerable increase in alligator cracking
11-18-79	83,068	Section dug up; hot asphalt placed

Section 4

10-25-79	5,875	Round the clock track operation begun
11-02-79	28,152	No visible cracks
11-06-79	43,225	No visible cracks
11-12-79	60,968	Longitudinal cracks beginning to form
11-23-79	87,447	3 ft longitudinal crack on inner half of wheel path; only crack evident
11-24-79	91,324	Gauge lost cover
11-29-79	108,090	No change; transition 4-5 forming transverse cracks at patch joint; some settlement occurring
11-30-79	111,481	Longitudinal crack expanded to 5 ft length
12-14-79	129,323	No change
12-18-79	133,698	No change
01-02-80	138,659	Transverse cracks beginning to form from longitudinal crack

Section 4 (continued)

<u>Date</u>	<u>Revolutions</u>	<u>Description of Events</u>
01-21-80	145,311	At outside of track middle of section, 4 transverse cracks 2 ft in length; no change in longitudinal crack
1-23-80	152,000	7 ft longitudinal crack; 6 transverse cracks, about 2 ft wide, center of section

Section 5

10-25-79	5,875	Round the clock track operation begun
11-02-79	28,152	No visible cracks
11-06-79	43,225	No visible cracks
11-12-79	60,968	A few small transverse cracks beginning to form (5" to 8" in length)
11-15-79	77,713	A few small transverse cracks beginning to form (5" to 8" in length)
11-18-79	83,068	Alligator cracking and permanent deformation at beginning end of section; transverse cracks the width of the wheel path across remaining center of the section; water ponding in depressions Section dug up, replaced with asphalt
12-07-79	121,732	Section dug up again and portland cement concrete placed

Section 6

10-25-79	5,875	Round the clock track operation begun
11-02-79	28,152	No cracks
11-06-79	43,225	No cracks
11-29-79	108,090	No visible evidence of cracking
12-02-79	120,567	No visible evidence of cracking
12-06-79	129,323	Cracking progressing from 6-7 line into section 6 (transverse and longitudinal cracking) approximately 3 ft into section 6
12-18-79	133,698	No change; 5-6 transition patched with portland cement concrete

Section 6 (continued)

<u>Date</u>	<u>Revolutions</u>	<u>Description of Events</u>
01-02-80	138,543	Section 6 showing no evidence of cracking
01-14-80	143,302	No change
01-16-80	144,096	No change
01-22-80	148,785	No change
01-23-80	152,000	No evidence of cracking in section 6, except around transition zones

Section 7

10-25-79	5,875	Round the clock track operation begun
11-02-79	28,152	7 transverse cracks within wheel path, 2½ ft lengths
11-06-79	43,225	Subgrade squeezed out at center of section, 3 ft X width of wheel path; covered with alligator cracking; longitudinal cracks along inside and outside edge of wheel path; noticeable permanent deformation
11-09-79	50,639	Shear failure developing along outside edge of wheel path
11-11-79	55,215	7 and 8 transition zone 2" depression
11-11-79	57,698	Alligator cracking expanding throughout section; increasing permanent deflection; noticeable heaving of outside edge of wheel path
11-12-79	60,968	Entire section covered by alligator cracking; permanent deflection full length of section
11-12-79	62,052	Cold patched
11-17-79	81,475	Entire section failed; outside of wheel path heaving
11-18-79	83,068	Section dug up; hot asphalt patch placed
12-07-79	121,732	Portland cement concrete placed because of patch break-up

Section 8

<u>Date</u>	<u>Revolutions</u>	<u>Description of Events</u>
10-25-79	5,875	Round the clock track operation begun
11-02-79	28,152	No crack development
11-06-79	43,225	Transition 7 and 8, transverse cracking developing
11-12-79	62,052	No change
11-29-79	108,090	Longitudinal crack (2 ft length) formed center section
12-01-79	119,043	No change
12-14-79	129,323	Longitudinal crack expanding at center of section; no evidence of any transverse cracks; longitudinal crack progressing inward from both transition zones
12-18-79	133,698	Center longitudinal crack 5 ft long, longitudinal from section 7, 6 ft long
12-22-79	137,565	Section 9 collapse progressing 3 ft into section 8
01-02-80	138,659	Longitudinal crack from Section 7 expanded 8 ft into section 8
01-14-80	143,302	No change
01-23-80	152,000	No change

Section 9

10-25-79	5,875	Round the clock track operation begun
11-02-79	28,152	No cracks
11-06-79	43,225	Fatigue cracking at 9 and 10 transition zone
11-10-79	51,953	8" transverse crack; slight deflection with wheel pass
11-10-79	52,438	Transverse cracks spreading from 9 and 10 transition zone
11-11-79	58,324	No development of longitudinal cracks as of yet
11-12-79	60,968	Alligator cracks beginning to form at 9 and 10 transition zone
11-14-79	69,920	Same

Section 9 (continued)

<u>Date</u>	<u>Revolutions</u>	<u>Description of Events</u>
11-18-79	83,068	Transverse cracks throughout entire section; noticeable permanent deformation at center of section; subgrade pumping. Section dug up; hot asphalt placed

Section 10

10-25-79	5,875	Round the clock track operation begun
11-02-79	28,152	No cracks
11-06-79	43,225	Fatigue cracking at 9 and 10 transition zone
11-12-79	60,968	Evidence of small transverse crack
11-14-79	72,140	Transverse cracking continuing to form within the section
11-18-79	83,068	Transverse cracking throughout entire section; noticeable permanent deflection; hot asphalt placed at 9 and 10 transition zone; zealous paving crew replaced almost half of the section with asphalt
11-22-79	85,806	Extreme alligator cracking, plus longitudinal cracking inside and outside edges of wheel path; mud working up from subgrade; permanent deflection on remaining unpaved part of section
11-26-79	95,750	Deep depression, continued break-up
12-07-79	121,732	Portland cement concrete placed over entire section

Section 11

10-25-79	5,875	Round the clock track operation begun
11-02-79	28,152	2 ft x 4 ft fatigue failure; alligator cracking developing
11-05-79	38,562	Alligator cracking developed throughout entire section; pumping of subgrade; longitudinal cracking (14 ft) along outside edge of wheel path; noticeable deformation
11-06-79	43,225	Outside edge heaving; 3 ft x ½" deep shear failure outside edge, continued development of alligator cracking
11-09-79	50,639	1" to ½" vertical pavement separation along entire outside edge of the wheelpath; extreme alligator cracking developing over entire section area

Section 11 (continued)

<u>Date</u>	<u>Revolutions</u>	<u>Description of Events</u>
11-12-79	62,052	Continued pavement separation on edge of outside wheel path, extreme permanent deformation for entire length of section Cold patch applied to reduce wheel bounce
11-14-79	72,140	3½" separation heave on outside of wheel path; cold patch applied
11-18-79	83,068	Section dug up; asphalt hot mix placed

Section 12

10-25-79	5,875	Round the clock track operation begun
11-02-79	28,152	No cracking
11-06-79	43,225	No cracking
11-09-79	50,639	11 and 12 transition zone break-up
11-14-79	72,140	Longitudinal crack from section 11 expanding through transition zone of 11 and 12; center of section 12 still intact
11-18-79	83,068	Center section still okay
11-29-79	108,090	14" longitudinal crack at center of section
11-30-79	111,481	3 transverse cracks (1 ft length), center of section; longitudinal crack 2 ft long
12-01-79	110,043	5 (1 ft) transverse cracks; longitudinal crack 30" in length
12-14-79	129,323	8 transverse cracks now extend across wheel path; longitudinal crack 33" long
12-15-79	131,620	Alligator cracking developing; noticeable subgrade expulsion
12-22-79	137,565	2 ft x 3 ft alligator cracking around area by sensor
01-02-80	138,543	Transverse cracks developing throughout entire section within wheel path
01-14-80	143,302	No increase or change
01-16-80	144,096	No increase or change

Section 12 (continued)

<u>Date</u>	<u>Revolutions</u>	<u>Description of Events</u>
01-23-80	152,000	3 ft by width of wheel path around center of section covered with alligator cracks; rest of section okay, only slightly visible evidence of transverse cracking

APPENDIX B

CALIBRATION OF BISON STRAIN GAGES

The Bison strain gages (manufactured by Bison Instruments Inc.) were used extensively in the research described in this report. To enable a better understanding of how these instruments were used, a review of the calibration process is appropriate.

The calibration process involves three distinct steps. These are:

1. Development of coil spacing versus amplitude plots for Ranges 1, 2 and 3 for the 1-in., 2-in. and 4-in. diameter strain gages.
2. Development of coil spacing versus inches per volt relationships for the 1-in., 2-in. and 4-in. diameter strain gages.
3. Development of strain multiplication factors (K') versus calibration signal.

Item 1 described above resulted in the initial relationships which enable measurement of the distance between any two strain coils. Thus, deflections between two strain coils can be measured over time or between a load or no load condition. These relationships can be directly used for static loading conditions. Dynamic measurements require additional relationships which will subsequently be described.

The results of these initial calibration efforts are shown as Figures B-1 through B-5 and indicate the relationship between coil spacing and amplitude. The amplitude is used to achieve a signal balance or null condition, i.e., the difference between two amplitude readings correlates with change in coil spacing. Also shown in these figures are three coil separation ranges. These ranges cor-

AD-A083 725

ARMY MILITARY PERSONNEL CENTER ALEXANDRIA VA
INITIAL ANALYSIS OF THE SULFUR-EXTENDED TEST TRACK CONSTRUCTED --ETC(U)
MAR 80 R L GARMAN

F/G 11/4
--ETC(U)

UNCLASSIFIED

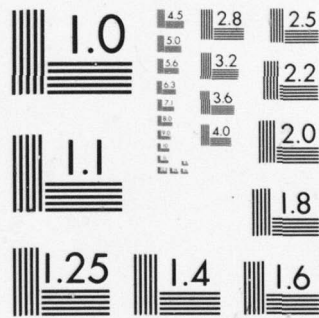
NL

3 OF 3

AD
A083 725



END
DATE
FILMED
6-80
DTIC



MICROCOPY RESOLUTION TEST CHART
 NATIONAL BUREAU OF STANDARDS-1963-A

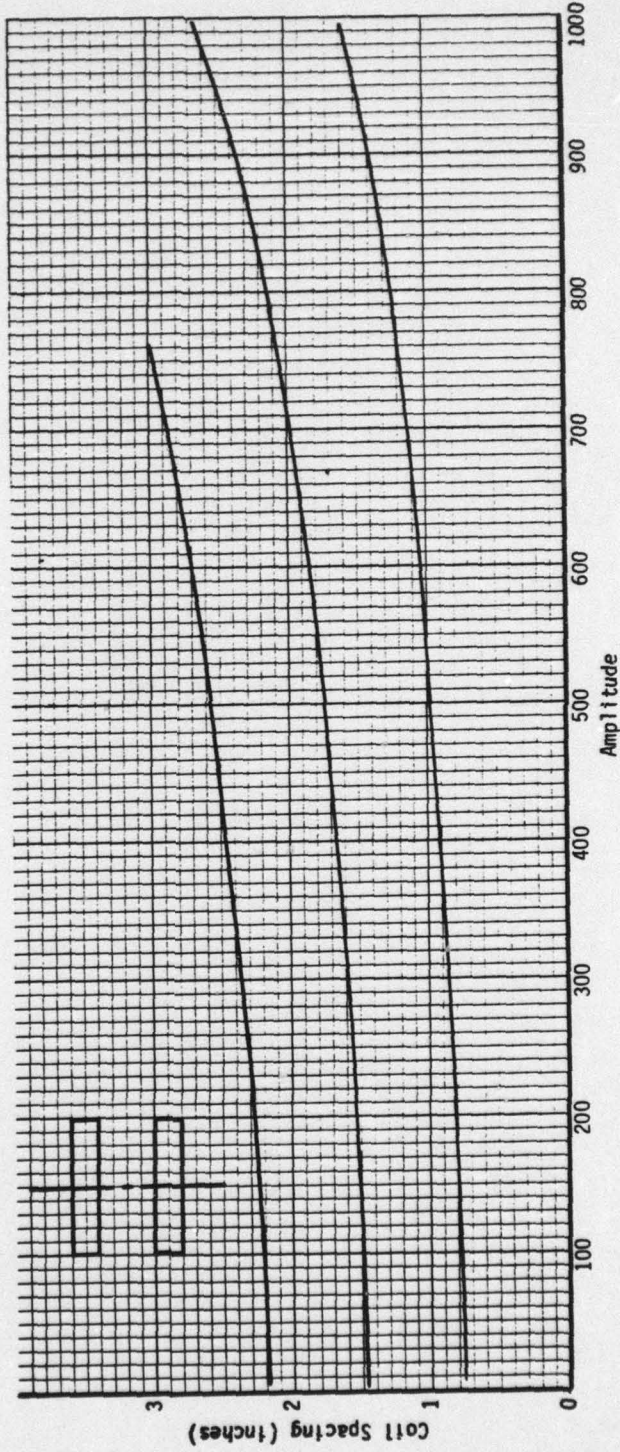


Figure B-1. COIL SPACING VS AMPLITUDE FOR 1-INCH DIAMETER BISON STRAIN COILS (PARALLEL CONFIGURATION AND MAXIMUM SENSITIVITY)

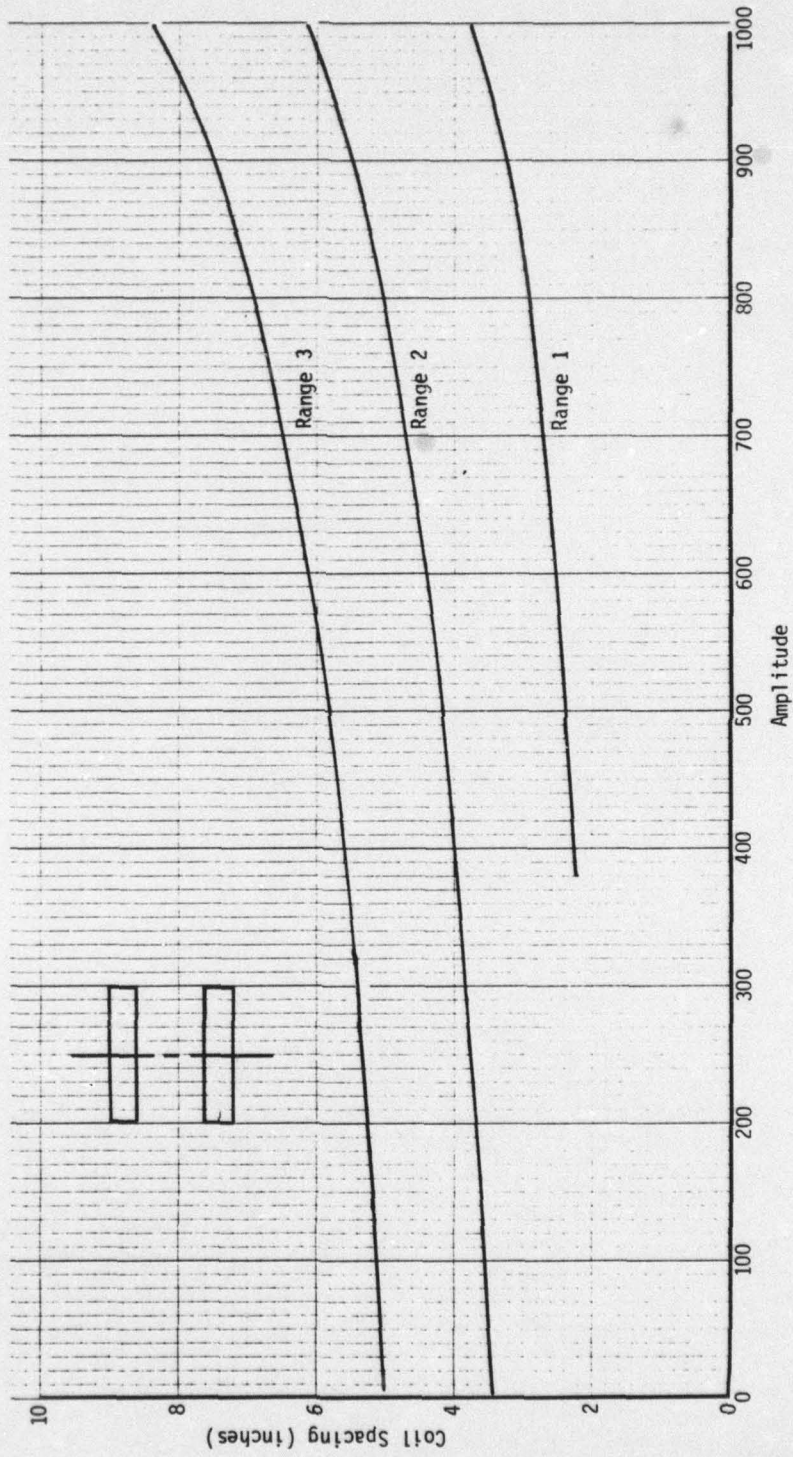


Figure B-2. COIL SPACING VS AMPLITUDE FOR 2-INCH DIAMETER BISON STRAIN COILS (PARALLEL CONFIGURATION AND MAXIMUM SENSITIVITY)

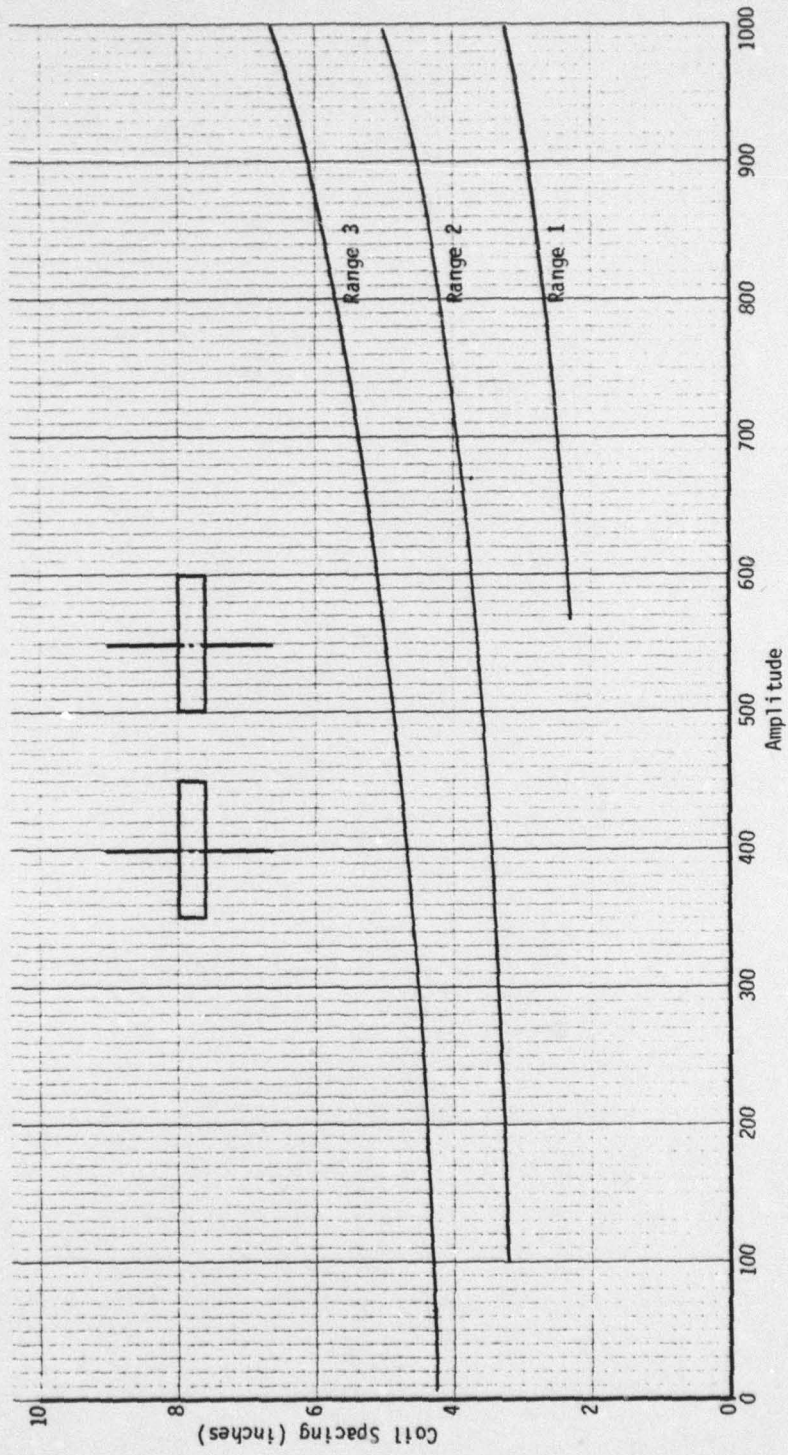


Figure B-3. COIL SPACING VS AMPLITUDE FOR 2-INCH DIAMETER BISON STRAIN COILS (COPLANAR CONFIGURATION AND MAXIMUM SENSITIVITY)

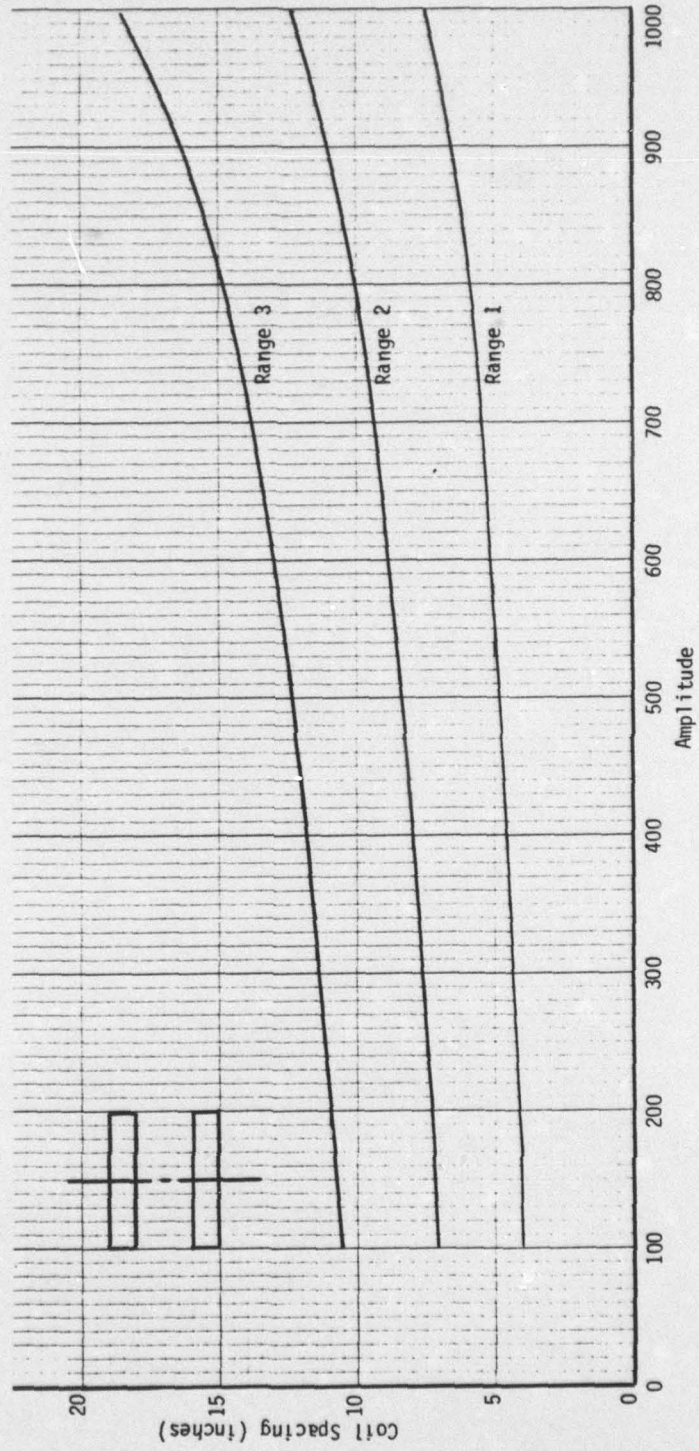


Figure B-4. COIL SPACING VS AMPLITUDE FOR 4-INCH DIAMETER BISON STRAIN COILS (PARALLEL CONFIGURATION AND MAXIMUM SENSITIVITY)

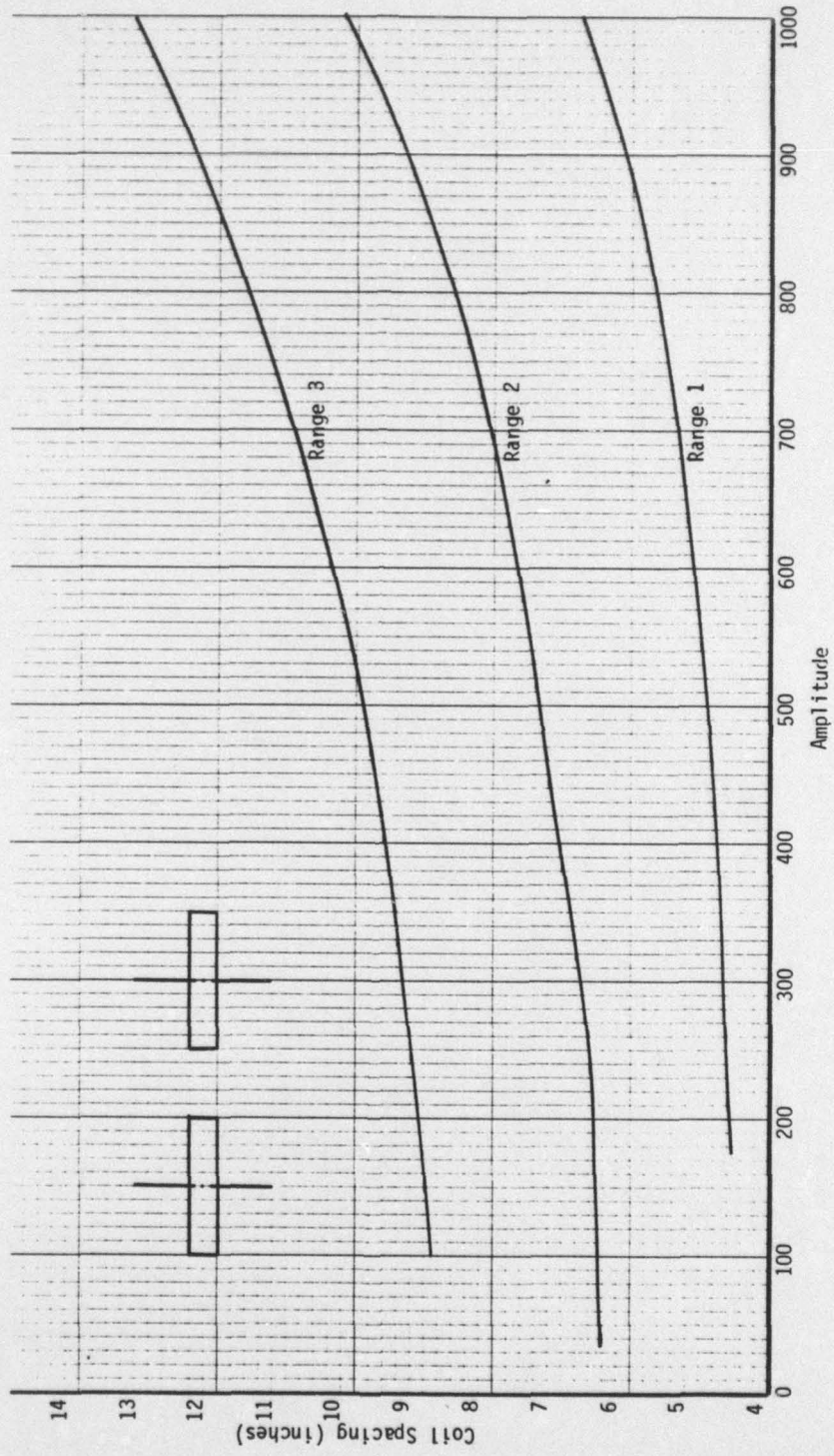


Figure B-5. COIL SPACING VS AMPLITUDE FOR 4-INCH DIAMETER BISON STRAIN COILS (COPLANAR CONFIGURATION AND MAXIMUM SENSITIVITY)

respond to a rough measure of coil separation distance (in terms of coil diameter) as follows:

Range 1: 1 to 2 diameters

Range 2: 1.5 to 3 diameters

Range 3: 2.5 to 4.5 diameters

The same generalized curvilinear relationships for coil separation versus amplitude hold for 1-in. diameter (Figure B-1), 2-in. diameter (Figures B-2 and B-3) and 4-in. diameter (Figures B-4 and B-5) strain coils. For the 2-in and 4-in. diameter coils, calibrations for both parallel and coplanar configurations were necessary. Only one calibration was necessary for the 1-in. diameter coil because the 1-in. coils were used only in a parallel configuration.

The procedure used to obtain the relationships shown in Figures B-1 through B-5 was to place two coils in a wooden jig designed and constructed for this purpose. The two coils were then connected to the Bison instrument. One coil was slowly moved via use of a micrometer and corresponding amplitude readings were obtained. In this way a full series of coil spacing versus amplitude readings were obtained. The initial coil spacing was measured with a scale at three separate locations around the circumference of the coils. This distance was taken as a center-to-center coil measurement. The sensitivity of the Bison instrument during this calibration process was at the maximum possible value.

Although the previously described calibration process was adequate for measurements made in a static loading mode, additional calibrations were required to allow measurement of dynamic deflections

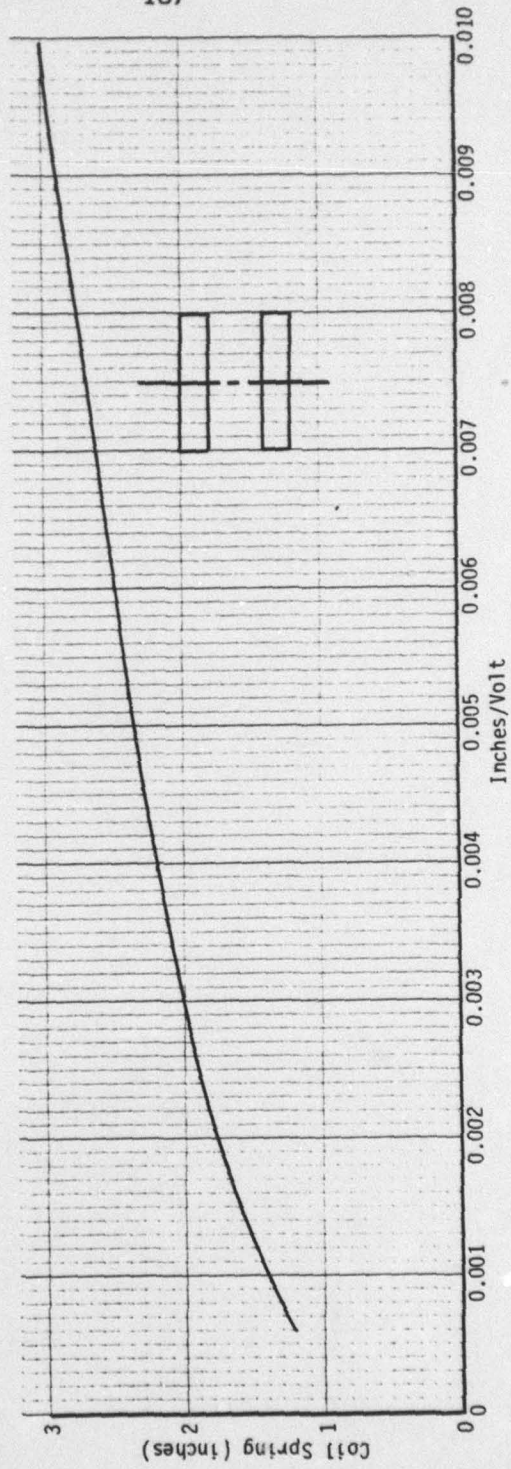


Figure B-6. COIL SPACING VS INCHES PER VOLT FOR 1-INCH DIAMETER BISON STRAIN COILS (PARALLEL CON-FIGURATION AND MAXIMUM SENSITIVITY)

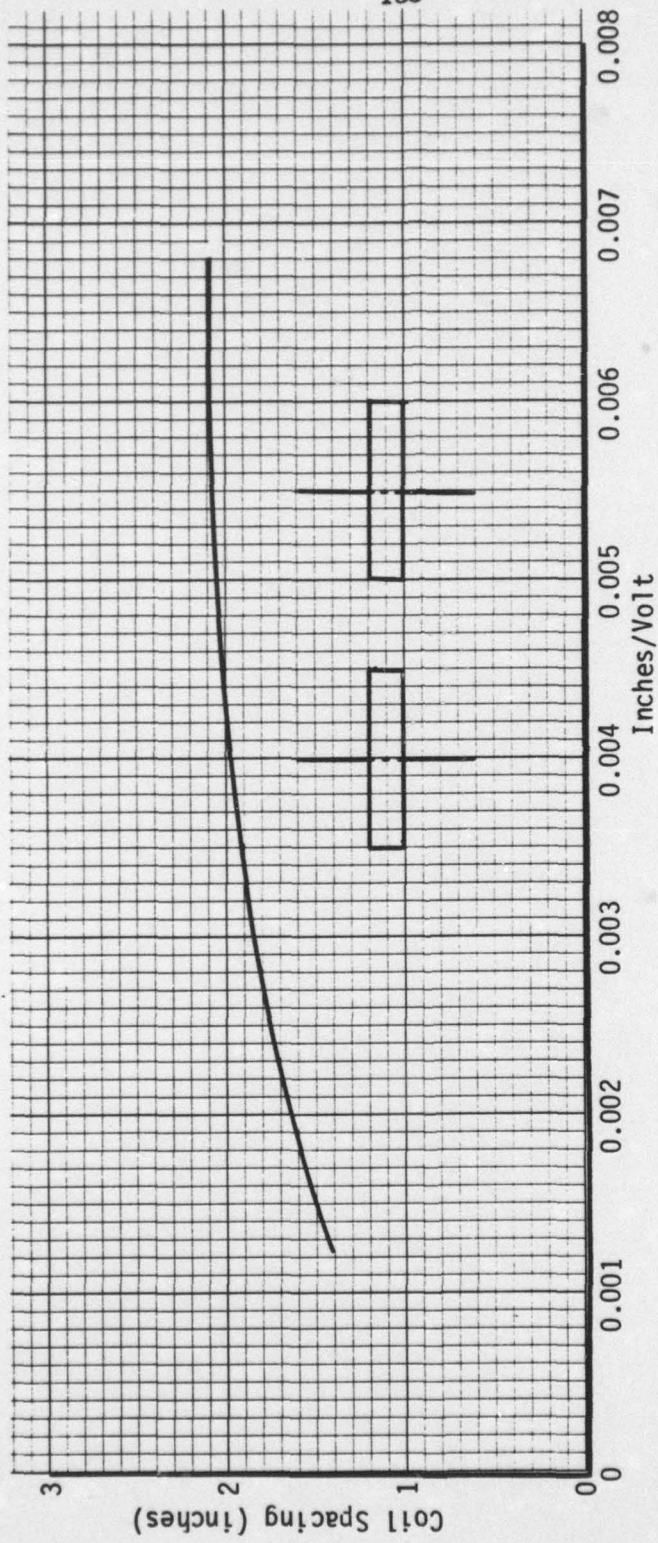


Figure B-7. COIL SPACING VS INCHES PER VOLT FOR 1-INCH DIAMETER BISON STRAIN COILS (COPLANAR CONFIGURATION AND MAXIMUM SENSITIVITY)

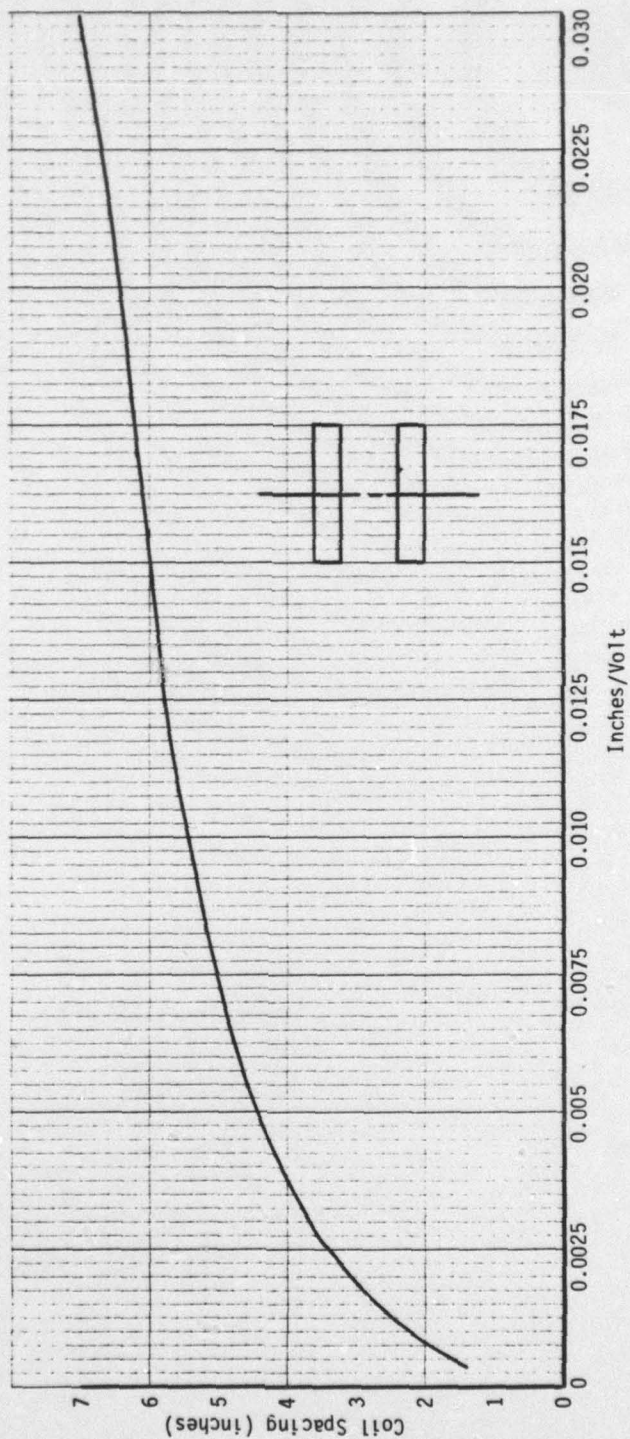


Figure B-8. COIL SPACING VS INCHES PER VOLT FOR 2-INCH DIAMETER BISON STRAIL COILS (PARALLEL CONFIGURATION AND MAXIMUM SENSITIVITY)

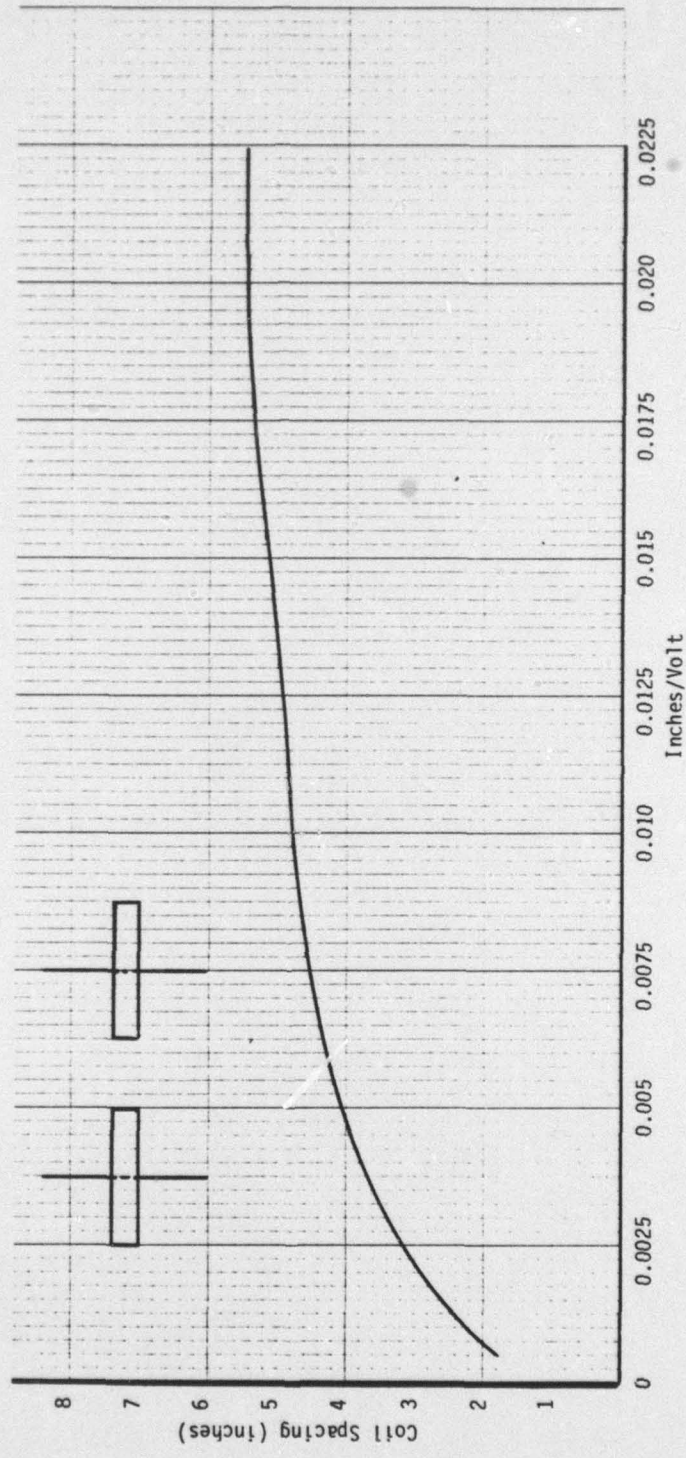


Figure B-9. COIL SPACING VS INCHES PER VOLT FOR 2-INCH DIAMETER BISON STRAIN COILS (COPLANAR CONFIGURATION AND MAXIMUM SENSITIVITY)

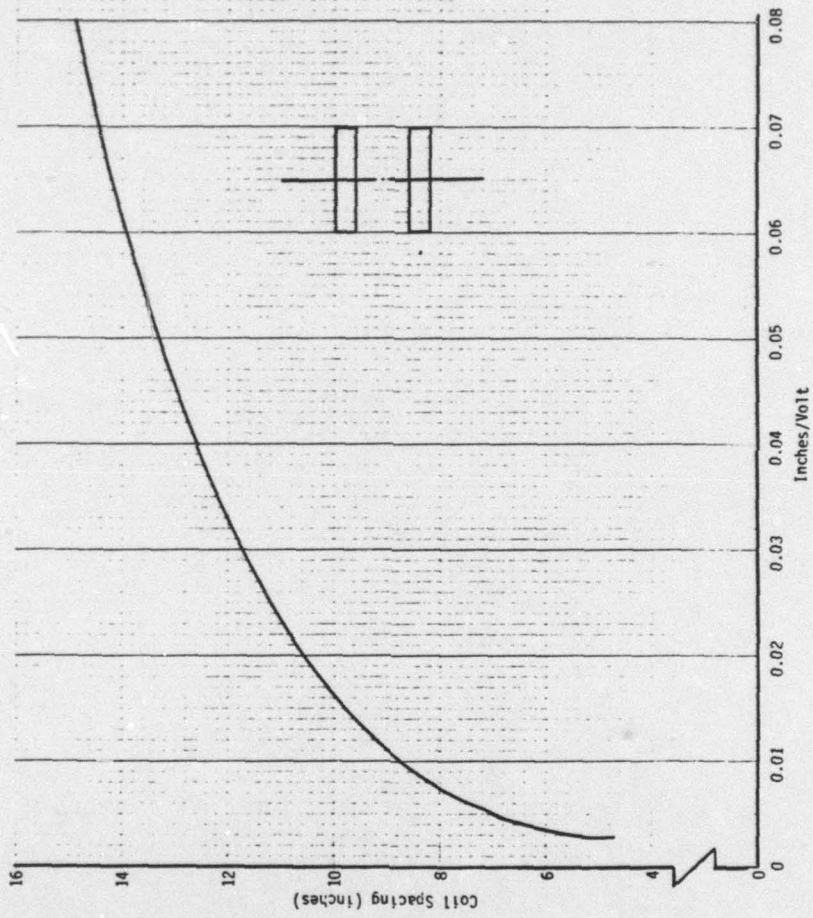


Figure B-10. COIL SPACING VS INCHES PER VOLT FOR 4-INCH DIAMETER BISON STRAIN COILS (PARALLEL CON-FIGURATION AND MAXIMUM SENSITIVITY)

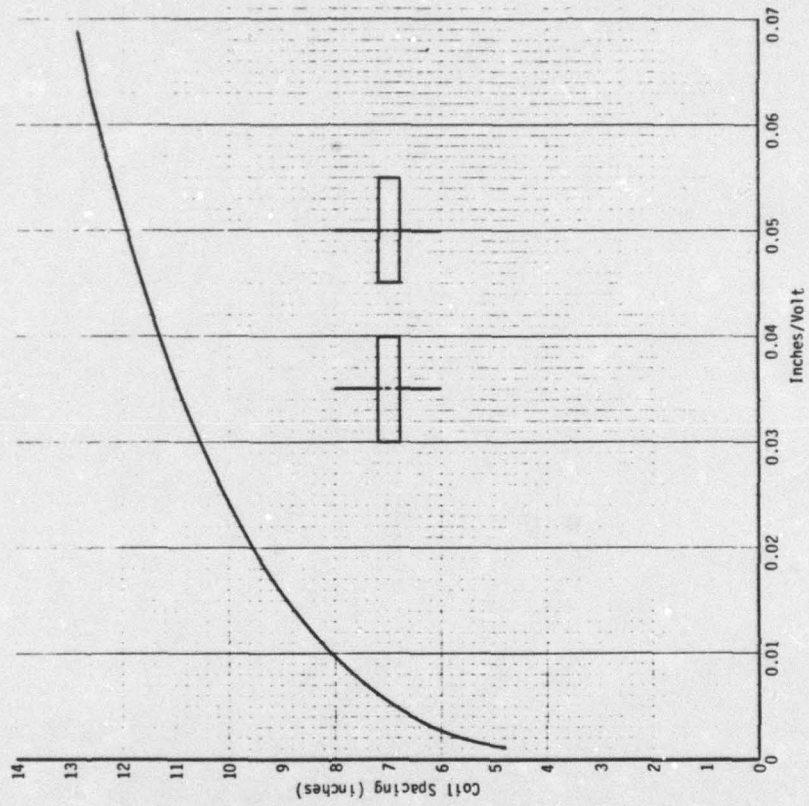


Figure B-11. COIL SPACING VS INCHES PER VOLT FOR 4-INCH DIAMETER BISON STRAIN COILS (COPLANAR CONFIGURATION AND MAXIMUM SENSITIVITY)

(hence strains). Dynamic deflection measurements required the use of voltages to determine changes in coil spacings. Thus amplitude readings were not sufficient and coil spacing versus inches of deflection per volt were made. This calibration process was similar to that previously described except that a volt meter was used to measure changes in coil spacings. These calibrations were made for all three coil sizes and both configurations (parallel and coplanar). This information is shown in Figures B-6 through B-11.

The calibrations shown in Figures B-6 through B-11 allow the use of a known coil spacing to determine a value of inches of deflection per volt. By measuring the voltage change between two coils during loading, the change in distance between coils can be computed. This relationship does not need to be modified if the Bison instrument is at full sensitivity. During the test track operation, lower sensitivities were necessary thus requiring additional calibrations.

The final series of calibrations were used to find relationships between change in deflection for constant voltage changes taken over a range of Bison instrument sensitivities. The sensitivity of the Bison instrument was quantified by use of the "Calibration Signal" which ranges from 1000 (maximum sensitivity) to 0 (no sensitivity). The ratio of the change in deflection at any calibration signal level and the change in deflection at a calibration signal level of 1000 was calculated and denoted as k' . This value is used as a multiplier to increase the deflection value determined from the calibrations shown in Figure B-1 through B-11. Thus appropriate deflections can be determined for any Bison instrument sensitivity. The results of these cali-

brations are shown as Figures B-12 through B-14 for the three coil sizes. The k' values were determined for both the parallel and coplanar coil configurations but resulted in essentially the same relationship. Thus the overall calibration procedure simplified slightly.

All calibration relationships were quantified by use of regression techniques. This enabled more accurate determinations of deflections (strains) to be made from the raw data.

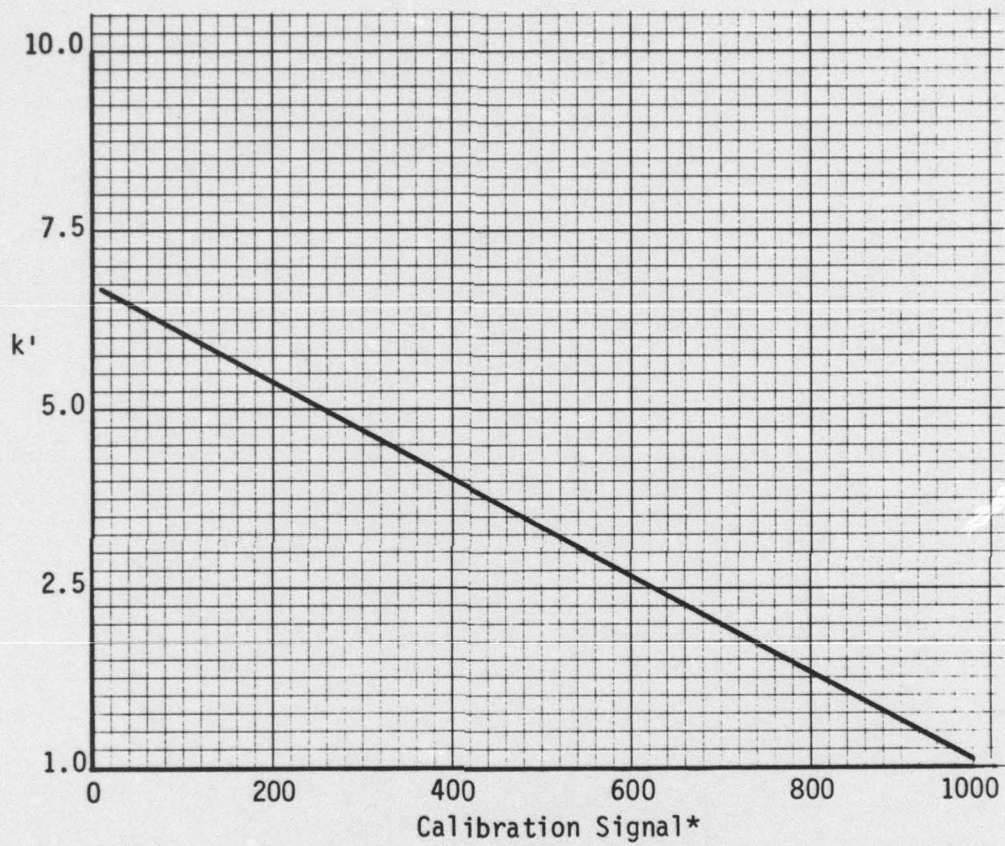


Figure B-12. k' VS CALIBRATION SIGNAL
FOR 1-INCH DIAMETER BISON
STRAIN COILS (PARALLEL AND
COPLANAR CONFIGURATIONS)

*Note: calibration signal = 1000 maximum sensitivity

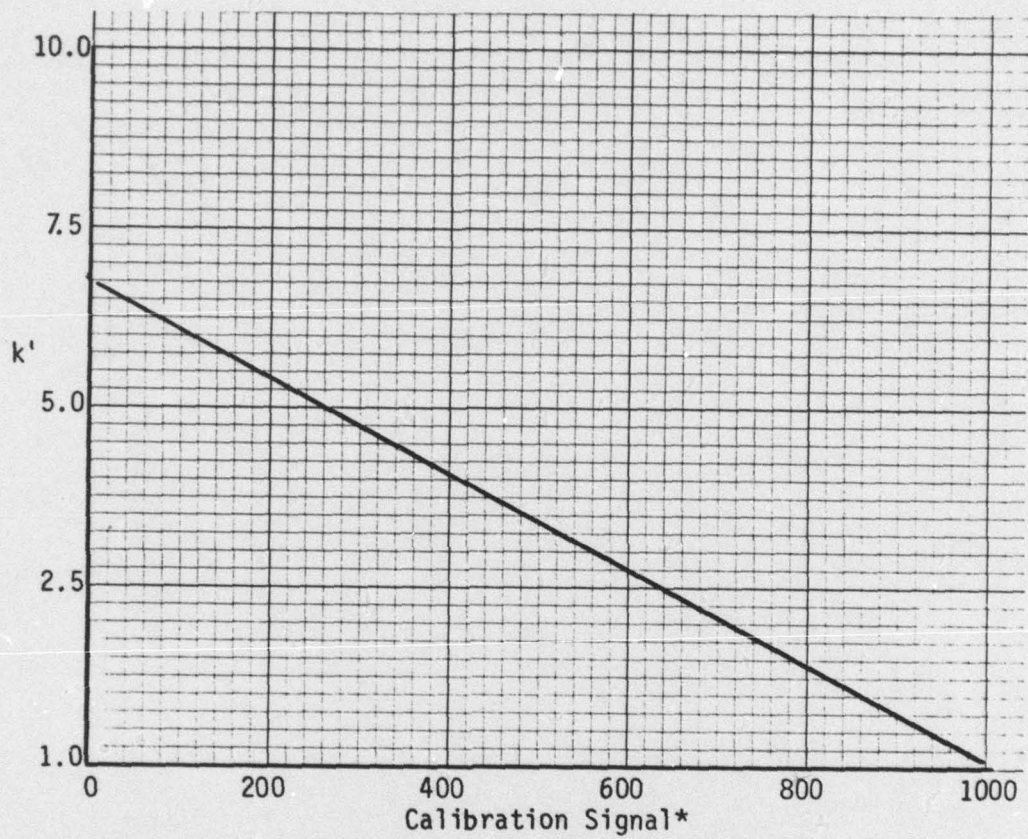


Figure B-13. k' VS CALIBRATION SIGNAL
FOR BISON STRAIN COILS
(PARALLEL AND COPLANAR
CONFIGURATIONS -2 INCH)

*Note: calibration signal = 1000 maximum sensitivity

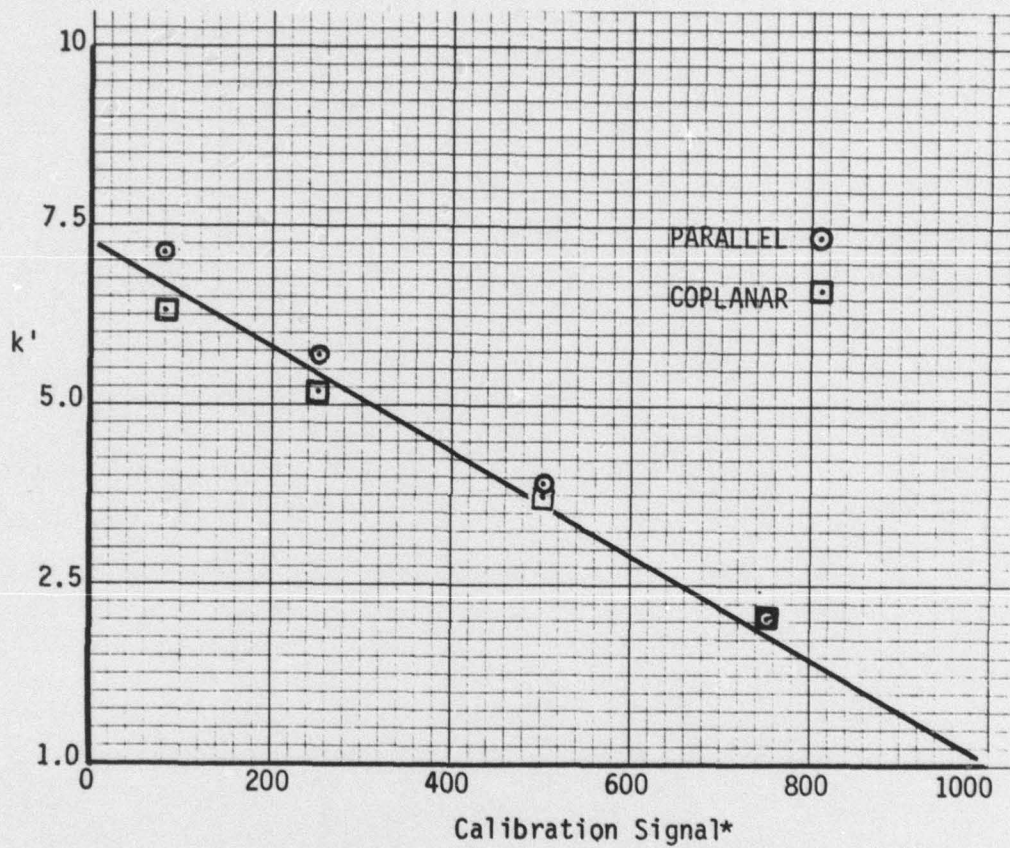


Figure B-14. k' VS CALIBRATION SIGNAL FOR 4-INCH DIAMETER BISON STRAIN COILS (PARALLEL AND COPLANAR CONFIGURATIONS)

*Note: calibration signal = 1000 maximum sensitivity

LMED
-8